CONSTRUCTION OF CHAOTIC REGIONS FOR DUFFING'S EQUATION WITH A QUADRATIC TERM

By

Xiong Chen

B. Sc. Zhejiang University, M. Eng. Dalian Institute of Technology

A THESIS SUBMITTED IN PARTIAL FULFILLMENT OF

THE REQUIREMENTS FOR THE DEGREE OF

MASTER OF APPLIED SCIENCE

in

THE FACULTY OF GRADUATE STUDIES

CIVIL ENGINEERING

We accept this thesis as conforming

to the required standard

.....	....
.....	....
.....	....
.....	....
.....	....

THE UNIVERSITY OF BRITISH COLUMBIA

June 1992

In presenting this thesis in partial fulfilment of the requirements for an advanced degree at the University of British Columbia, I agree that the Library shall make it freely available for reference and study. I further agree that permission for extensive copying of this thesis for scholarly purposes may be granted by the head of my department or by his or her representatives. It is understood that copying or publication of this thesis for financial gain shall not be allowed without my written permission.

CIVIL ENGINEERING
The University of British Columbia
2324 Main Mall
Vancouver, Canada
V6T 1Z4

Date: Aug. 19. 1992

abstract

Non-linear oscillators can exhibit non-periodic responses under periodic excitation. A point in the parametric space is said to be within a chaotic region if the response under periodic excitation is chaotic. The Lyapunov exponent analysis is developed herein to construct chaotic regions for Duffing's equation. Structural background of Duffing's equation is given. Phase plane and Poincaré plots are made to check some questionable chaotic points in the parametric space. In order to help understand chaotic behaviour, bifurcation and stability analyses are presented. Theoretical and heuristic criteria are also discussed for specific cases, and plotted to compare with numerical results.

Numerical results are obtained for Duffing's equation with two kinds of quadratic terms, (1) $X|X|$ term, (2) X^2 term. Some other cases are also included in order to compare with previous work. In general, good agreement is obtained.

Table of Contents

List of Tables

List of Figures

Acknowledgement

The author wishes to take this opportunity to express his appreciation to his supervisor Dr. M.D. Olson for his patient guidance, advice and encouragement throughout the course of research work and in the preparation of this thesis. I am also deeply grateful to Dr. Jian-Ping Jiang for numerous helpful discussions.

Financial support in the form of a research assistantship from the Natural Sciences and Engineering Research Council is gratefully acknowledged.

Chapter 1

INTRODUCTION AND LITERATURE REVIEW

1.1 GENERAL REMARKS

In recent years, there has been growing interest in nonperiodic, randomlike or chaotic behaviour of nonlinear differential equations in applications to many physical systems. The equations governing these systems are deterministic while for certain control parameters chaotic motions appear. The clues to the emergence of chaotic motions in deterministic dynamical systems have been uncovered by new topological methods in mathematics, and at the same time, supporting evidence has been provided by experimental measurement and numerical simulation. In spite of the deterministic nature of these systems, randomlike behaviour is observed for certain parameters and initial conditions without random inputs.

There are several good books which study nonlinear differential equations using classical methods, such as the perturbation method and averaging techniques etc., which can describe some characteristics of these nonlinear equations [1]. However, these methods usually assume periodic solutions which is not valid for chaotic motion. Due to the presence of nonlinearities in the equation, analytical solutions are rarely obtainable, and numerical simulation is widely used to study these equations.

Systems which exhibit chaotic motion include mechanical devices with nonlinear springs, atmospheric dynamics, electrical circuits, elastic structures, elastic - plastic structures, convective flows, aeroelastic systems, and chemical and biological systems.

The term 'CHAOS' is generally used to distinguish randomlike behaviour from a true random process, and chaotic motion has also been called 'strange attractors' to distinguish it from classical limit cycle and forced periodic motion. Key to an understanding of these motions is the concept of maps. For continuous motions, this amounts to discrete time sampling of the motion in phase space. A particular map that is common to all strange attractor systems is the horseshoe map. Chaotic motions are also related to classic bifurcation theory in dynamical systems. A common feature of a chaotic system is a succession of bifurcations to higher and higher subharmonics as a parameter is varied. In some simple systems this occurs as a sequence of period doubling bifurcations with a limit point beyond which strange attractors occur. The most important characteristics of chaos is its sensitivity to initial conditions which makes the precise time history unpredictable but still bounded. Because of this potential unpredictability, it is important for engineering designs to study chaotic motion.

Representative equations of these nonlinear dynamical systems are Duffing's and the Lorenz equations. There have been many papers and reports published for Duffing's equation which include only a cubic term or both linear and nonlinear cubic terms using either numerical or experimental methods. However, few papers considered the additional quadratic term, and no chaotic region was constructed. It appears that Duffing's equation with linear term, cubic term, and absolute value quadratic term has not been studied before. The major part of this thesis is devoted to constructing chaotic regions of Duffing's equation with two kinds of quadratic terms in the parametric space using numerical simulation. The basic idea of the numerical simulation is based on the characteristics of chaotic motions, in which the solution is sensitive to the initial conditions. This method was developed by Lyapunov, and is called Lyapunov exponent[2]. Some other Duffing's equations are also studied in order to compare the results with previous work. Analytical and heuristic criteria of chaotic motion, which have been discussed in many papers, are

presented in this thesis, as well.

1.2 LITERATURE REVIEW OF PREVIOUS STUDIES

Although randomlike behaviour of nonlinear dynamical systems was first observed a century ago by Poincaré et al, significant attention has been devoted since Ueda [3-4] first explored chaos in a special form of the stable Duffing's equation for electrical circuits which includes only the cubic term. An analogous computer simulation and Lyapunov analysis were used, and chaotic regions were constructed in the damping coefficient and forcing amplitude plane. Almost at the same time, the vibration of a buckled beam was studied by P.J.Holmes [5], who considered the unstable Duffing's equation with negative linear term and cubic term. A mathematical analysis using bifurcation theory was also attempted in his work, and an analytical criterion based on the work of Melnikov was obtained. Due to the restriction of this analytical criterion, it is very difficult to apply this criterion to the general Duffing's equation. Later attention has been directed towards the unstable Duffing's system, which is often referred to as a buckled beam model [6-8].

In reference [6], F.C.Moon studied the same problem as in [5], using experimental methods to simulate chaotic phenomenon. He suggested a heuristic criterion for two - well potential problems based partly on a perturbation solution for forced periodic motion and experimental observation. This criterion, according to [6] and his later published book [9], is much better than the Holmes analytical method [5] for the low damping case. Later, Li applied the same idea to a multi - well potential problem, and this criterion has been verified successfully in experiments for a vibrating beam with three equilibrium points [10].

A very good summary of previous work on systems that may cause chaotic motion

was given by P.J.Holmes [7], which included the buckled beam, flow of fluid over a buckled plate, electrical circuits, magnetic torque on a magnet, feedback control systems, and chemical systems, etc. Analytical methods are also presented for some specific problems. E.H.Dowell, et al. [8] have explained how the potential wells, associated with the statically unstable nature of the system, promote the transition to chaos. Another heuristic criterion was posed for the two - well potential problem – buckling beam model in [8]. Instead of comparing the size of periodic orbits with the undamped, unforced problem that was used in [6], they compared the boundary of the basin of attraction for the damped, unforced problem. This boundary represents a set of initial conditions for which the orbit goes to the left or right equilibrium point without crossing the zero displacement line in the phase plane. They also observed, through numerical simulation, that the driven motion becomes chaotic when the forcing amplitude is larger than the value for which a periodic orbit touches the basin boundary.

A more general and stable Duffing's system, with positive linear term and cubic term, was examined by E.H.Dowell [11] using numerical simulation. Chaotic motion was found at much higher forcing amplitude than what was obtained in [3-4]. It was also found that in addition to the multi-level responses which may occur occasionally in the system, dual responses are usually possible as well. Whether it is periodic or chaotic, it is always sensitive to the initial conditions. Finally, it is suggested that for transition to chaos, the system behaviour might follow a certain pattern: dual periodic responses — period doubling — almost periodic motion — chaos.

An experimental study was performed by F.C.Moon [12], of the harmonically forced motion of a buckled rod and beam - plate system. These models simulate the responses of one and two dimensional Duffing's type nonlinear differential equations with multiple equilibrium points. A chaotic motion threshold criterion for forcing amplitude as a function of frequency was discussed as well. Tongue [13] showed that the existence of

multiple static equilibria is not a necessary requirement for chaos to occur.

A.H.Nayfeh [14-16] studied the parametrically excited Duffing's oscillator which is representative of many physical systems. In [14], the quadratic nonlinearity as well as linear and cubic terms were considered, and its response to a fundamental parametric resonance was examined. The classical perturbation results were verified by integrating the governing equation using a digital computer and an analogue computer. It was found that for small excitation amplitude, the analytical results were in excellent agreement with the numerical solutions. But, as the amplitude of excitation increases, the accuracy of the perturbation solution deteriorates. After investigating the case of single - and double - well potential problems, Nayfeh concluded that systems with double - well potentials exhibit complicated dynamic behaviours including period multiplying and demultiplying, bifurcation and chaos. Responses of two - degree - of - freedom systems with quadratic nonlinearities are discussed in [17-18].

The dynamical behaviour of Duffing's equation with linear and negative quadratic terms was studied by M.S. Soliman [19] and J.M.T. Thompson [20] et al, in which attention was focused on basins of attraction and their boundaries rather than the intricate steady states of the bifurcating patterns. Transient behaviour was studied. The theoretical criterion for chaos in this type of problem was obtained by using Melnikov's analysis [20].

Construction of chaotic regions in parameter space for nonlinear differential equations was investigated (in [21]) using a numerical method. The incremental harmonic balance method and Newtonian iteration method were applied to construct chaotic regions. Due to the complexity of the Floquet theory which is used to determine the bifurcation points, it usually needs much more analytical work and CPU time than the Lyapunov exponent method. The latter is quite simple for obtaining analytical and numerical solutions. As an example, Ueda's case was treated in [21], and good agreement was obtained as

compared to the previous study.

As mentioned before, Duffing's equation can be obtained not only from a buckled beam model, but also from many other structural and mechanical systems. B.Poddar et al. [22] considered chaotic behaviour of an elastic - plastic beam, which leads to Duffing's equation, with constant, linear and cubic terms. It was found that geometric and material nonlinearities in the structure may lead to extreme sensitivity to small changes in parameters and cause unpredictability, (i.e. chaotic motion). It is important for engineering design to investigate chaotic motion for these problems.

It is noted that there are some other remarkable structural and mechanical systems which are not governed by Duffing's equation. Chaotic behaviour of a periodically forced piecewise linear oscillator was studied by using the analytical method [23] and the experimental method [24], respectively. The nonlinearity is in the restoring force which is piecewise linear with a single change in slope [23]. In [24] a beam with a nonlinear boundary condition was considered. Chaotic motion was obtained for both cases. Also flutter of a buckled plate was discussed by Dowell [25], and chaos may occur with both compressive load and a fluid flow.

1.3 SCOPE OF PRESENT INVESTIGATION

It is clear from a survey of the pertinent literature that there are very few studies reported for Duffing's equation including a quadratic term. It appears that there is no publication which shows chaotic regions for this kind of equation. It is the purpose of this thesis, therefore, to investigate such systems and to construct chaotic regions in parametric space using Lyapunov exponent analysis.

In Chapter 2, the structural background of Duffing's equation is described, and some fundamentals of mathematical analysis are presented. Three kinds of beam problems

are considered, and three kinds of Duffing's equations are obtained. The bifurcation and stability analysis are carried out. The concept of homoclinic orbits, Melnikov method and Lyapunov exponent analysis are introduced, and are used to construct analytical criteria and to perform numerical simulations. Some analytical and heuristic criteria are also discussed.

The details of numerical procedures and formulations are described in Chapter 3. Two kinds of Duffing's equations with quadratic terms are considered: (i) $X|X|$ term, and(ii) X^2 term. In order to compare the results with previous work, some other kinds of Duffing's equations are also considered here.

In Chapter 4, the numerical results and chaotic regions are presented in parametric space. In order to confirm suspected points and regions of chaotic motion, plots in the phase plane and Poincaré plane are also provided. The analytical and heuristic criteria are plotted as well.

Conclusions and suggestions for further study are presented in Chapter 5.

Chapter 2

STRUCTURAL BACKGROUND AND MATHEMATICAL ANALYSIS

2.1 STRUCTURE BACKGROUND OF DUFFING'S EQUATION

2.1.1 GENERAL REMARKS

In this section, the structural background of Duffing's equation is described. A simple supported elastic beam with axial preload, a simple supported rigid - plastic beam, and a rigid - plastic beam with some elastic behaviour are considered, respectively, by using some modelling assumptions. Different types of Duffing's equations are obtained, that is, Duffing's equation involving only cubic term, linear and cubic terms, and extra quadratic term.

2.1.2 ELASTIC SIMPLY SUPPORTED BEAM WITH PRELOAD IN AXIAL DIRECTION

From Figure (2.1), the governing equation of this beam is given by

$$EI\frac{\partial^4 W}{\partial X^4} + (-N_x + N_o)\frac{\partial^2 W}{\partial X^2} + C\frac{\partial W}{\partial t} + M\frac{\partial^2 W}{\partial t^2} = F(X,t) \tag{2.1}$$

where E is modulus of elasticity, A is the area of the beam cross-section , EI is the bending rigidity, M is the mass per unit length, C is the damping coefficient of the beam, N_x is the axial load, N_o is axial compressive preload, W is the deflection of the beam, and $F(X,t) = q_o \sin(\pi X/L)\cos\Omega t$ is the time dependent loading.

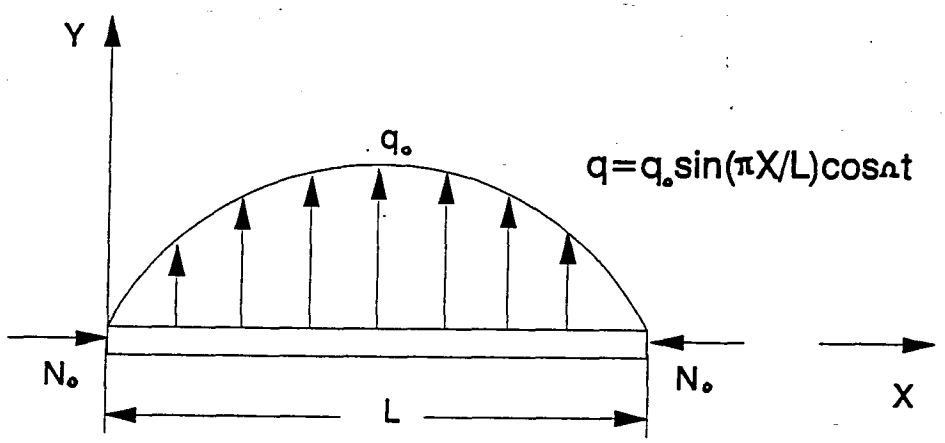

Figure 2.1: Elastic Simply Supported Beam

The axial load in the beam due to stretching is

$$N_x = EA\epsilon_x \tag{2.2}$$

where ϵ_x is axial extension of the beam, which is

$$\epsilon_x = (1/2L)\int_0^L (W')dx \tag{2.3}$$

Nondimensionalize the governing eqn. (2.1)

Introduce:

$\xi = X/L$ is nondimensional variable.

$\bar{t} = W_o t$ is nondimensional time.

$\eta = W/L$ is nondimensional deflection.

$\Omega_o^2 = EI/ML^4$ is natural frequency.

$c = C\Omega_o L^4/EI$ is nondimensional damping coefficient.

$a_1 = N_x L^2/EI, a_2 = N_o L^2/EI$ are coefficients.

$F(\xi, \bar{t}) = q_o L^3/EI \sin \pi\xi \cos(\Omega_1/\Omega_o)\bar{t}$ is nondimensional external load.

Then (2.1) becomes

$$\frac{\partial^4 \eta}{\partial \xi^4} + (-a_1 + a_2)\frac{\partial^2 \eta}{\partial \xi^2} + c\frac{\partial \eta}{\partial \bar{t}} + \frac{\partial^2 \eta}{\partial \bar{t}^2} = F(\xi, \bar{t}) \tag{2.4}$$

Using one mode approximation (i.e. first mode solution)

$$\eta(\bar{t}) = \eta_o(\bar{t}) \sin \pi\xi \tag{2.5}$$

Then

$$\epsilon_x = (1/2L)\int_0^L (W')dx = (\pi/2L)^2 \eta_o^2 L^2 \tag{2.6}$$

Thus

$$N_x = EA\epsilon_x = EA(\pi/2L)^2 \eta_o^2 L^2 \tag{2.7}$$

Therefore (2.4) becomes

$$\ddot{\eta}_o + c\dot{\eta}_o + k\eta_o + \beta\eta_o^3 = B\cos\Omega\bar{t} \tag{2.8}$$

where

$k = \pi^4 - N_o(L\pi)^2/EI$, $\beta = AL^2\pi^4/4I$,

$B = q_o L^3/EI$, $\Omega = \Omega_1/\Omega_o$,

$\ddot{\eta}_o = d^2\eta_o/dt^2$, $\dot{\eta}_o = d\eta_o/dt$

Equation (2.8) is Duffing's equation with linear and cubic terms.

If $k = 0$, i.e. $N_o L^2/EI = \pi^2$. Eqn. (2.8) becomes

$$\ddot{\eta}_o + c\dot{\eta}_o + \beta\eta_o^3 = B\cos\Omega\bar{t} \tag{2.9}$$

2.1.3 RIGID - PLASTIC SIMPLY SUPPORTED BEAM

Now a rigid - plastic simply supported beam is considered, which has uniform rectangular cross - section with width b and depth h.The beam is subjected to a uniformly distributed load. The load is harmonic in time with maximum intensity of P_o (force per

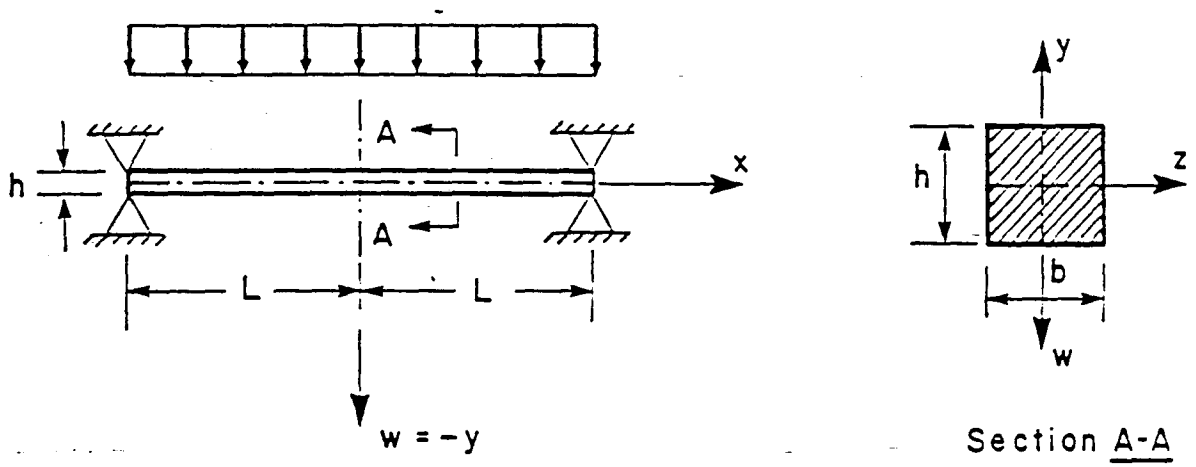

Figure 2.2: Rigid - Plastic Simply Supported Beam

unit length). The edge restranints are such that the ends of the beam at the centroidal axis are prevented from in - plane movements along the x-axis. Tensile axial forces N are induced in the beam due to the transverse deflection and increased length of the beam, as shown in Figure 2.2.

At the limit load the beam tends to deform plastically in a single - hinge mechanism (Figure 2.3). This mechanism, however, is only correct at zero deflection when no membrane forces are generated. Exact theoretical solutions including finite deflection effects are difficult to obtain, thus one has to resort to approximate solutions.

To develop an approximate method, we consider the single - hinge configuration of Figure 2.3 as a first approximation to the deformed shape of the beam during small but finite deflections. The membrane forces are no longer zero and must be included in the formulation.

Consider equilibrium configuration of the beam at the instant of plastic collapse (Figure 2.4). This mode of deformation has one degree of fredom defined by the rotation

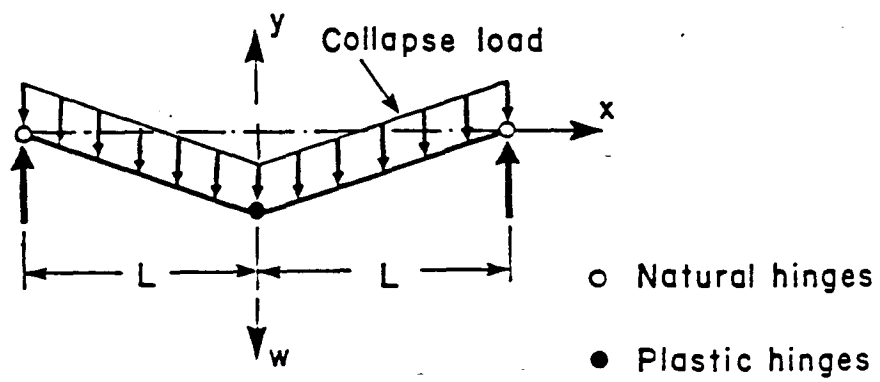

Figure 2.3: Configuration of the simply supported beam after development of a central plastic hinge

θ of each half of the beam. The angular dislacement θ is considered as an incremental displacement in the collapse state and is therefore a "small" quantity.

Let θ have a variation $\delta\theta$ in the neighbourhood of the given configuration (Figure 2.4). Then observing that the hinge rotation at the central section is the sum of the rotations of the two portions of the beam, we have

$$\delta\psi = 2\delta\theta \tag{2.10}$$

where $\delta\psi$ is the increment of rotation at the hinge point.

Due to the increment $\delta\theta$, the length of the beam will have a virtual extension $\delta\epsilon$ given by

$$\delta\epsilon = \delta(2L\cos^{-1}\theta) = 2L\cos^{-1}\theta\tan\theta\delta\theta \tag{2.11}$$

For sufficiently small θ such that $\theta^2 \ll 1$, then

$$\delta\epsilon = 2L\theta\delta\theta \tag{2.12}$$

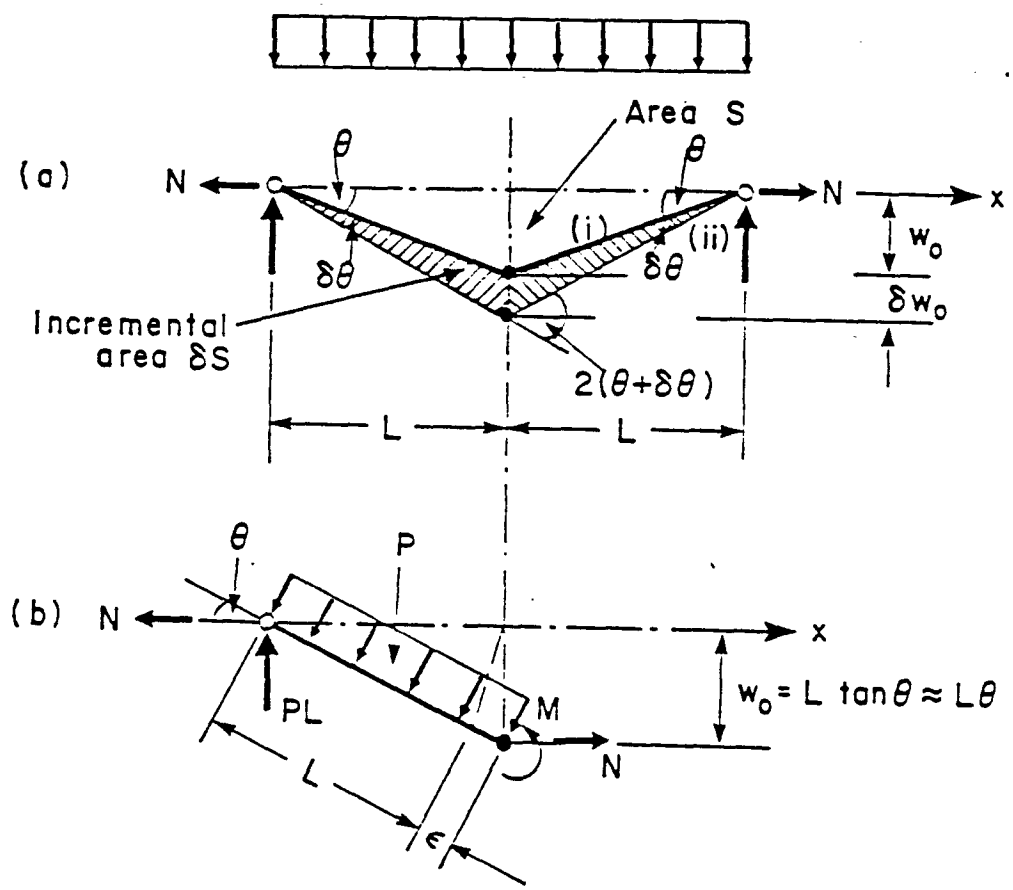

Figure 2.4: Nomenclature and free body diagram for a static analysis of the simply supported beam. (a) (i) Deflected form during collapse. (ii) Virtually disturbed configuration. (b) Free body diagram

According to [26], using the principle of virtual work and considering small deflection, we can get:

$$N\delta\epsilon + M\delta\psi = \int_{-L}^{L}(F(t) - m\ddot{W}(x,t) + C\dot{W}(x,t))\delta W(x,t)dx \tag{2.13}$$

There exists a function of the nondimensional stress components $(\overline{n}, \overline{m})$, the so-called "yield function" given by

$$f(\overline{n}, \overline{m}) \equiv \overline{m} + 2\overline{n}y_e/r_p - 1 \tag{2.14}$$

where $\overline{n} = N/N_o$ and $\overline{m} = M/M_o$.

The beam reaches its limit state of stress under a critical combination of axial load and bending moment when f=0. The material cannot tolerate stress distributions for which $f > 0$. Therefore the yield condition is satisfied everywhere in the beam if $f \leq 0$ is maintained.

In the above equation, y_e denotes the distance of the centroid of the transferred area A_e from the equal area axis and is given by

$$y_e = \int_0^e b(y)ydy / \int_0^e b(y)dy \tag{2.15}$$

where b(y) is the width of the section at a distance y from the equal area axis (Figure 2.5).

$r_p = y_1 + y_2$ is the lever arm of the plastic moment (Figure 2.6).

For a rectangular cross - section, we have

$r_p = h/2, y_e = e/2, N = 2\sigma_o be, N_o = \sigma bh, M_o = \sigma_o bh^2/4$

So the yield condition turns out to be

$$M/M_o = 1 - (N/N_o)^2 \tag{2.16}$$

Then the yield surface is

$f = \overline{m} + \overline{n}^2 - 1$ (see Figure 2.7), and from Fig. 2.4

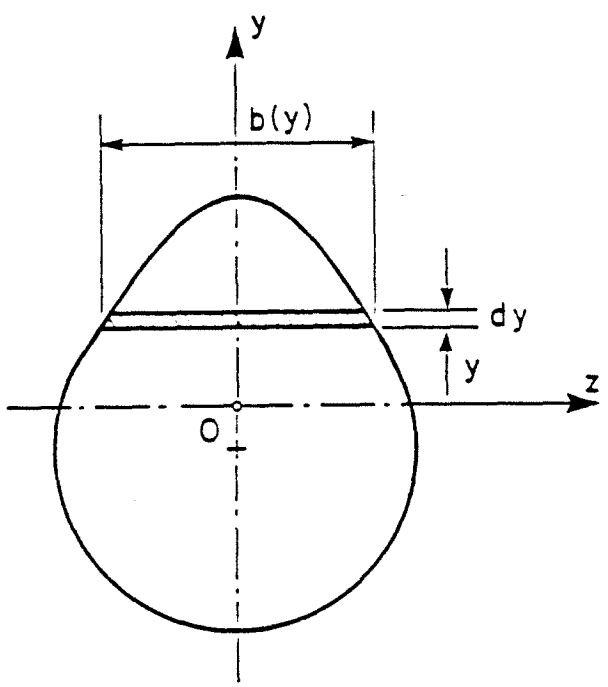

Figure 2.5: Schematic of the cross - section showing a typical differential element

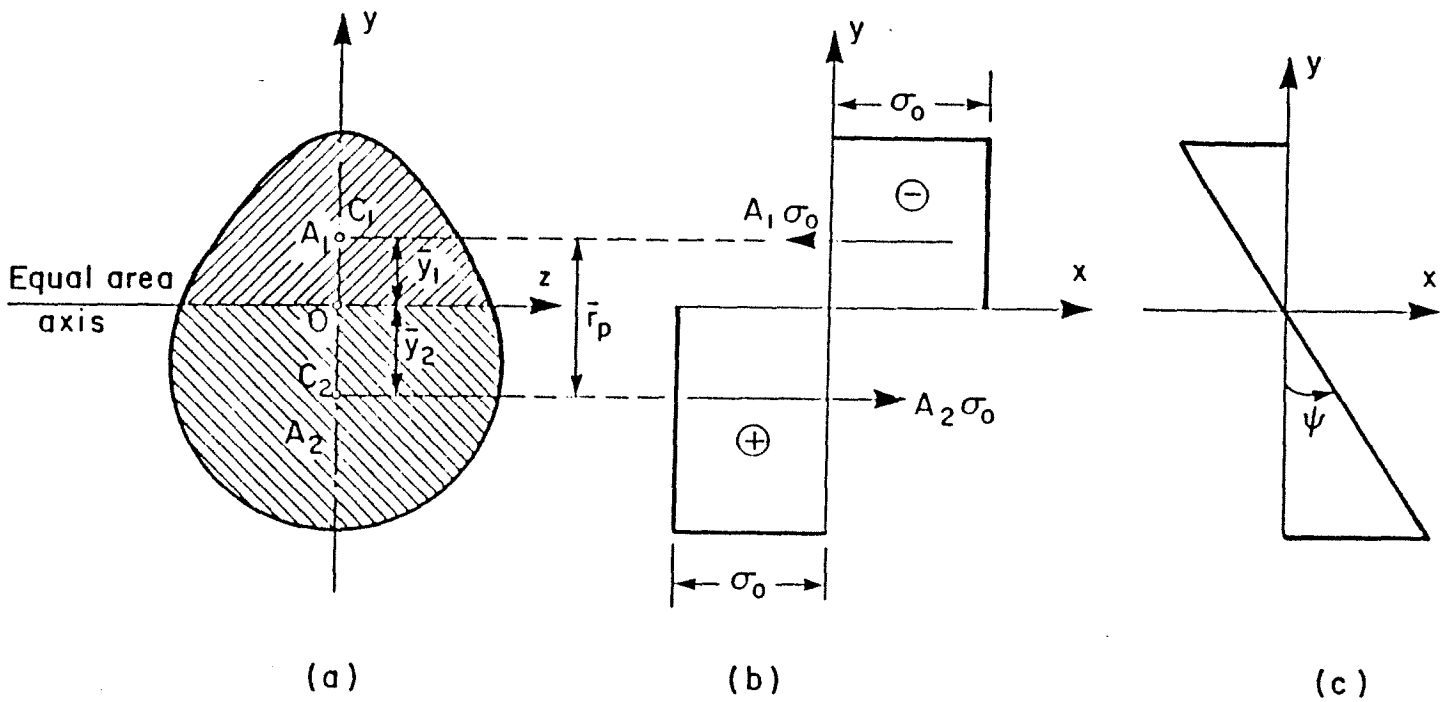

Figure 2.6: Resolution of the fully plastic stress distribution (a) fully plastic stress distribution (b) fully plastic stress distribution in the absence of axial load (c) fictitious stress distribution

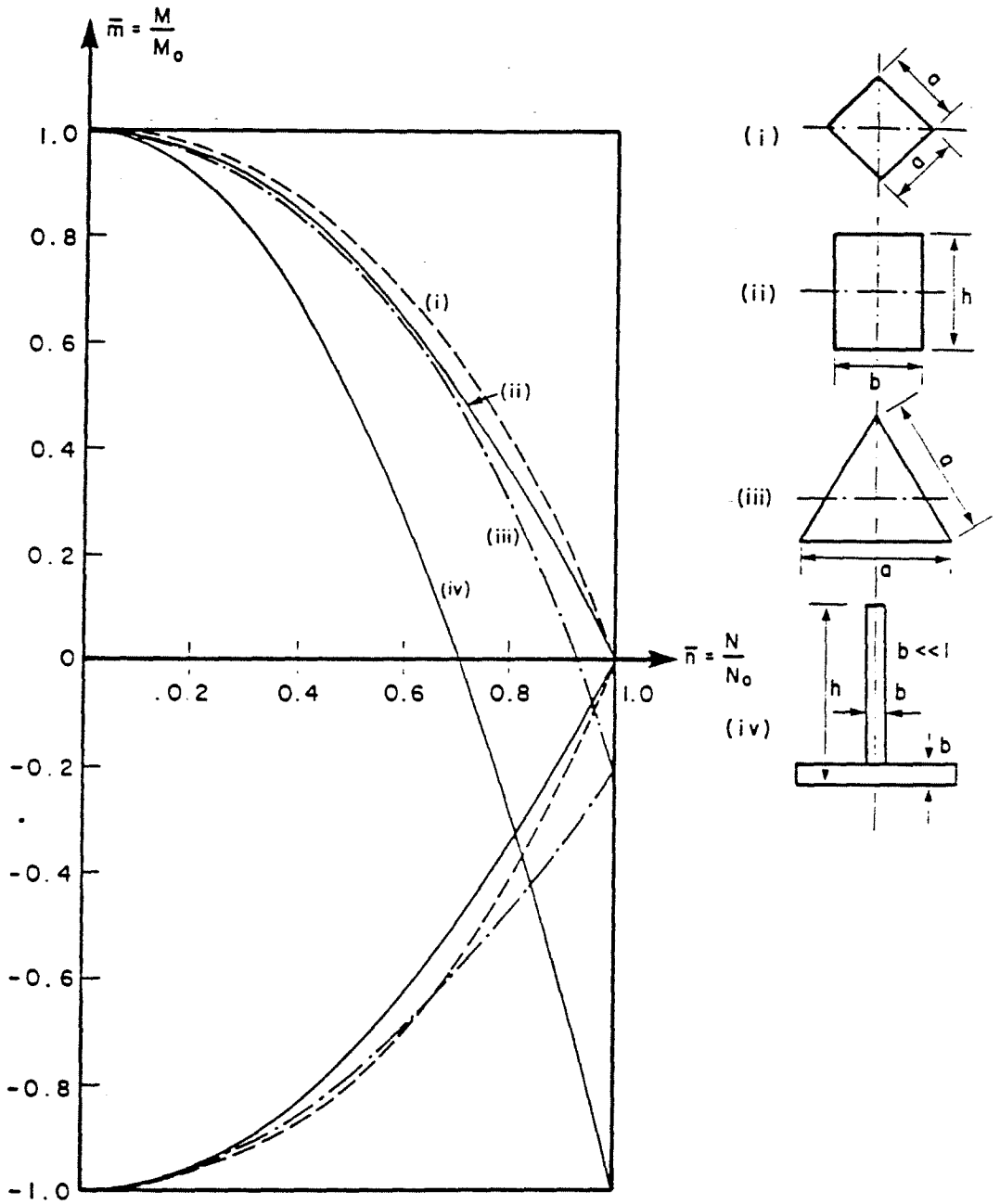

Figure 2.7: Yield curves for some typical cross - section geometries

$$W(x,t) = W_o(t)(1 - |x|/L) \qquad -L \leq x \leq L$$

$$\delta W_o = L\delta\theta \tag{2.17}$$

The flow rule which using the parabolic yield function $f \equiv \overline{m} + \overline{n}^2 - 1$ requires that

$$N_o/M_o\delta\epsilon/\delta\psi = 2N/N_o \tag{2.18}$$

Thus

$$W_oN_o/M_o = 2N/N_o \tag{2.19}$$

For a rectangular section:

$$N_o = \sigma_o bh, \qquad M_o = \sigma_o bh^2/4$$

So:

$$N/N_O = 2W_o/h \tag{2.20}$$

Therefore (2.13) becomes

$$M_o[1 + 4/h^2W_o(t)|W_o(t)|] = L^2/2[f(t) - 3/2m\ddot{W}_o(t) - 3/2C\dot{W}_o(t)] \tag{2.21}$$

i.e.

$$\ddot{W}_o(t) + c\dot{W}_o(t) + \alpha W_o(t)|W_o(t)| = \frac{3}{2m}\,(B_o\cos\Omega t - B_1) \tag{2.22}$$

where $\quad c = C/m, \alpha = 6B_o/mh^2, B_1 = 2M_o/L^2$

Equation (2.22) is Duffing's equation only with quadratic term.

2.1.4 RIGID - PLASTIC BEAM WITH ELASTIC EFFECT

As we already discussed above, the elastic beam leads to linear and cubic terms, while the rigid-plastic beam leads to a quadratic term. So, for a rigid-plastic beam with elastic effect, the governing equation of this beam should have all these terms. i.e.

$$\ddot{X}(t) + c\dot{X}(t) + kX + \alpha X|X| + \beta X^3 = B\cos\Omega t \tag{2.23}$$

In the following study, another form of Duffing's equation with a quadratic term is also considered, which is

$$\ddot{X}(t) + c\dot{X}(t) + kX + \alpha X^2 + \beta X^3 = B\cos\Omega t \tag{2.24}$$

Both equations (2.23) and (2.24) are investigated in the following Chapter on constructing chaotic regions.

2.2 MATHEMATICAL ANALYSIS

2.2.1 GENERAL REMARK

Some useful mathematical analysis is discussed in this section, First, bifurcation and stability analysis is given which is important to predict whether it is possible to have chaos. Then the concept of homoclinic orbits and the Melkinov method is presented and are used to construct theoretical criteria for chaos. Finally, based on these mathematical analyses, some theoretical and heuristic threshold criteria are derived.

2.2.2 BIFURCATION AND STABILITY ANALYSIS

Here the local bifurcation and stability study is given for the fixed points (or equilibria in engineering) of Duffing's equation.

Considering an autonomous Duffing's equation:

$$\ddot{X} + c\dot{X} + kX + \alpha X^2 + \beta X^3 = 0 \tag{2.25}$$

it can be shown that, if $\alpha^2 < 4k\beta$, there is a single equilibrium point at $(X, \dot{X}) = 0$, while if $\alpha^2 \geq 4k\beta$, there are three equilibria at $X = 0, (-\alpha \pm \sqrt{\alpha^2 - 4k\beta})/2\beta$ and

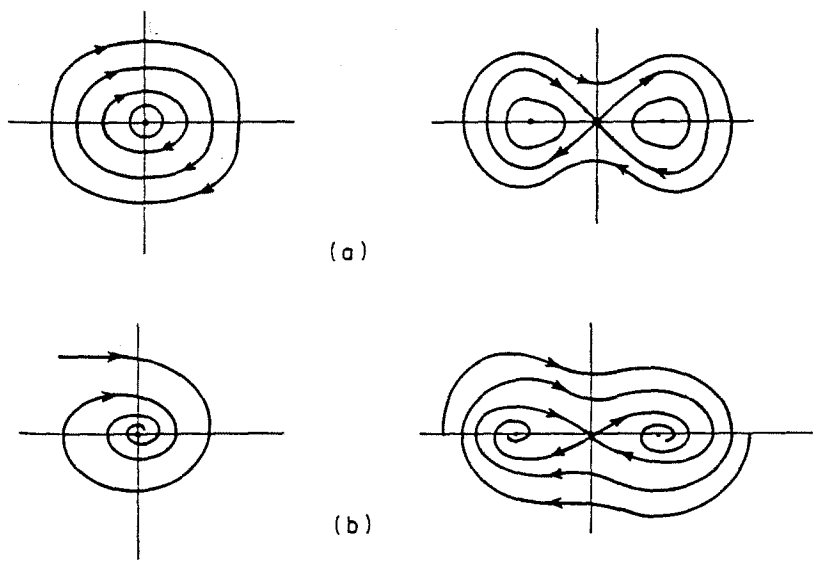

Figure 2.8: Phase plane examples for Duffing's equation without external forcing. (a) $\delta = 0$, (b) $\delta > 0$.

$\dot{X} = 0$. If $c > 0$, the equilibria are, respectively, a sink (for $\alpha^2 < 4k\beta$) and two sinks and a saddle (for $\alpha^2 \geq 4k\beta$). According to [28], Eqn.(2.25) undergoes a pitchfork bifurcation of equilibria as k passes though zero.

To obtain global information on the phase portrait, we note that, for $c = 0$, the system is Hamiltonian with Hamiltonian energy given by

$$H(X,Y) = \frac{Y^2}{2} + k\frac{X^2}{2} + \alpha\frac{X^3}{3} + \beta\frac{X^4}{4} \tag{2.26}$$

where $Y = \dot{X}$.

The phase portraits of both $c = 0$ and $c > 0$ are shown in Figure 2.8(a,b), which are very important to understand the behaviour of Eqn.(2.25)

In general, chaotic motion will occur when there are two sinks and a saddle between them (i.e. $\alpha^2 \geq 4k\beta$ here), but it is not always valid to say that there is no chaos with only a stable sink. Why a static stable equilibrium can cause chaos is still largely unknown.

A similar analysis can be applied to the autonomous system of (2.23).

2.2.3 HOMOCLINIC ORBIT AND MELKINOV METHOD

It appears that the mysteries of nonlinear dynamics and chaos are often deciphered by looking at a digital sampling of motion such as a Poincaré map. Here, the Poincaré map is introduced to describe a homoclinic orbit. If there are saddle points, in the case of small forcing, the stable and unstable manifolds only intersect at saddle points. If the stable and unstable manifolds intersect at other points (it will occur at large forcing), then the points of intersections of stable and unstable manifolds are called homoclinic points. A Poincaré point near one of the intersection points will be mapped into all the rest of the intersection points. This is called a homoclinic orbit.

If near the homoclinic points, a volume of points transform to a conventional shaped volume, the regular solution is obtained. When the volume is stretched, contracted and folded as in the Baker's transformation or horseshoe map, chaotic motion occurs. That is, if the homoclinic orbit leads to a horseshoe map, then the motion will be chaotic.

A good discussion of homoclinic orbits may be found in the books [27,28].

The Melkinov function is used to measure the distance between unstable and stable manifolds when that distance is small (see [28]). It has been applied to problems where the dissipation is small and the equations for the manifolds of the zero dissipation problem are known. For example(see [9]), suppose we consider the forced motion of a nonlinear oscillator where (q,p) are the generalized coordinate and momentum variables. We assume that both the damping and forcing are small and then we can write the

equations of motion in the form

$$\begin{cases} \dot{q} = \partial H/\partial p + \epsilon g_1 \\ \dot{p} = -\partial H/\partial q + \epsilon g_2 \end{cases} \tag{2.27}$$

where $g = g(p, q, t) = (g_1, g_2)$, ϵ is a small parameter, and H(q,p) is the Hamiltonian for the undamped, unforced problems ($\epsilon = 0$). We also assume that g(t) is periodic, so that

$$g(t + T) = g(t) \tag{2.28}$$

and that the motion takes place in a three-dimensional phase space $(q, p, \Omega t)$, where Ωt is the phase of the periodic force and T is the period.

In many nonlinear problems, a saddle point exists in the unperturbed Hamiltonian problem ($\epsilon = 0$ in Eqn.(2.27)). When $\epsilon \neq 0$ one can take a Poincaré section of the three-dimensional torus flow synchronized with the phase Ωt. It has been shown (see [26]) that the Poincaré map also has a saddle point with stable and unstable manifolds, W^s and W^u (see [9]), respectively.

The Melkinov function provides a measure of the separation between W^s and W^u as a function of the phase of the Poincaré map Ωt. This function is given by the integral

$$M(t_o) = \int_{-\infty}^{\infty} g^{\star} \bullet \nabla H(q^{\star}, p^{\star}) dt \tag{2.29}$$

where $g^{\star} = g(q^{\star}, p^{\star}, t + t_o)$ and $q^{\star}$ and $p^{\star}$ are the solutions for the unperturbed homoclinic orbit originating at the saddle point of the Hamiltonian problem. The variable t_o is a measure of the distance along the original unperturbed homoclinic trajectory in the phase plane.

2.2.4 THEORETICAL AND HEURISTIC CRITERIA OF CHAOS

For some specific coefficients of Duffing's equations, theoretical criteria may be derived by using homoclinic orbits and the Melkinov method. Heuristic criteria are also derived by multiwell potential method (see [9]) in this section.

The theoretical criteria for the following equation has already obtained (see [28]) by using the Melkinov method.

$$\ddot{X} + c\dot{X} - X + X^3 = B\cos\Omega t \tag{2.30}$$

The lower bound on the chaotic region in (B, Ω, c) space is

$$B_c = \frac{4c\cosh(\pi\Omega/2)}{3\sqrt{2}\pi\Omega} \tag{2.31}$$

and this has been verified in experiments by Moon [6].

Because only a few problems have analytical Melkinov functions, theoretical criteria for chaotic motion can only be derived for a few cases, as given in the following.

Consider Duffing's equation with the form

$$\ddot{X} + c\dot{X} - \frac{1}{2}X + \frac{1}{2}X^3 = B\cos\Omega t \tag{2.32}$$

The Hamiltonian for the unperturbed problem is

$$H(X, \dot{X}) = \frac{1}{2}\dot{X}^2 - \frac{1}{4}X^2 + \frac{1}{8}X^4 \tag{2.33}$$

For $H = 0$, there are two homoclinic orbits originating and terminating at the saddle point at the origin. The variables X^* and $\dot{X}^*$ take on values along the right half plane curve given by solving Eqn.(2.33) when $H = 0$. This is

$$\begin{cases} X^* = \sqrt{2}\cosh^{-1}(t/\sqrt{2}) \\ \dot{X}^* = -(t/\sqrt{2})\tanh(t/\sqrt{2}) \end{cases} \tag{2.34}$$

Substituting $g_1 = 0$ and $g_2 = \overline{B}\cos\Omega t - \overline{c}\dot{X}$ into Eqn.(2.27), where $c = \epsilon\overline{c}$ and $B = \epsilon\overline{B}$, leads to the Melkinov function

$$M(t_o) = -B\int_{-\infty}^{\infty}\cosh^{-1}(t/\sqrt{2})\tanh(t/\sqrt{2})\cos\Omega(t+t_o)dt - c\int_{-\infty}^{\infty}\cosh^{-2}(t/\sqrt{2})\tanh^2(t/\sqrt{2})dt \tag{2.35}$$

which can be integrated exactly using methods of contour integration.

Then

$$M(t_o) = -2\sqrt{2}c/3 + 2\mathrm{B}\pi\Omega\cosh^{-1}(\sqrt{2}\pi\Omega/2)\,\sin\Omega t_o$$

Thus, the lower bound on the chaotic region in (B, Ω, c) space is

$$B_c = \frac{\sqrt{2}c}{3}\,\frac{\cosh(\sqrt{2}\pi\Omega/2)}{\pi\Omega} \tag{2.36}$$

If $c = 0.1$, $B_c = 0.01501\cosh(2.2211\Omega)/\Omega$

For Eqn.(2.30), Moon [9] describes an ad hoc criterion by using the multiwell potential method. The lower bound on the criterion for chaotic motion is

$$B_c = \frac{\alpha}{2\Omega}\,[(1 - \Omega^2 - 3\alpha^2/8\Omega^2)^2 + c^2\Omega^2]^{\frac{1}{2}} \tag{2.37}$$

where $\alpha \approx 0.86$ is a factor obtained from experiments by Moon [6].

Using the same method, the heuristic criterion of Eqn(2.32) can also be obtained, that is

$$B_c = \frac{\sqrt{2}\alpha}{2\Omega}\,[(2 - \Omega^2 - 3\alpha^2/2\Omega^2)^2 + c^2\Omega^2]^{\frac{1}{2}} \tag{2.38}$$

2.3 LYAPUNOV EXPONENT ANALYSIS

2.3.1 GENERAL REMARKS

Lyapunov exponent analysis, which is a numerical tool for diagnosing whether or not a system is chaotic, is presented in this section. An excellent review of Lyapunov exponents

and their use in experiments to diagnose chaotic motion was given by Wolf et al.[2]. The basic concept of this analysis is dependent on the characteristics of chaotic motion, that is, a sensitive dependence on initial conditions. This means that if two trajectories start close to one another in phase plane, they will move exponentially away from each other for small times on the average. Any system containing at least one positive Lyapunov exponent is defined to be chaotic, with the magnitude of the exponent reflecting the time scale on which system dynamics become unpredictable. Thus, if d_o is a measure of the initial distance between the two starting points. At a small but later time the distance is

$$d(t) = d_o e^{\lambda t}$$

The symbol λ is called the Lyapunov exponent. If $\lambda > 0$, the distance between two points is divergent. This is interpretted as chaos. Then the criterion for chaos becomes

$\lambda > 0$ chaotic

$\lambda \leq 0$ regular motion

More details of this concept may be found in the book [9].

2.3.2 NUMERICAL CALCULATION OF LYAPUNOV ANALYSIS

As we already mentioned above, as far as a criterion for chaos is concerned, one need only calculate the largest exponent which tells whether nearby trajectories diverge ($\lambda > 0$) or converge ($\lambda < 0$) on the average. At the present time, calculations of Lyapunov exponents must be done by digital computer.

Considering a set of differential equations of the form

$$\dot{\vec{x}} = \vec{f}(\vec{x}; \vec{c}) \tag{2.39}$$

where $\vec{x}$ is a set of n state variables and $\vec{c}$ is a set of n parameters. The main idea in calculating λ is to be able to determine the length ratio $d(t_k)/d(t_{k-1})$. A direct method is to use the equation to find the variation of trajectories in the neighbourhood

of the reference trajectory $\vec{x}^*(t)$. That is, using an initial condition of some nearby point $\vec{x}^*(t_k) + \zeta$, at each step t_k we solve the variational equations

$$\dot{\vec{\zeta}} = \vec{A} \bullet \vec{\zeta} \tag{2.40}$$

where $\vec{A}$ is the matrix of partial derivatives $\nabla \vec{f}(\vec{x}^*(t_k))$. We note that, in general, the elements of $\vec{A}$ depend on time.

Thus, the numerical scheme goes as follows

(i) Integrate (2.39) to find $\vec{x}^*(t)$. Allow a certain time to pass before calculating d(t) in order to get rid of transients. After all, we are assuming we are on a stable attractor.

(ii) After the transients are judged to be small, begin to integrate (2.40) to find $\zeta(t)$. One can choose $|\zeta(0)| = 1$, but choose the initial direction to be arbitrary.

(iii) Then numerically integrate $\dot{\vec{\zeta}} = \vec{A}(x^*(t)) \bullet \vec{\zeta}$, taking into account the change in $\vec{A}$ through $x^*(t)$.(In practice one can integrate both (2.39) and (2.40) simultaneously).

(iv) After a given time interval $t_{k+1} - t_k = \tau$, take

$d(t_{k+1})/d(t_k)$=$|\vec{\zeta}(\tau; t_k)|/|\vec{\zeta}(0; t_k)|$

(v) To start the next time step, use the direction of $\vec{\zeta}(\tau; t_k)$ for the new initial condition. That is

$\vec{\zeta}(0; t_{k+1})$ =$\vec{\zeta}(\tau; t_k)/|\vec{\zeta}(\tau; t_k)|$

where we have normalized the initial distance to unity, and

$\lambda_k = Ln(d(t_{k+1})/d(t_k))$

Repeat this step many times until λ converges. It is the largest Lyapunov exponent. Check whether or not $\lambda > 0$.

It should be mentioned that one should not rely solely on this technique to certify a region as chaotic. Other tests such as phase plane plots, Poincaré maps,or fractal dimension should also be used to confirm suspected regions of chaotic motion.

Chapter 3

FORMULATION OF NUMERICAL INVESTIGATION

3.1 GENERAL REMARKS

This chapter presents the numerical formulations for different forms of the Duffing's equation using the Lyapunov exponent method.

3.2 DUFFING'S EQUATION WITH CUBIC TERM

Chaotic behaviour of Duffing's equation with only a cubic term was observed first by Ueda [3-4] using numerical simulation. After that, this equation has been studied widely. As an example, it is very useful to consider this equation again using the present method.

The governing equation is

$$\ddot{X} + c\dot{X} + \beta X^3 = B\cos\Omega t \tag{3.1}$$

It can be written as

$$\begin{cases} \dot{X} = Y \\ \dot{Y} = -cY - \beta X^3 + B\cos\Omega t \end{cases} \tag{3.2}$$

As we discussed in Chapter 2, in order to obtain the largest Lyapunov exponent, the variational equations (2.40) should be solved.

The resulting matrix of equation (3.2) is

$$\vec{A} = \begin{bmatrix} 0 & 1 \\ -3\beta X^2 & -c \end{bmatrix}$$

where $\vec{A}$ is dependent on time.

Then, the variational equation (2.40) becomes

$$\begin{cases} \dot{\zeta}_1 = \xi_2 \\ \dot{\zeta}_2 = -c\zeta_2 - 3\beta X^2 \zeta_1 \end{cases} \tag{3.3}$$

Thus, we can solve the variational Eqn. (3.3) and Eqn. (3.2) simultaneously, to get Lyapunov exponents and construct chaotic region. Runge-Kutta numerical integration, which has second order accuracy, is used to solve these equations. The inner matrix in $\vec{A}$ is updated at every Runge-Kutta time step Δt.

The results of numerical investigation for different parameters are presented in Chapter 4, and the comparison between this method and previous work is also given there.

3.3 DUFFING'S EQUATION WITH LINEAR AND CUBIC TERMS

Duffing's equation with positive linear and cubic terms was investigated by E.H. Dowell [11] using numerical simulation, but no chaotic regions were constructed. There are many other papers discussing this equation by using either numerical or experimental methods. We consider this equation again with either positive or negative linear terms to construct chaotic regions.

The governing equation is

$$\ddot{X} + c\dot{X} + kX + \beta X^3 = B\cos\Omega t \tag{3.4}$$

Rewritting in the form

$$\begin{cases} \dot{X} = Y \\ \dot{Y} = -cY - kX - \beta X^3 + B\cos\Omega t \end{cases} \tag{3.5}$$

the resulting matrix $\vec{A}$ of equation (3.5) becomes

$$\vec{A} = \begin{bmatrix} 0 & 1 \\ -k - 3\beta X^2 & -c \end{bmatrix}$$

So the variational equation (2.40) becomes

$$\begin{cases} \dot{\zeta}_1 = \zeta_2 \\ \dot{\zeta}_2 = -c\zeta_2 - k\zeta_1 - 3\beta X^2 \zeta_1 \end{cases} \tag{3.6}$$

As we mentioned earlier, the numerical procedure is to solve equations (3.5) and (3.6) simultaneously. The numerical investigation is presented in detail in Chapter 4.

3.4 DUFFING'S EQUATION WITH QUADRATIC TERM (I)

The governing equation of this kind of Duffing's equation is

$$\ddot{X} + c\dot{X} + kX + \alpha X|X| + \beta X^3 = B\cos\Omega t \tag{3.7}$$

Rewritting in the form

$$\begin{cases} \dot{X} = Y \\ \dot{Y} = -cY - kX - \alpha X|X| - \beta X^3 + B\cos\Omega t \end{cases} \tag{3.8}$$

the matrix $\vec{A}$ of this problem is

$$\vec{A} = \begin{bmatrix} 0 & 1 \\ -k - 2\alpha|X| - 3\beta X^2 & -c \end{bmatrix}$$

Thus, the variational equation (2.40) becomes

$$\begin{cases} \dot{\zeta}_1 = \zeta_2 \\ \dot{\zeta}_2 = -c\zeta_2 - k\zeta_1 - 2\alpha|X|\zeta_1 - 3\beta X^2\zeta_1 \end{cases} \tag{3.9}$$

3.5 DUFFING'S EQUATION WITH QUADRATIC TERM (II)

Here the governing equation is

$$\ddot{X} + c\dot{X} + kX + \alpha X^2 + \beta X^3 = B\cos\Omega t \tag{3.10}$$

It can be rewritten in the form

$$\begin{cases} \dot{X} = Y \\ \dot{Y} = -cY - kX - \alpha X^2 - \beta X^3 + B\cos\Omega t \end{cases} \tag{3.11}$$

Here, the matrix $\vec{A}$ is

$$\vec{A} = \begin{bmatrix} 0 & 1 \\ -k - 2\alpha X - 3\beta X^2 & -c \end{bmatrix}$$

Then the variational equation (2.22) becomes

$$\begin{cases} \dot{\zeta}_1 = \zeta_2 \\ \dot{\zeta}_2 = -c\zeta_2 - k\zeta_1 - 2\alpha X\zeta_1 - 3\beta X^2\zeta_1 \end{cases} \tag{3.12}$$

It is clear from Chapter 2 that the Lyapunov exponent λ is a statistical property of the motion. That is, one must average the changes in lengths over a long time in order to get a reliable value. Also, one has to be careful in choosing the Runge-Kutta step size Δt as well as the Lyapunov exponent step size τ.

The details of numerical investigation are presented in the next Chapter.

Chapter 4

NUMERICAL RESULTS AND PLOTS

4.1 GENERAL REMARKS

In this Chapter, numerical results are obtained for five different kinds of Duffing's equations with various parameters or coefficients by using Lyapunov exponent analysis. Chaotic regions constructed in parametric space are shown in Section 4.2. Simulation and/or calculation errors are unavoidable in the computer solutions for the different equations. Therefore, in Section 4.3 phase plane and Poincaré plane plots are presented to check suspected points.

Analytical and heuristic criterion curves of chaos are also plotted in Section 4.2 to compare with numerical results.

4.2 CONSTRUCTION OF CHAOTIC REGION IN PARAMETRIC SPACE

4.2.1 PLOT IN DAMPING COEFFICIENT AND FORCING AMPLITUDE SPACE

The form of Duffing's equation investigated here is

$$\ddot{X} + c\dot{X} + kX + \alpha X|X| + \beta X^3 = B\cos\Omega t \tag{4.1}$$

The formulation and numerical procedure is presented in Chapter 2 and 3, the parameters which are chosen to investigate chaotic motion are listed in tables, while chaotic regions of these parameters are plotted in figures.

Table 4.1: Duffing's equation including only cubic term

Parameter		*Value*
Linear coeff.	k	0.0
Quadratic coeff.	α	0.0
Cubic coeff.	β	1.0
Force frequency	Ω	1.0
Damping coeff.	c	0.0 - 0.4
Force amplitude	B	0.0 - 15.0

DUFFING'S EQUATION WITH CUBIC TERM

In order to compare to previous results, we consider Duffing's equation including only the cubic term with $\beta = 1.0$ again, as shown in Table 4.1.

For the plot in Figure (4.1), the time step for numerical integration is $\Delta t = 0.01$ and the number of time steps to integrate $\eta(t)$ is chosen to be 10, or $\tau = 0.1$, and $\Delta c = 0.05$, $\Delta B = 0.5$.

From the plot, chaotic motion is indicated between B=5.5 - 13.0 and c=0.05 - 0.4, and there is a gap between B=8.0 - 10.0. The points where $*$ and $\bigcirc$ overlap means unique chaos, while others mean periodic and chaotic motion co-existing, and the symbols $*$ and $\bigcirc$ represent chaotic motion from two different initial conditions respectively. The plot agrees well with Ueda's results shown in Figure (4.2). See [3] or [29]. A comparison of Lyapunov exponents for different parameters in the Duffing's equation is shown in Table (4.2). It is shown that good agreement is obtained.

DUFFING'S EQUATION WITH LINEAR AND CUBIC TERMS

The governing equation is Eqn.(4.1) with $\alpha = 0$, and the parameters investigated are listed in Tables 4.3 to 4.5.

The time step for numerical investigation is $\Delta t = 0.01$, and $\tau = 0.1$ $\Delta B = 0.5$

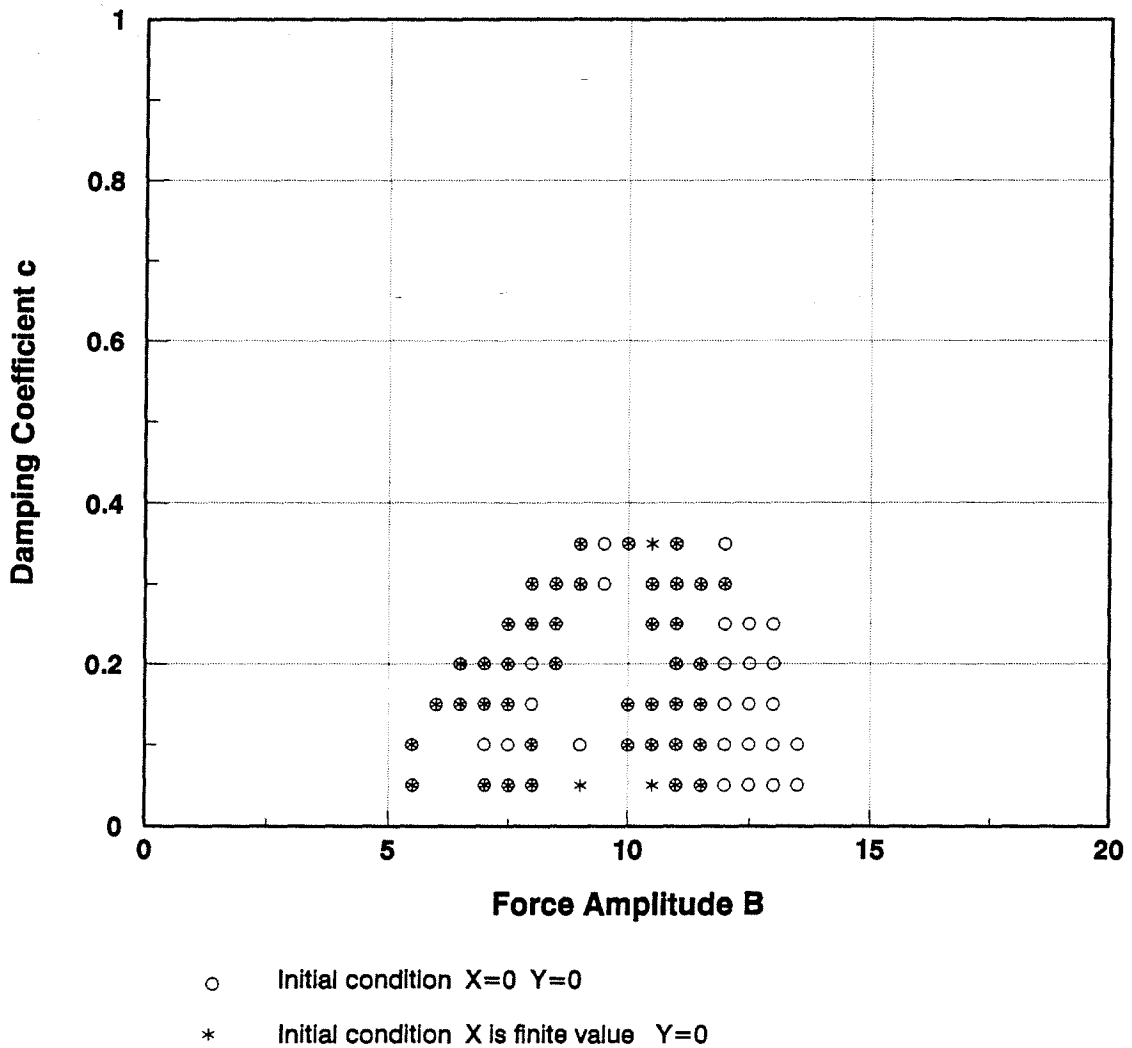

Figure 4.1: Duffing's equation including only cubic term in B–c plane ($k = 0.0$ $\alpha = 0.0$ $\beta = 1.0$ $\Omega = 1.0$)

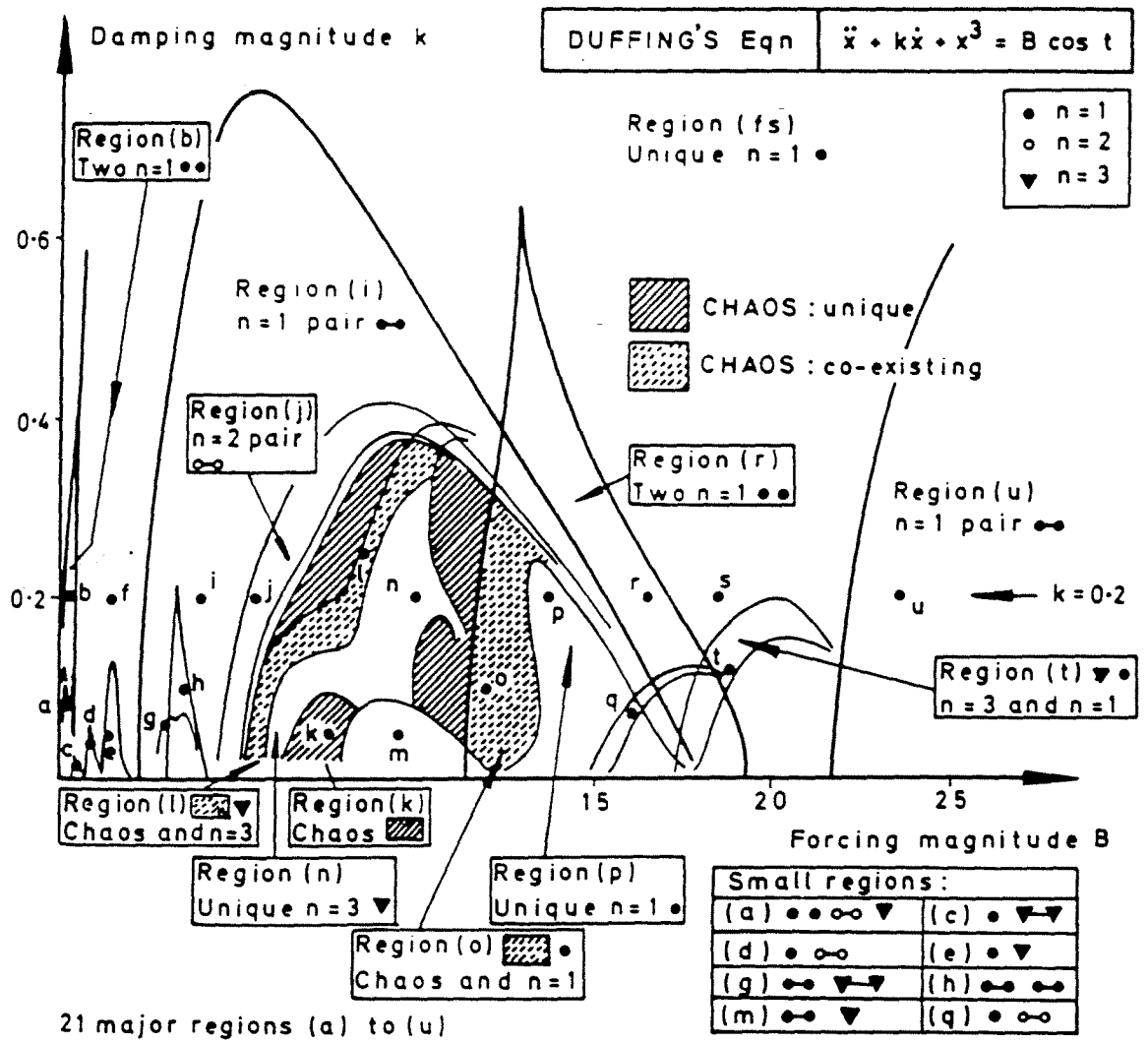

Figure 4.2: Regimes of the various long - term behaviours of Duffing's equation with cubic term, as a function of damping and forcing.

Table 4.2: Comparison of calculated Lyapunov exponent for Duffing's equation including only cubic term $\ddot{X} + 0.1\dot{X} + X^3 = B\cos t$

c	B	λ_1 [4]	λ_1 [9]	λ_1 (this thesis)
0.1	10	0.094	0.102	0.108
0.1	11	0.114	0.114	0.114
0.1	12	0.143	0.149	0.154
0.1	13	0.167	0.182	0.191

Table 4.3: Duffing's equation including positive linear and cubic terms

Parameter		*Value*
Linear coeff.	k	0.25
Quadratic coeff.	α	0.0
Cubic coeff.	β	1.0
Force frequency	Ω	1.0
Damping coeff.	c	0.0 - 0.4
Force amplitude	B	0.0 - 15.0

Table 4.4: Duffing's equation including positive linear and cubic terms

Parameter		*Value*
Linear coeff.	k	0.5
Quadratic coeff.	α	0.0
Cubic coeff.	β	1.0
Force frequency	Ω	1.0
Damping coeff.	c	0.0 - 0.4
Force amplitude	B	0.0 - 15.0

Table 4.5: Duffing's equation including positive linear and cubic terms

Parameter		*Value*
Linear coeff.	k	0.75
Quadratic coeff.	α	0.0
Cubic coeff.	β	1.0
Force frequency	Ω	1.0
Damping coeff.	c	0.0 - 0.4
Force amplitude	B	0.0 - 15.0

$\Delta c = 0.05$.

Chaotic regions of different linear coefficients are shown in Figure (4.3) - Figure (4.6). Comparing Figure (4.3) to Figure (4.1), it is seen that the chaotic region becomes smaller as we increase the linear term from zero.

From Figure (4.3) - Figure (4.6), it is obvious that the chaotic region decreases as k increases, which means the linear term kills the chaos while cubic term leads to chaos.

DUFFING'S EQUATION WITH QUADRATIC AND CUBIC TERMS

The governing equation is Eqn.(4.1) with $k = 0$.

As we see in Figure (4.7) - Figure (4.10) and compared to Figure (4.1), it is very interesting. As α increases, the chaotic region decreases as well, but it is much slower

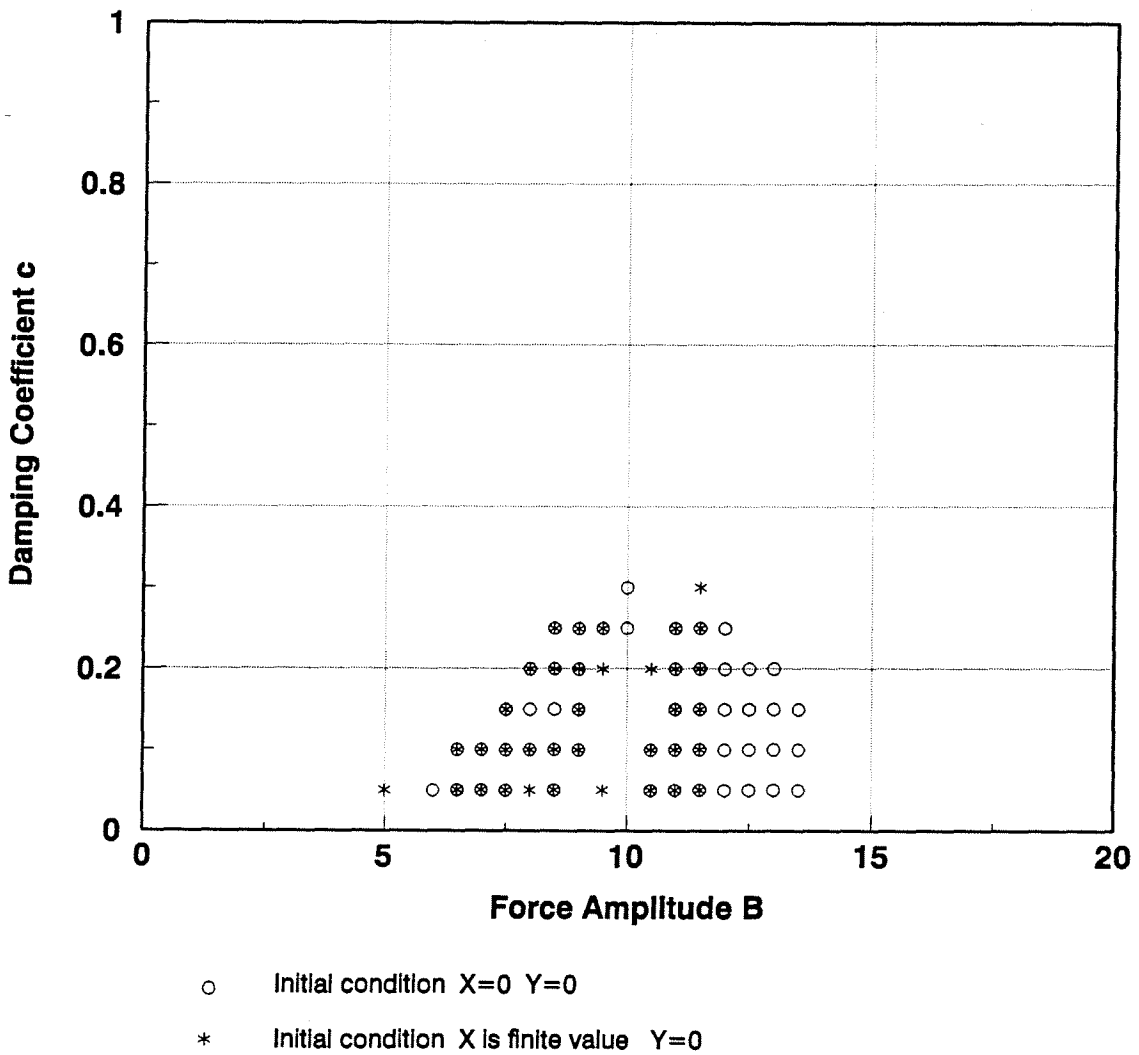

Figure 4.3: Duffing's equation including positive linear and cubic terms in B–c plane ($k = 0.25$ $\alpha = 0.0$ $\beta = 1.0$ $\Omega = 1.0$)

Table 4.6: Duffing's equation including positive linear and cubic terms

Parameter		*Value*
Linear coeff.	k	1.0
Quadratic coeff.	α	0.0
Cubic coeff.	β	1.0
Force frequency	Ω	1.0
Damping coeff.	c	0.0 – 0.4
Force amplitude	B	0.0 – 15.0

Table 4.7: Duffing's equation including quadratic and cubic terms

Parameter		*Value*
Linear coeff.	k	0.0
Quadratic coeff.	α	0.5
Cubic coeff.	β	1.0
Force frequency	Ω	1.0
Damping coeff.	c	0.0 – 0.4
Force amplitude	B	0.0 – 15.0

Table 4.8: Duffing's equation including quadratic and cubic terms

Parameter		*Value*
Linear coeff.	k	0.0
Quadratic coeff.	α	1.0
Cubic coeff.	β	1.0
Force frequency	Ω	1.0
Damping coeff.	c	0.0 – 0.4
Force amplitude	B	0.0 – 15.0

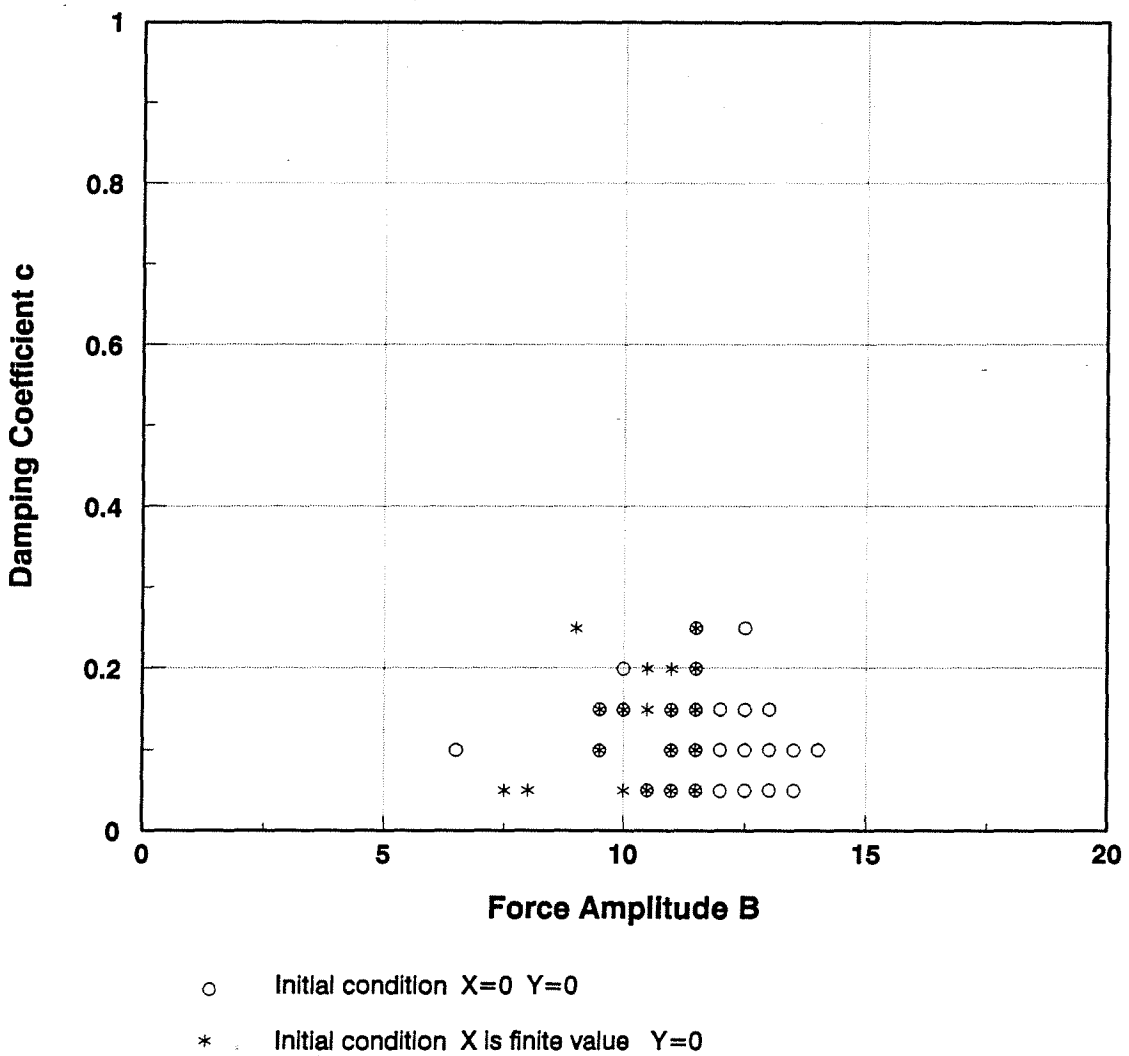

Figure 4.4: Duffing's equation including positive linear and cubic terms in B–c plane ($k = 0.5$ $\alpha = 0.0$ $\beta = 1.0$ $\Omega = 1.0$)

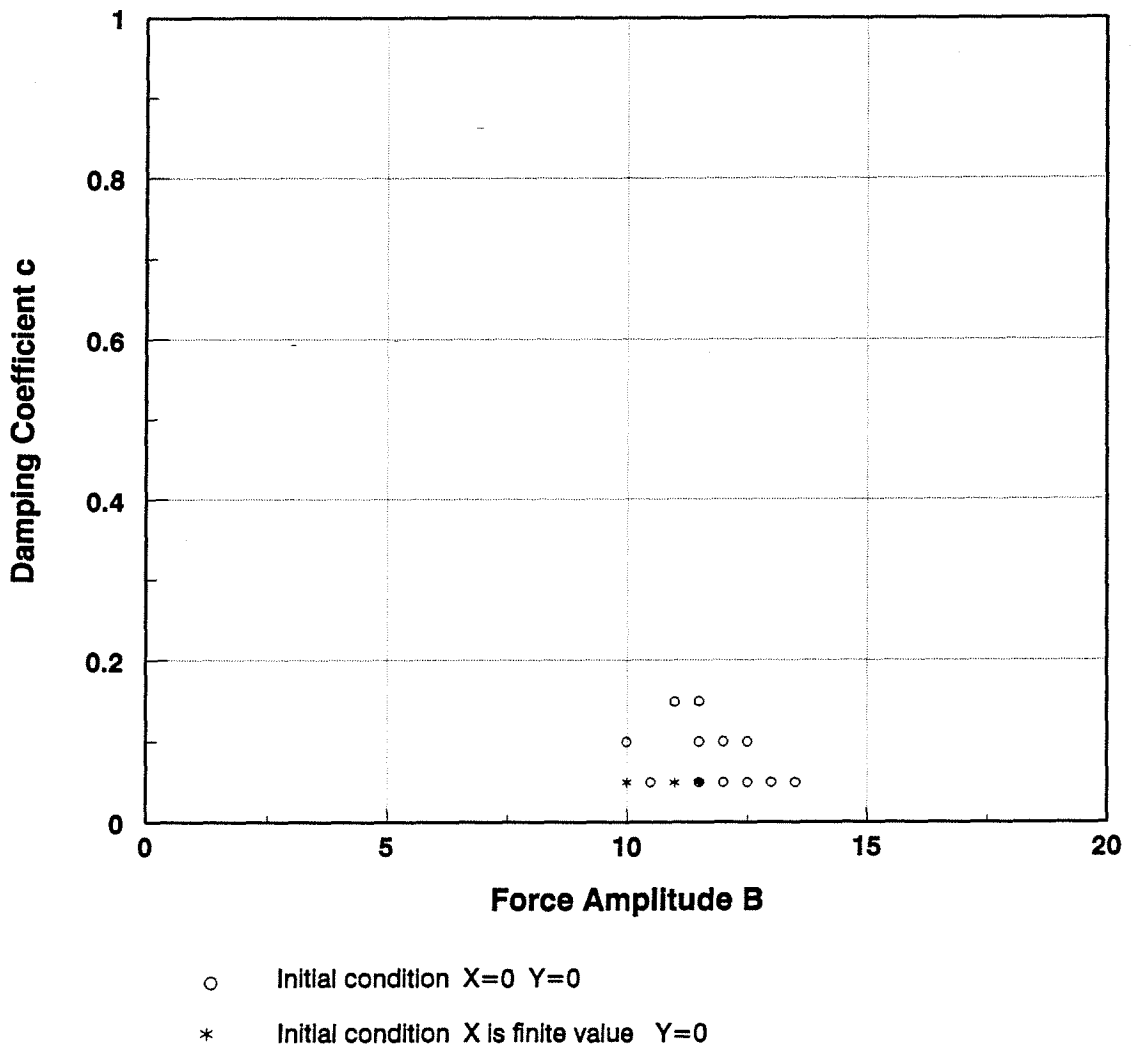

Figure 4.5: Duffing's equation including positive linear and cubic terms in B–c plane ($k = 0.75$ $\alpha = 0.0$ $\beta = 1.0$ $\Omega = 1.0$)

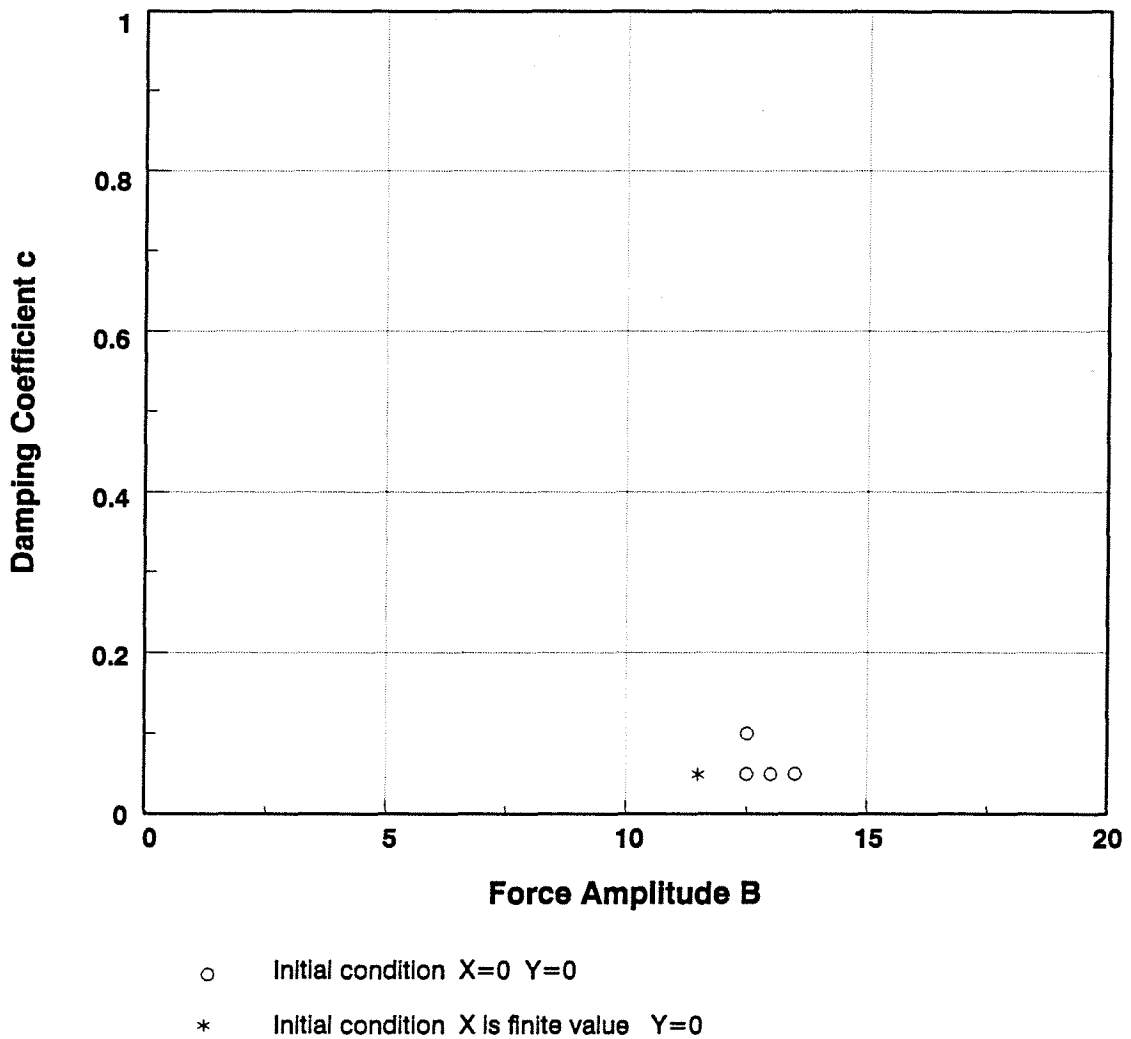

Figure 4.6: Duffing's equation including positive linear and cubic terms in B–c plane ($k = 1.0$ $\alpha = 0.0$ $\beta = 1.0$ $\Omega = 1.0$)

Table 4.9: Duffing's equation including quadratic and cubic terms

Parameter		*Value*
Linear coeff.	k	0.0
Quadratic coeff.	α	1.5
Cubic coeff.	β	1.0
Force frequency	Ω	1.0
Damping coeff.	c	0.0 - 0.4
Force amplitude	B	0.0 - 15.0

Table 4.10: Duffing's equation including quadratic and cubic terms

Parameter		*Value*
Linear coeff.	k	0.0
Quadratic coeff.	α	2.0
Cubic coeff.	β	1.0
Force frequency	Ω	1.0
Damping coeff.	c	0.0 - 0.4
Force amplitude	B	0.0 - 15.0

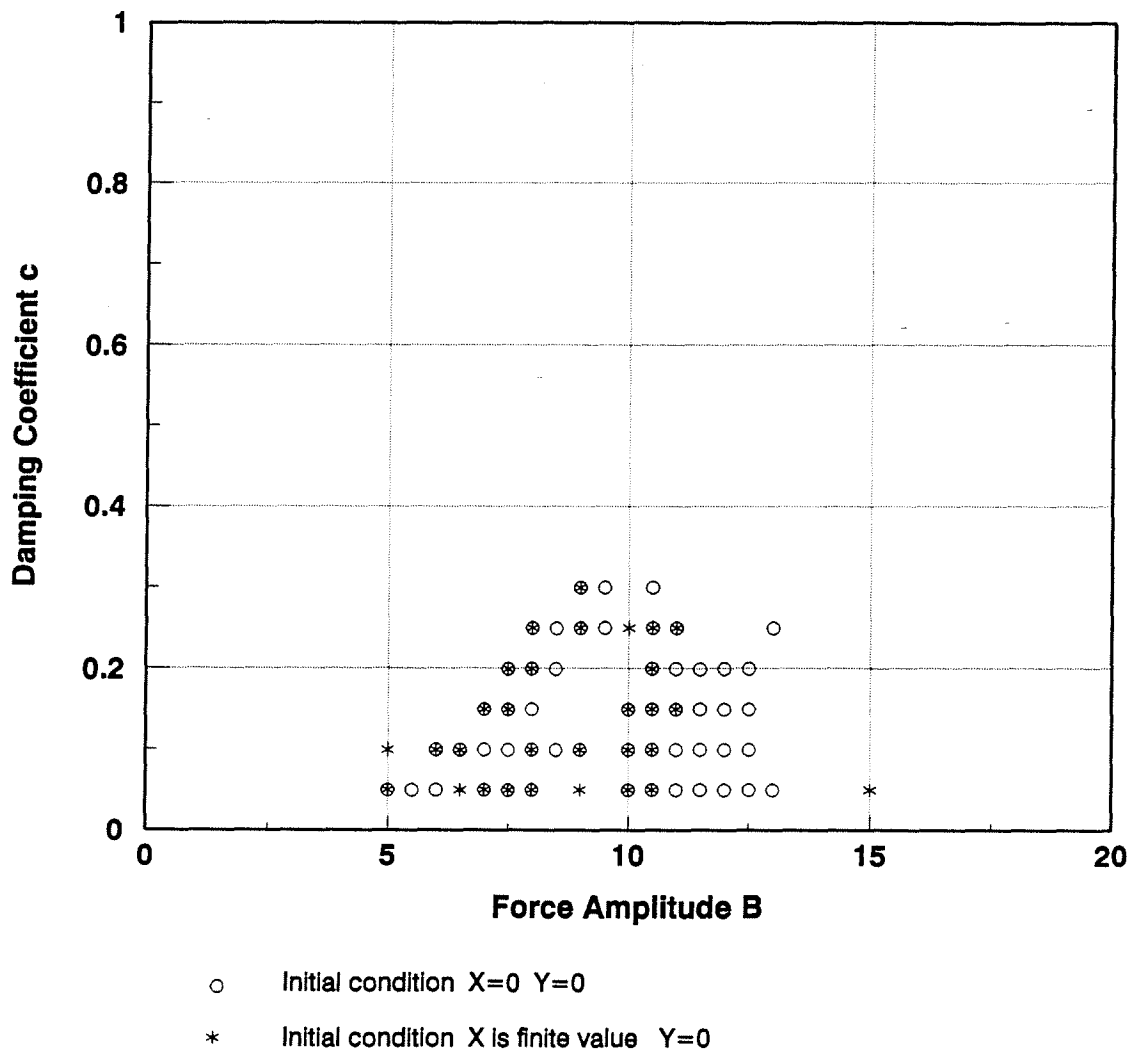

Figure 4.7: Duffing's equation including quadratic and cubic terms in B–c plane ($k = 0.0$ $\alpha = 0.5$ $\beta = 1.0$ $\Omega = 1.0$)

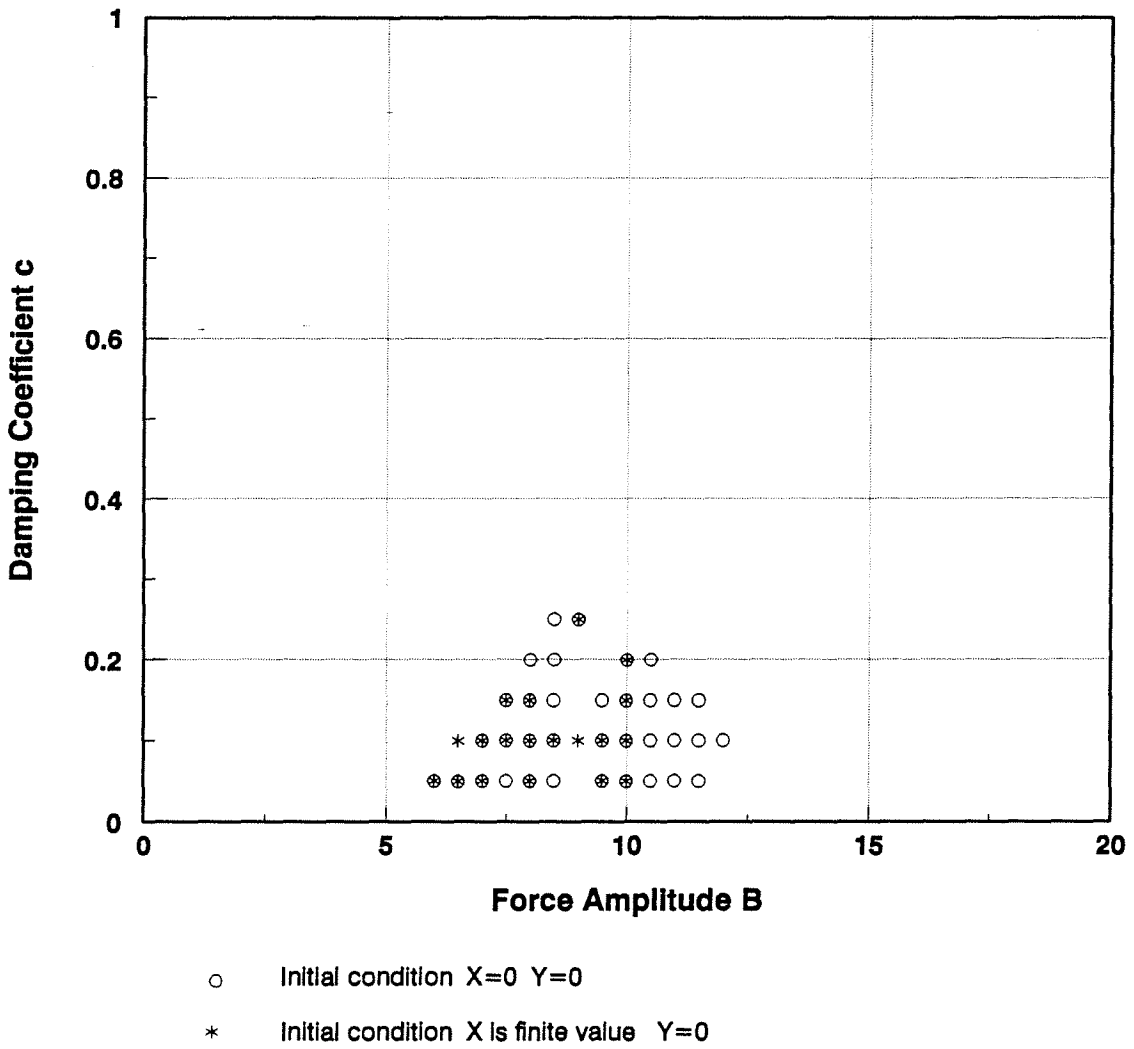

Figure 4.8: Duffing's equation including quadratic and cubic terms in B–c plane ($k = 0.0$ $\alpha = 1.0$ $\beta = 1.0$ $\Omega = 1.0$)

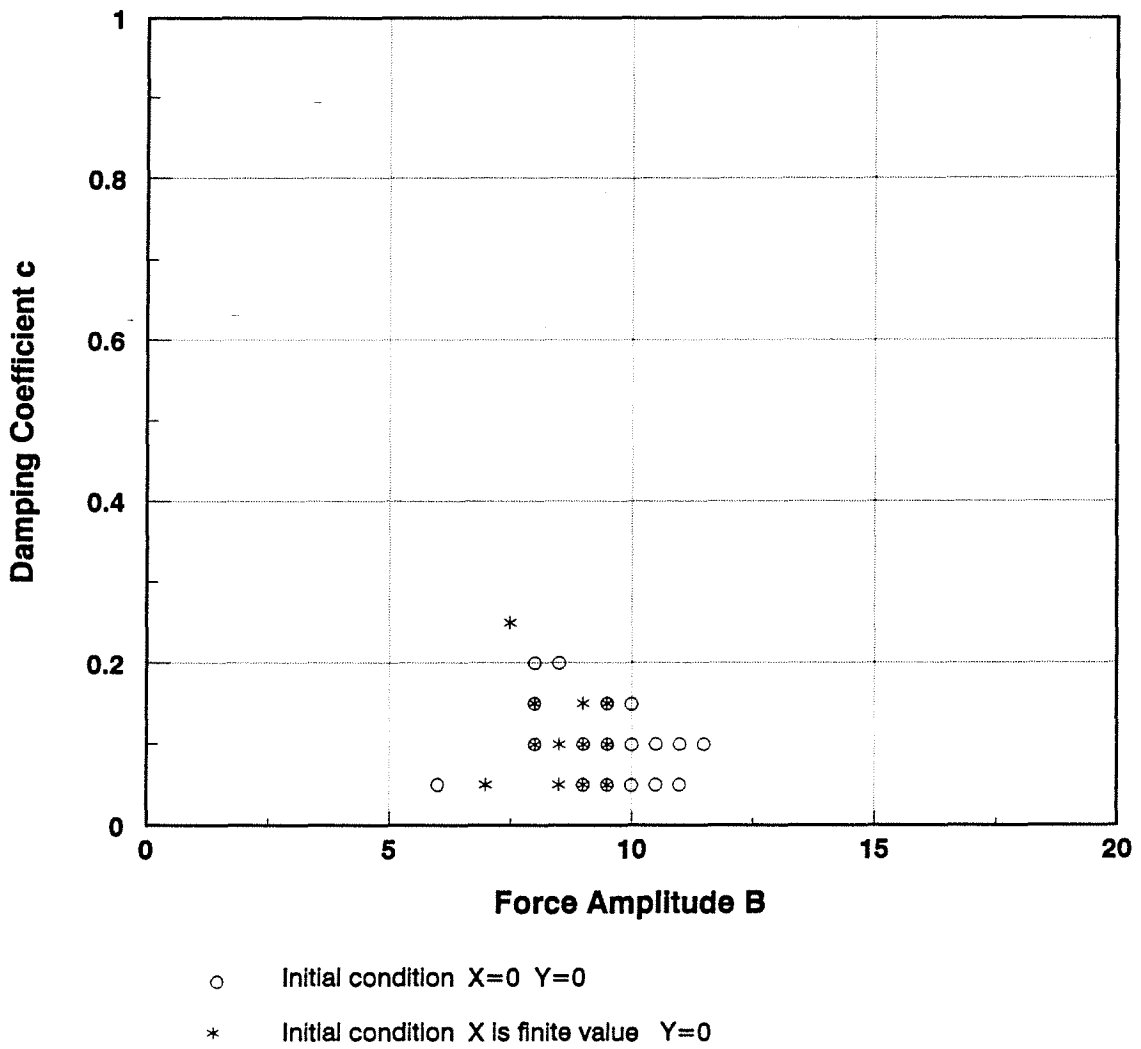

Figure 4.9: Duffing's equation including quadratic and cubic terms in B–c plane ($k = 0.0$ $\alpha = 1.5$ $\beta = 1.0$ $\Omega = 1.0$)

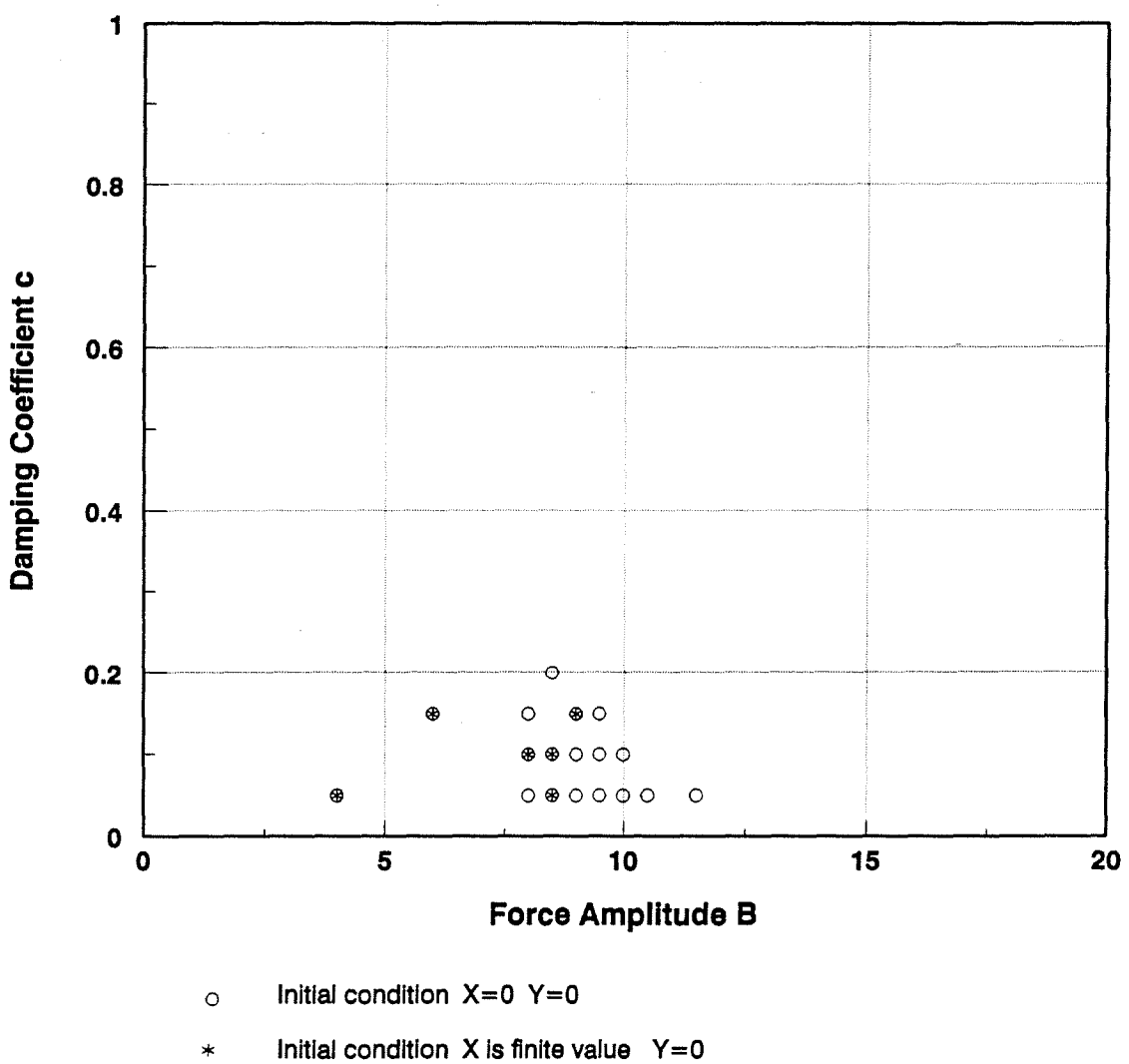

Figure 4.10: Duffing's equation including quadratic and cubic terms in B–c plane ($k = 0.0$ $\alpha = 2.0$ $\beta = 1.0$ $\Omega = 1.0$)

Table 4.11: Duffing's equation including only cubic term

Parameter		*Value*
Linear coeff.	k	0.0
Quadratic coeff.	α	0.0
Cubic coeff.	β	1.0
Damping coeff.	c	0.1
Force frequency	Ω	0.0 - 3.0
Force amplitude	B	0.0 - 30.0

than with the linear term. So the quadratic term also kills chaos but at a slower rate than the linear term.

4.2.2 PLOT IN FORCING AMPLITUDE AND FREQUENCY SPACE

In this section, different kinds of Duffing's equations are investigated using Lyapunov exponent analysis and chaotic regions are constructed in forcing amplitude and frequency plane. For some specific cases, the analytical and heuristic criteria of chaos are also plotted.

DUFFING'S EQUATION WITH CUBIC TERM

The governing equation is Eqn.(4.1) with $k = 0$ and $\alpha = 0$. The parameters of investigation are listed in Table (4.11)

Here, the time step for numerical integration is changed with frequency, which is $\Delta t = 2\pi/(\Omega C)$, where C is the cycles of calculation in one period. This means that the cycles of calculation in every period T are kept constant as the frequency is changed. Using this Δt, is much more efficient in numerical simulation. The number of time steps to integrate $\eta(t)$ is still chosen to be 10, or $\tau = 0.1$, and $\Delta B = 1.0$, $\Delta\Omega = 0.1$.

The results are shown in Figure (4.11). It is clear from Figure (4.11) that for small

Table 4.12: Duffing's equation including positive linear and cubic terms

Parameter		*Value*
Linear coeff.	k	0.5
Quadratic coeff.	α	0.0
Cubic coeff.	β	1.0
Damping coeff.	c	0.1
Force frequency	Ω	0.0 – 3.0
Force amplitude	B	0.0 – 30.0

Table 4.13: Duffing's equation including positive linear and cubic terms

Parameter		*Value*
Linear coeff.	k	1.0
Quadratic coeff.	α	0.0
Cubic coeff.	β	1.0
Damping coeff.	c	0.1
Force frequency	Ω	0.0 – 3.0
Force amplitude	B	0.0 – 30.0

forcing amplitude, chaotic motion exists only at small forcing frequency, and as B increases, the chaotic region expands with larger Ω, but the change is slower.

DUFFING'S EQUATION WITH LINEAR AND CUBIC TERMS

In this section, Duffing's equation with both positive linear and cubic terms and negative linear and cubic terms are investigated, which are listed in Tables (4.12) to (4.17). The analytical and heuristic criterions are plotted for negative linear and cubic term, but there are no analytical or heuristic criterions for positive linear and cubic terms.

The Δt, ΔB, Δc, and τ are chosen as the same as in the last section. Chaotic regions are constructed in Figure (4.12) – Figure (4.17).

It is shown, for the positive linear term, chaotic motion is obtained at large forcing

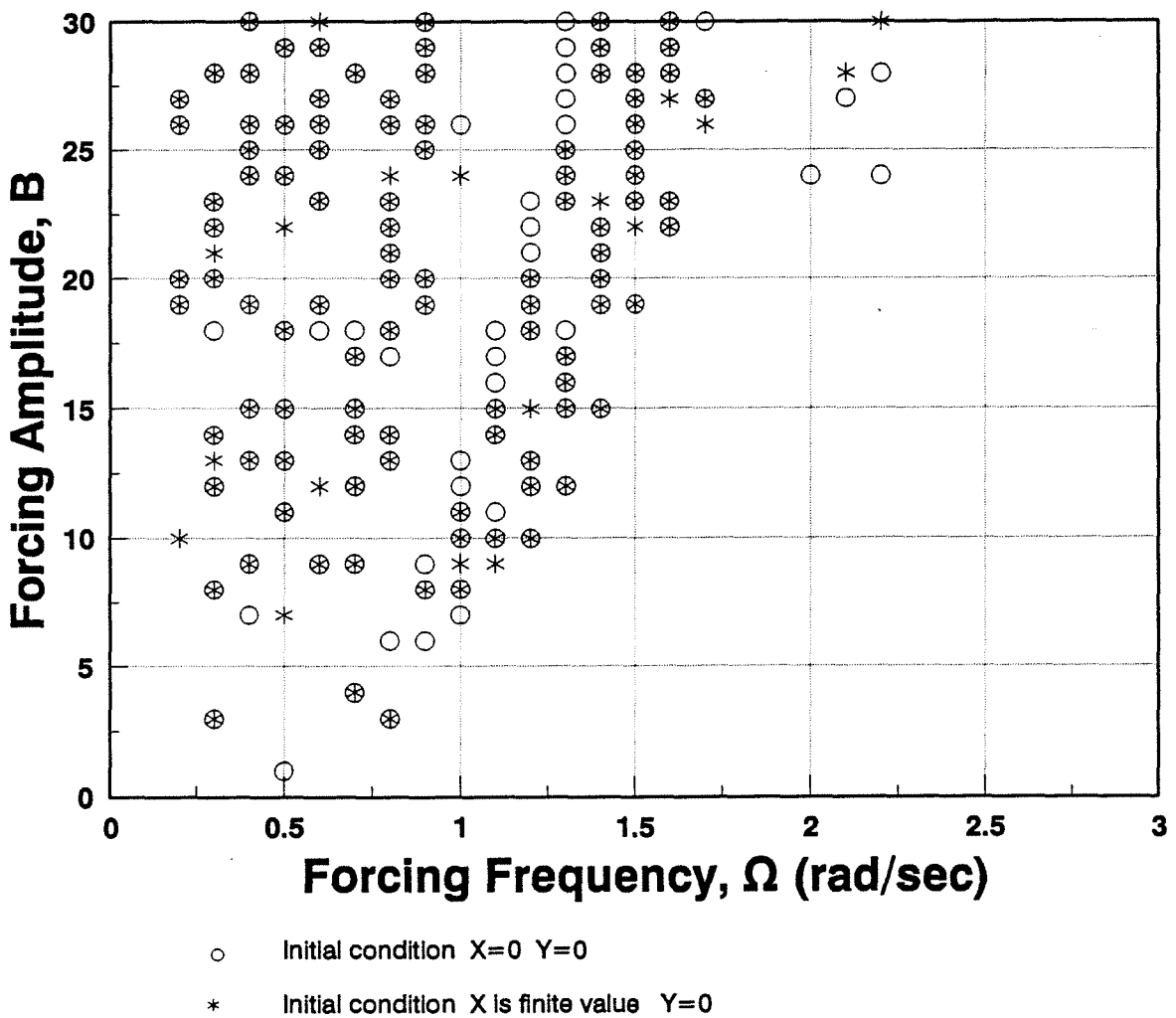

Figure 4.11: Duffing's equation including only cubic term in Ω–B plane ($k = 0.0$ $\alpha = 0.0$ $\beta = 1.0$ $c = 0.1$)

Table 4.14: Duffing's equation including negative linear and cubic terms

Parameter		*Value*
Linear coeff.	k	-0.5
Quadratic coeff.	α	0.0
Cubic coeff.	β	0.5
Damping coeff.	c	0.05
Force frequency	Ω	0.0 – 3.0
Force amplitude	B	0.0 – 1.5

Table 4.15: Duffing's equation including negative linear and cubic terms

Parameter		*Value*
Linear coeff.	k	-1.0
Quadratic coeff.	α	0.0
Cubic coeff.	β	1.0
Damping coeff.	c	0.05
Force frequency	Ω	0.0 – 3.0
Force amplitude	B	0.0 – 1.5

Table 4.16: Duffing's equation including negative linear and cubic terms

Parameter		*Value*
Linear coeff.	k	-0.5
Quadratic coeff.	α	0.0
Cubic coeff.	β	0.5
Damping coeff.	c	0.1
Force frequency	Ω	0.0 – 3.0
Force amplitude	B	0.0 – 1.5

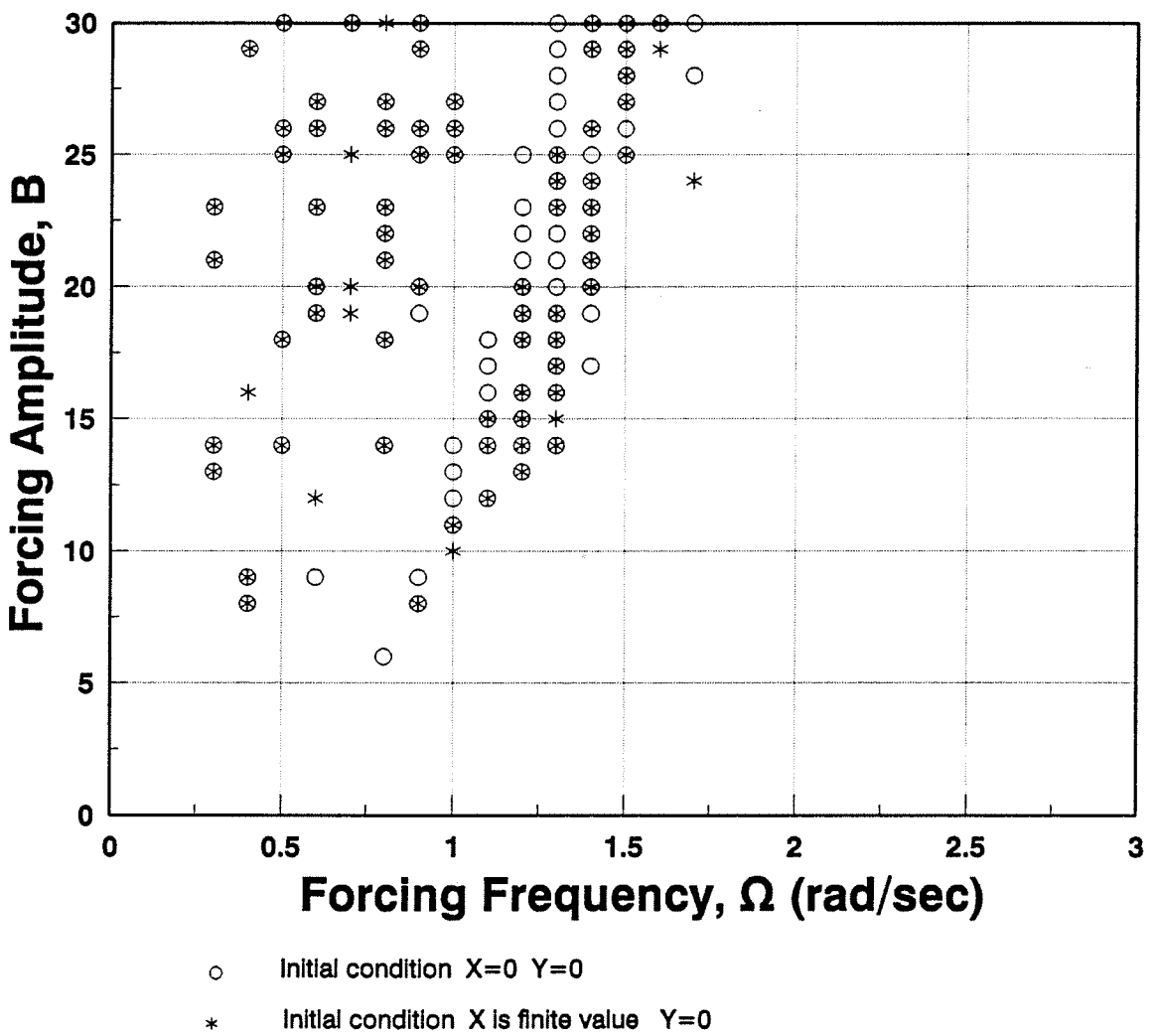

Figure 4.12: Duffing's equation including positive linear and cubic terms in Ω–B plane ($k = 0.5$ $\alpha = 0.0$ $\beta = 1.0$ $c = 0.1$)

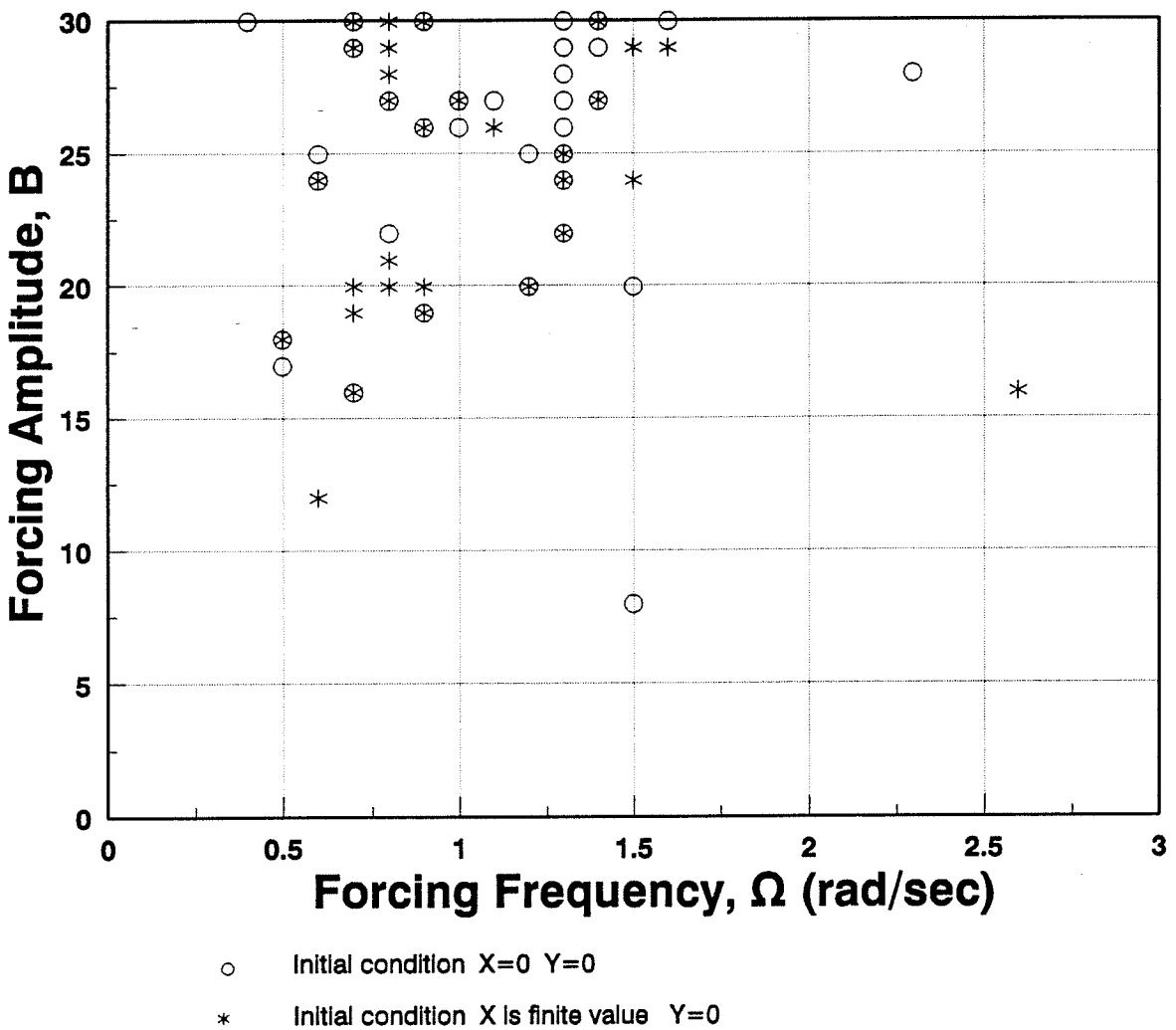

Figure 4.13: Duffing's equation including positive linear and cubic terms in Ω–B plane ($k = 1.0$ $\alpha = 0.0$ $\beta = 1.0$ $c = 0.1$)

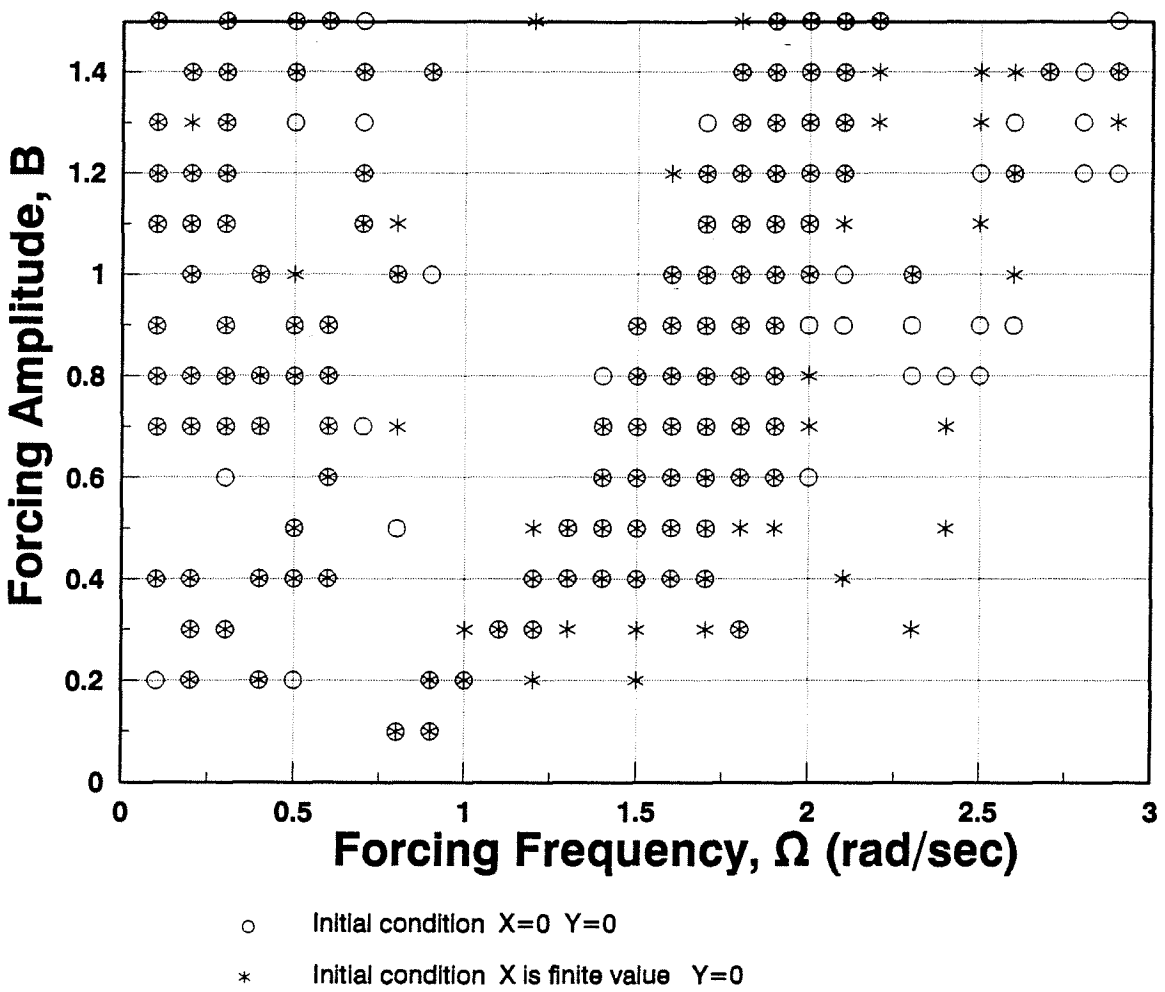

Figure 4.14: Duffing's equation including negative linear and cubic terms in Ω–B plane ($k = -0.5$ $\alpha = 0.0$ $\beta = 0.5$ $c = 0.05$)

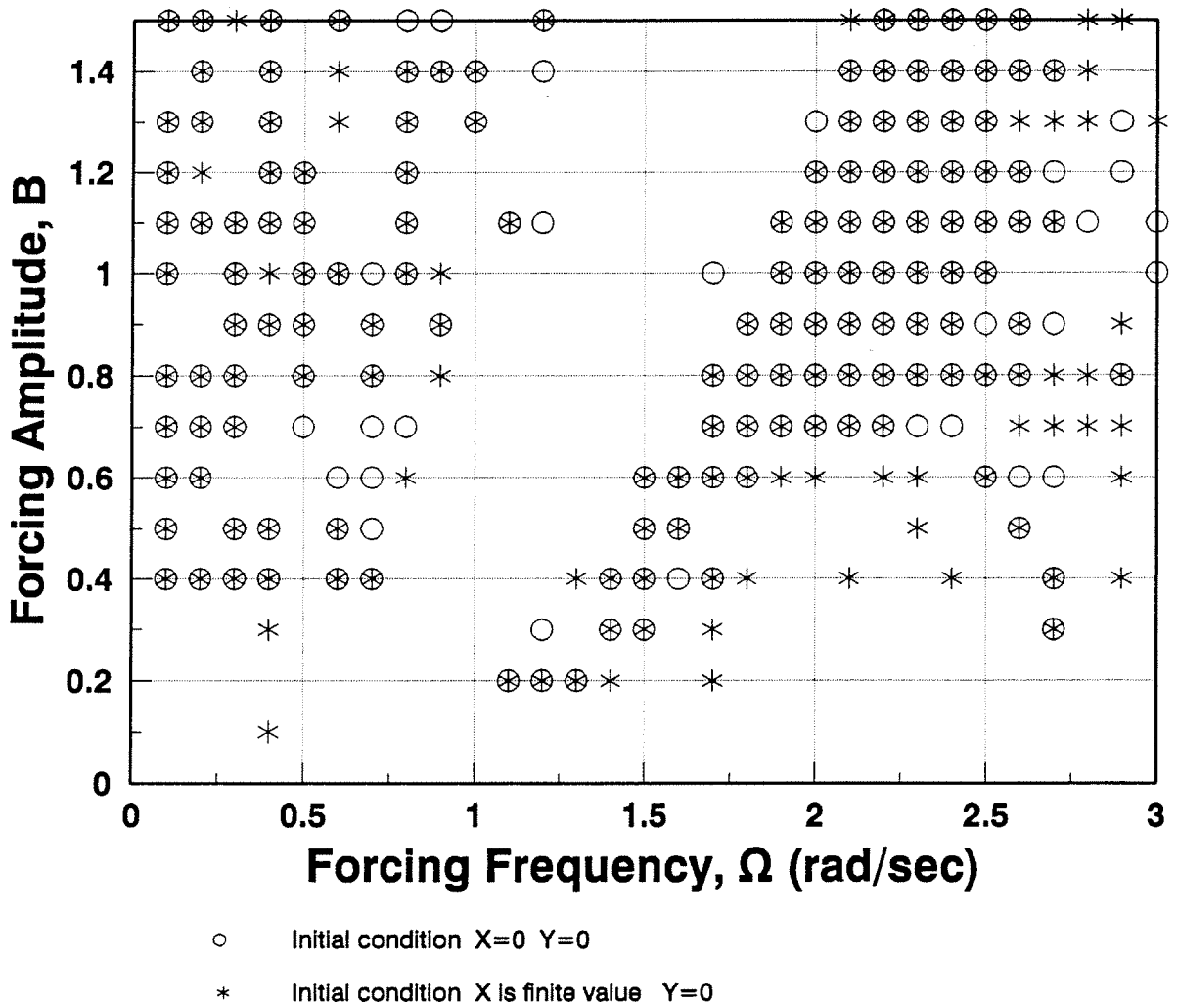

Figure 4.15: Duffing's equation including negative linear and cubic terms in Ω–B plane ($k = -1.0$ $\alpha = 0.0$ $\beta = 1.0$ $c = 0.05$)

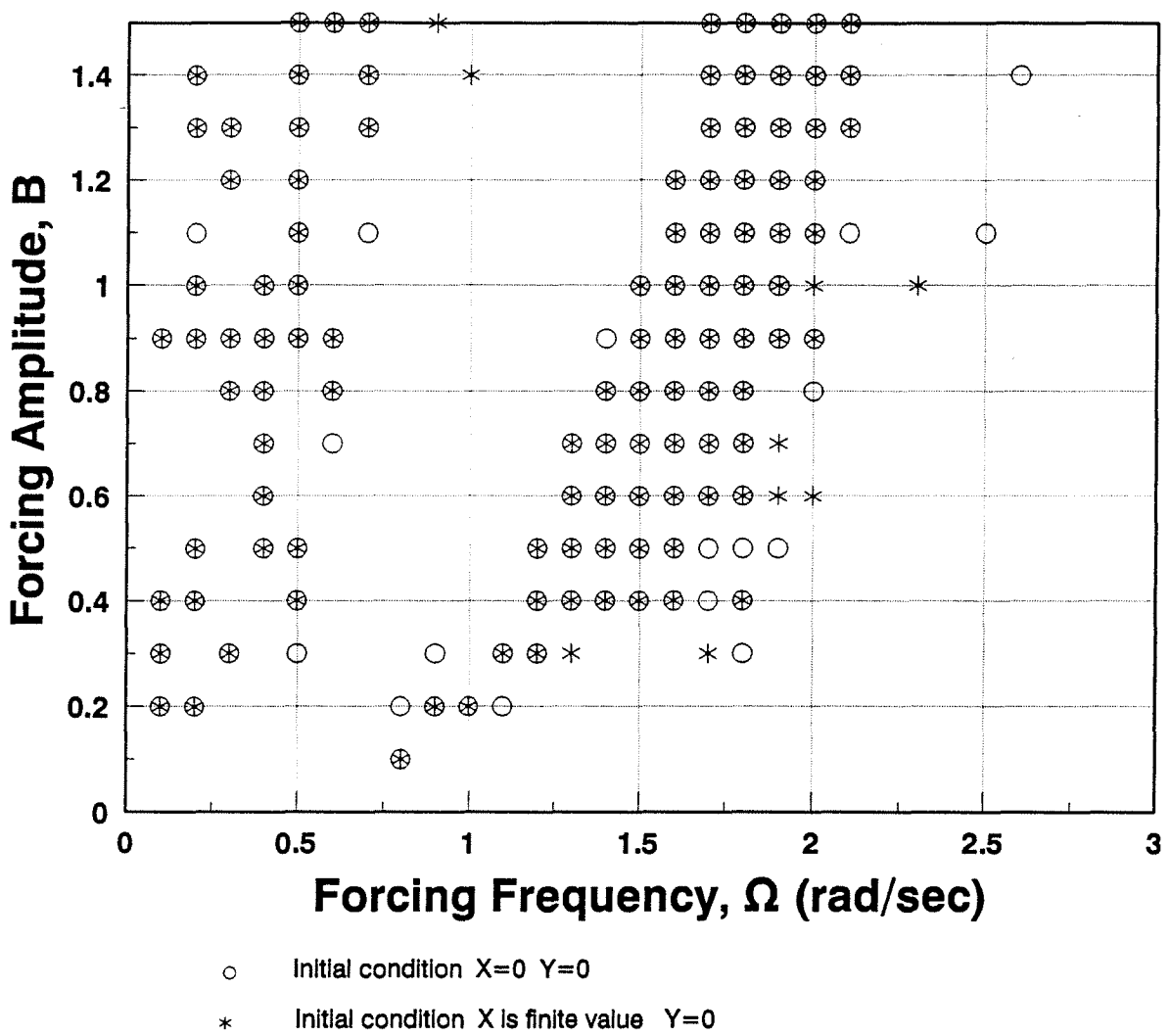

Figure 4.16: Duffing's equation including negative linear and cubic terms in Ω–B plane ($k = -0.5$ $\alpha = 0.0$ $\beta = 0.5$ $c = 0.1$)

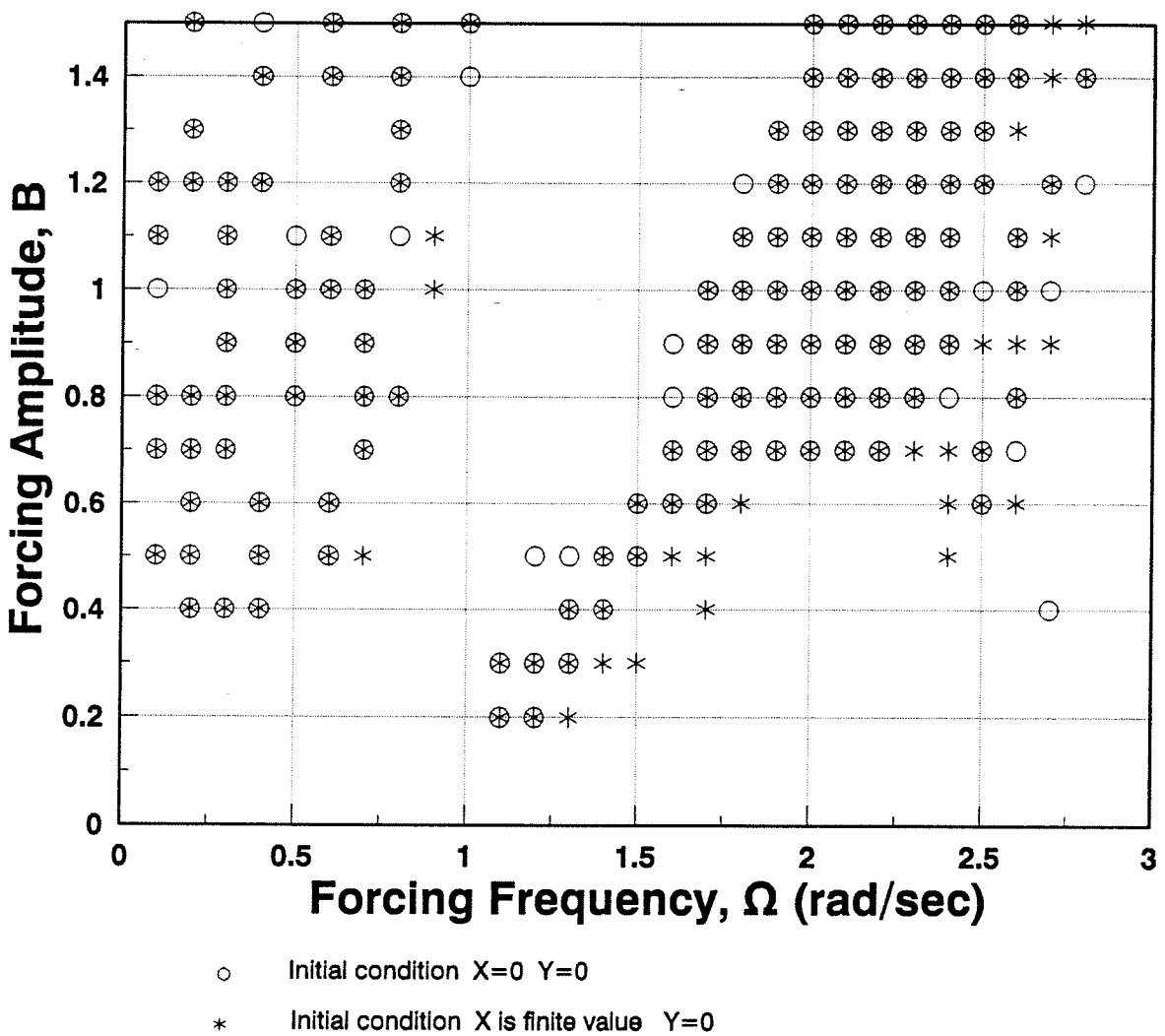

Figure 4.17: Duffing's equation including negative linear and cubic terms in Ω–B plane ($k = -1.0$ $\alpha = 0.0$ $\beta = 1.0$ $c = 0.1$)

Table 4.17: Duffing's equation including negative linear and cubic terms

Parameter		*Value*
Linear coeff.	k	-1.0
Quadratic coeff.	α	0.0
Cubic coeff.	β	1.0
Damping coeff.	c	0.1
Force frequency	Ω	0.0 - 3.0
Force amplitude	B	0.0 - 1.5

amplitude B and $\Omega < 2.0$, while chaotic motion is obtained at very small B and Ω from 0 to 3.0 for the negative linear term. For both cases, if $|k|$ increases, the forcing amplitude B that leads to chaos becomes larger.

Comparing Figure (4.14) and Figure (4.15) to Figure (4.16) and Figure (4.17), it is seen that for different damping coefficients 0.05 and 0.1, the whole chaotic regions look similar, but for small damping $c = 0.05$, there are more chaotic motions occurring near $\Omega = 3.0$.

DUFFING'S EQUATION INCLUDING QUADRATIC TERM (I)

Here, the governing equation is Eqn.(4.1). First, we consider Duffing's equation with quadratic and cubic terms only, i.e. $k = 0$. The parameters investigated are listed in Table (4.18) and Table (4.19).

From Figure (4.18) and Figure (4.19), it is shown that the quadratic term eliminates chaotic motions just as in Section 4.2.1. Chaotic motions only exist for $\Omega < 2.0$.

Now, Duffing's equation with all linear, quadratic and cubic terms is investigated. The cases of investigation are listed in Table (4.20) - Table (4.25), which includes two cases with negative linear terms.

From the numerical studies, chaotic motion exists for these cases, but will vanish

Table 4.18: Duffing's equation including quadratic and cubic terms (I)

Parameter		*Value*
Linear coeff.	k	0.0
Quadratic coeff.	α	0.5
Cubic coeff.	β	1.0
Damping coeff.	c	0.1
Force frequency	Ω	0.0 - 3.0
Force amplitude	B	0.0 - 30.0

Table 4.19: .Duffing's equation including quadratic and cubic terms (I)

Parameter		*Value*
Linear coeff.	k	0.0
Quadratic coeff.	α	1.0
Cubic coeff.	β	1.0
Damping coeff.	c	0.1
Force frequency	Ω	0.0 - 3.0
Force amplitude	B	0.0 - 30.0

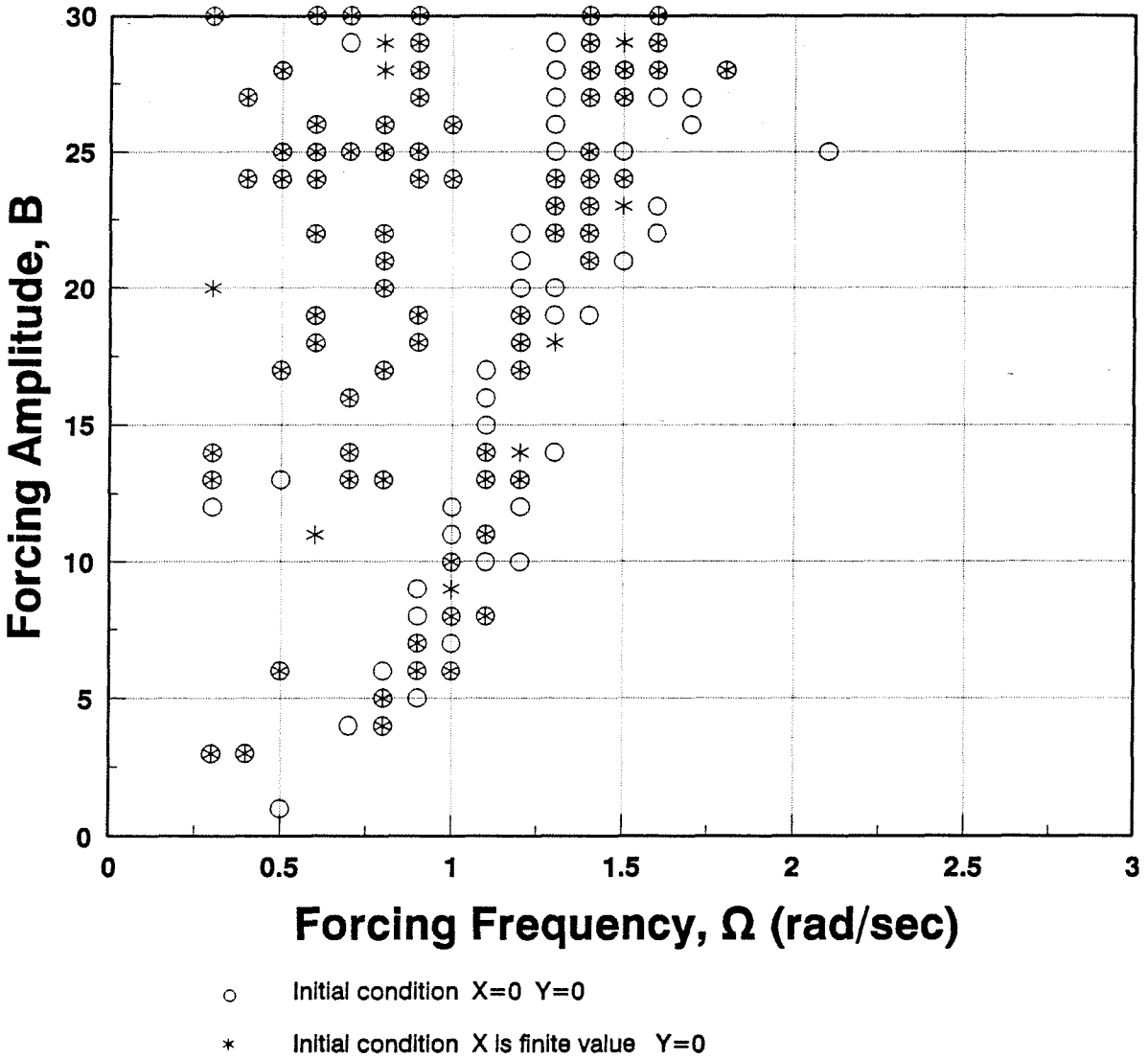

Figure 4.18: Duffing's equation including quadratic and cubic terms (I) in Ω–B plane ($k = 0.0$ $\alpha = 0.5$ $\beta = 1.0$ $c = 0.1$)

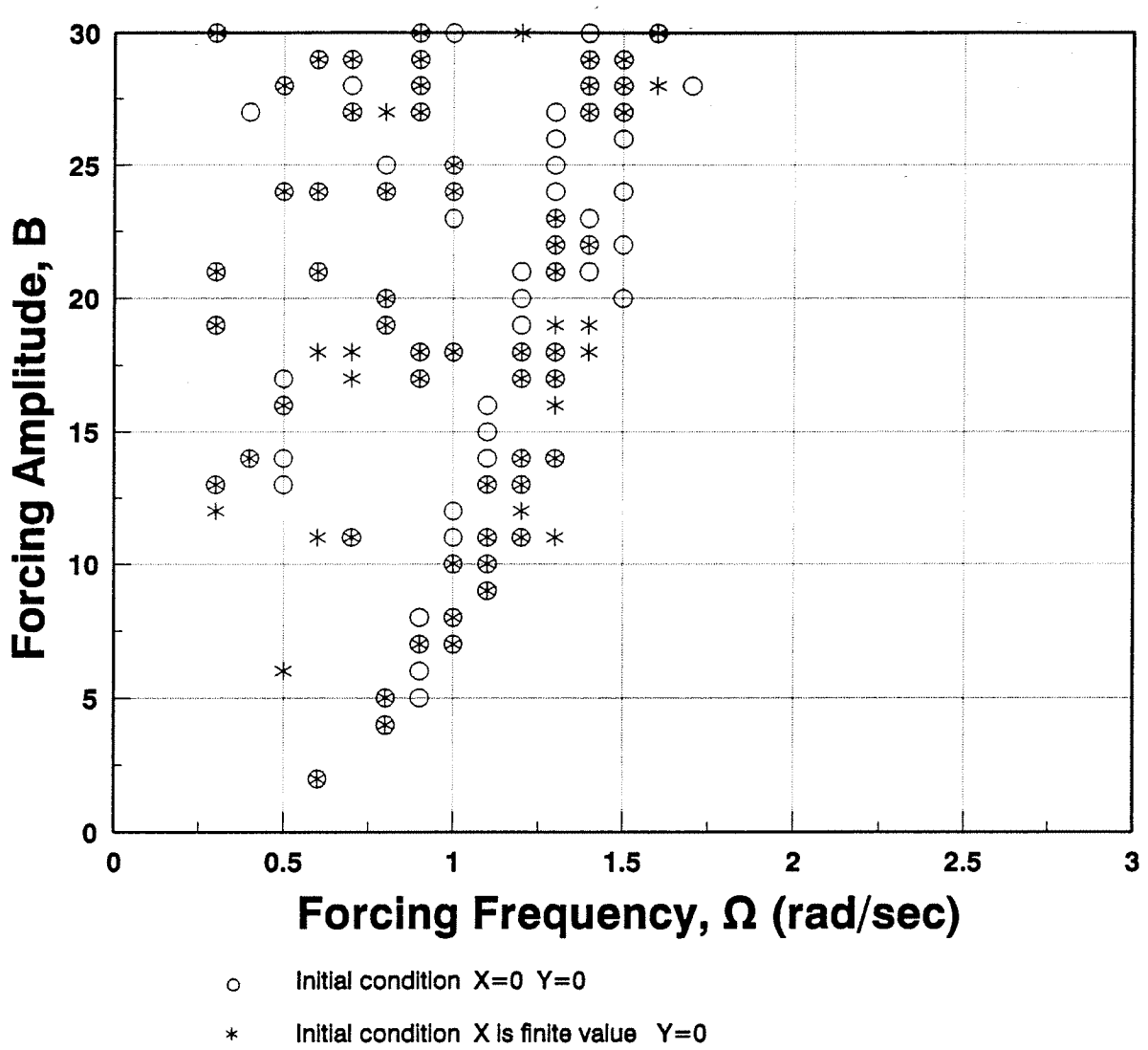

Figure 4.19: Duffing's equation including quadratic and cubic terms (I) in Ω–B plane ($k = 0.0$ $\alpha = 1.0$ $\beta = 1.0$ $c = 0.1$)

Table 4.20: Duffing's equation including quadratic nonlinearity (I)

Parameter		*Value*
Linear coeff.	k	0.5
Quadratic coeff.	α	0.5
Cubic coeff.	β	1.0
Damping coeff.	c	0.1
Force frequency	Ω	0.0 – 3.0
Force amplitude	B	0.0 – 30.0

Table 4.21: Duffing's equation including quadratic nonlinearity (I)

Parameter		*Value*
Linear coeff.	k	1.0
Quadratic coeff.	α	0.5
Cubic coeff.	β	1.0
Damping coeff.	c	0.1
Force frequency	Ω	0.0 – 3.0
Force amplitude	B	0.0 – 30.0

when the linear or quadratic term is large enough. For example, in Figure (4.23) there are only a few chaotic points. For the positive linear term, chaotic motion only exists at $\Omega < 2.0$, while for negative linear term, chaotic motion can exist at near $\Omega = 3.0$.

From the plot, there are some questionable points. The check of these points will be presented in Section 4.2.3 by using phase plane and Poincaré map plots.

DUFFING'S EQUATION INCLUDING QUADRATIC TERM (II)

The governing equation is

$$\ddot{X} + c\dot{X} + kX + \alpha X^2 + \beta X^3 = B\cos\Omega t \tag{4.2}$$

To compare with Section 4.2.1, we consider the same parameters, which are listed in

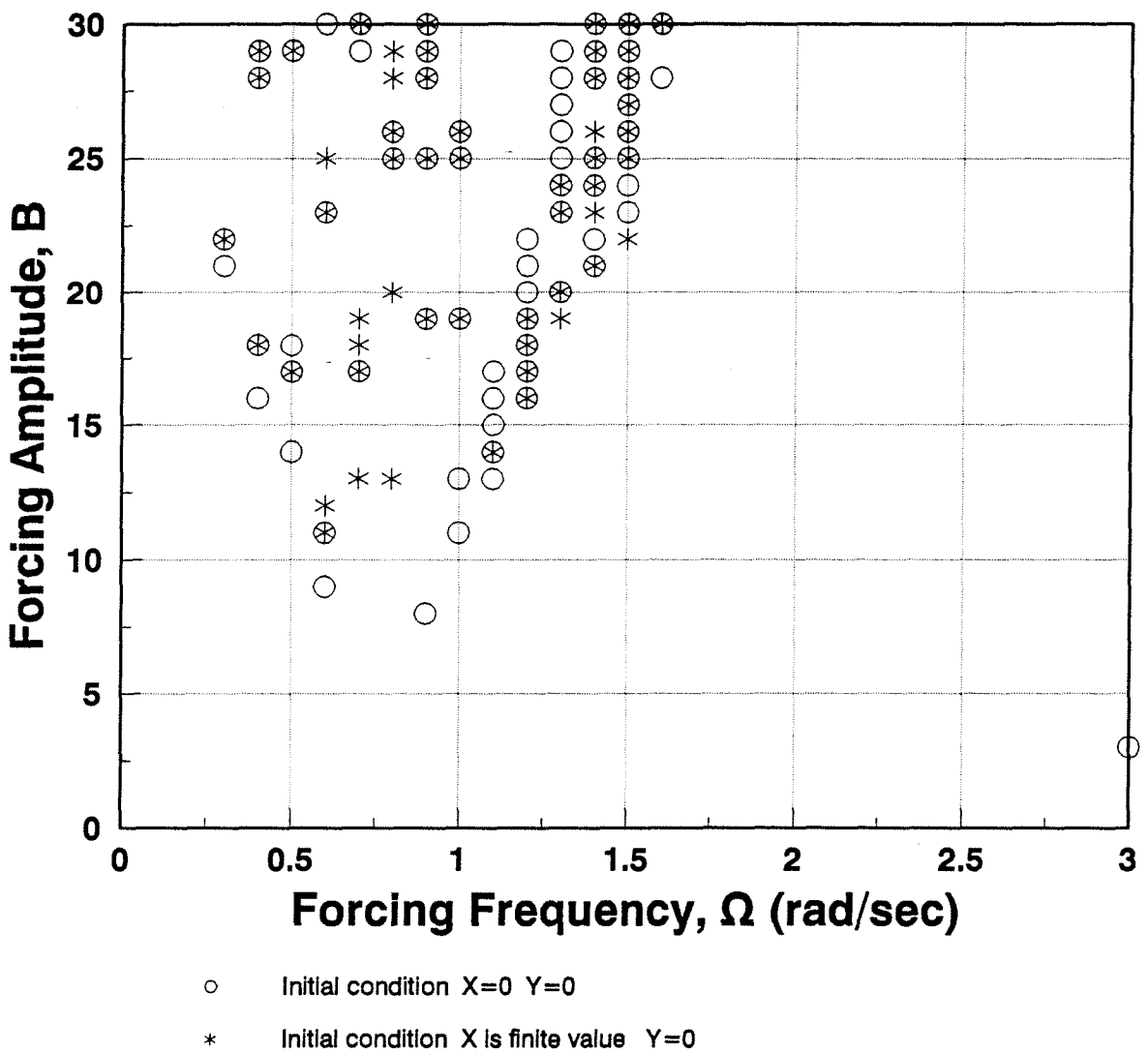

Figure 4.20: Duffing's equation including quadratic nonlinearity (I) in Ω–B plane ($k = 0.5$ $\alpha = 0.5$ $\beta = 1.0$ $c = 0.1$)

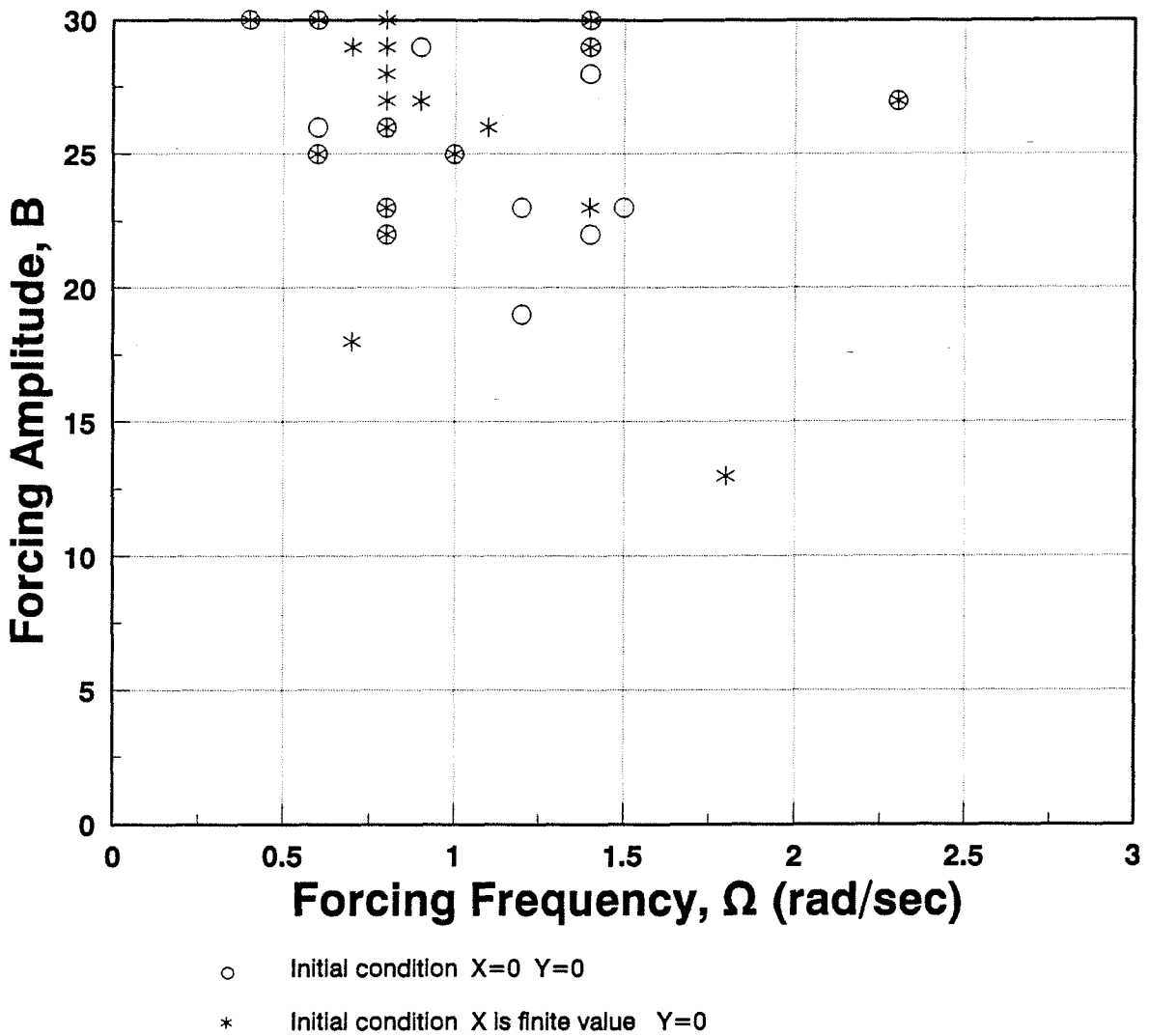

Figure 4.21: Duffing's equation including quadratic nonlinearity (I) in Ω–B plane ($k = 1.0$ $\alpha = 0.5$ $\beta = 1.0$ $c = 0.1$)

Table 4.22: Duffing's equation including quadratic nonlinearity (I)

Parameter		*Value*
Linear coeff.	k	0.5
Quadratic coeff.	α	1.0
Cubic coeff.	β	1.0
Damping coeff.	c	0.1
Force frequency	Ω	0.0 – 3.0
Force amplitude	B	0.0 – 30.0

Table 4.23: Duffing's equation including quadratic nonlinearity (I)

Parameter		*Value*
Linear coeff.	k	1.0
Quadratic coeff.	α	1.0
Cubic coeff.	β	1.0
Damping coeff.	c	0.1
Force frequency	Ω	0.0 – 3.0
Force amplitude	B	0.0 – 30.0

Table 4.24: Duffing's equation including quadratic nonlinearity (I)

Parameter		*Value*
Linear coeff.	k	-1.0
Quadratic coeff.	α	1.0
Cubic coeff.	β	1.0
Damping coeff.	c	0.1
Force frequency	Ω	0.0 – 3.0
Force amplitude	B	0.0 – 1.5

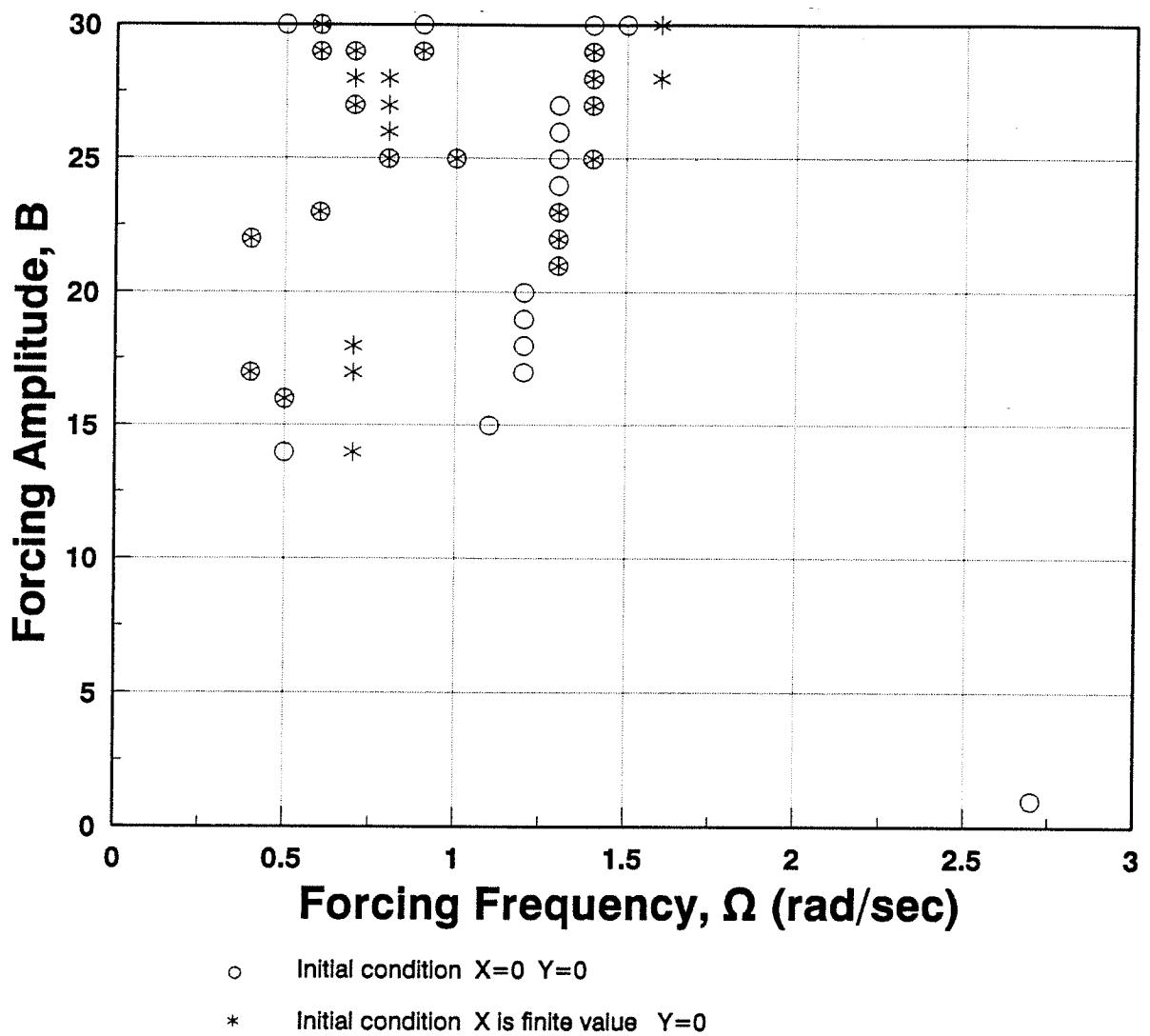

Figure 4.22: Duffing's equation including quadratic nonlinearity (I) in Ω–B plane ($k = 0.5$ $\alpha = 1.0$ $\beta = 1.0$ $c = 0.1$)

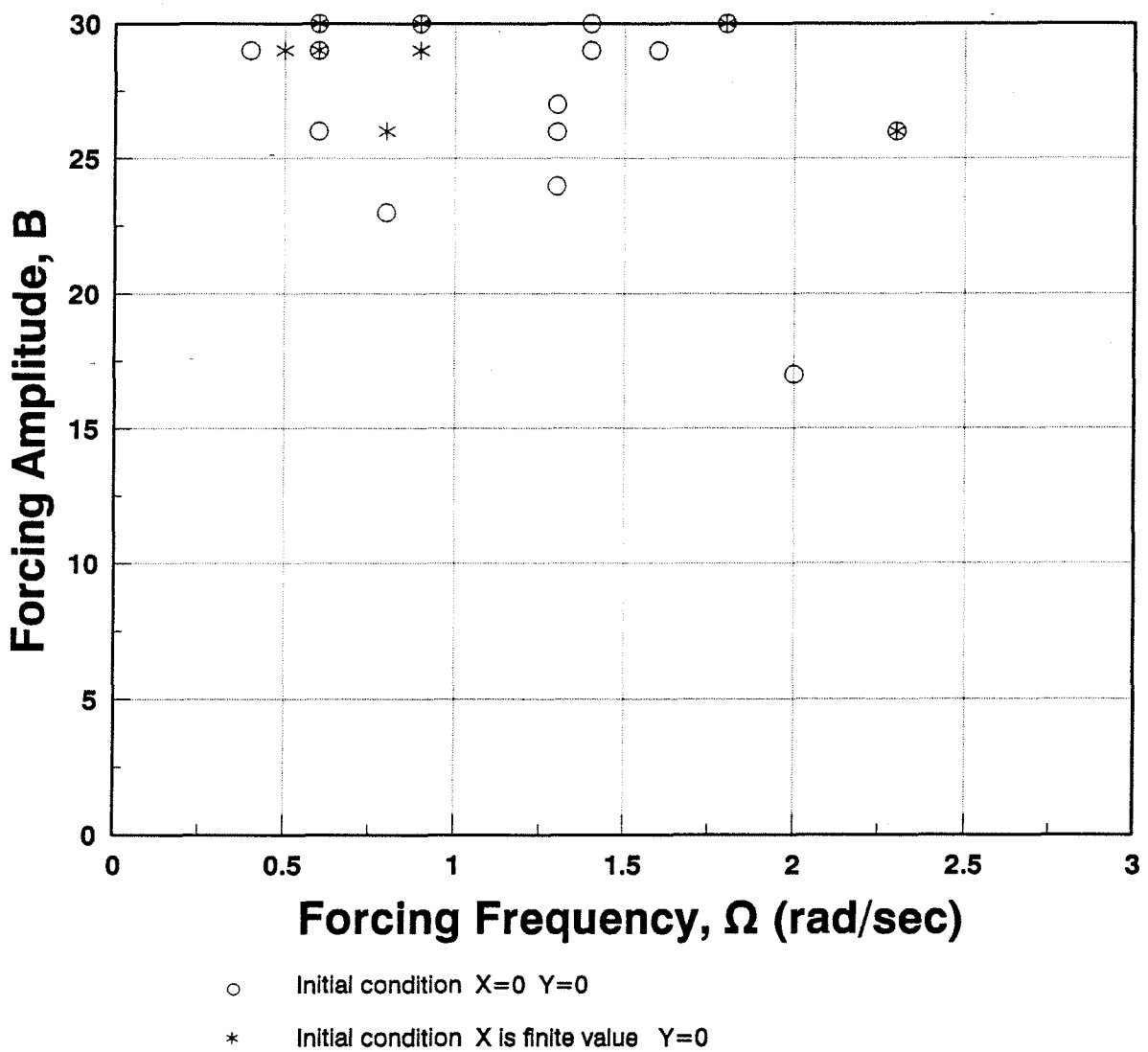

Figure 4.23: Duffing's equation including quadratic nonlinearity (I) in Ω–B plane ($k = 1.0$ $\alpha = 1.0$ $\beta = 1.0$ $c = 0.1$)

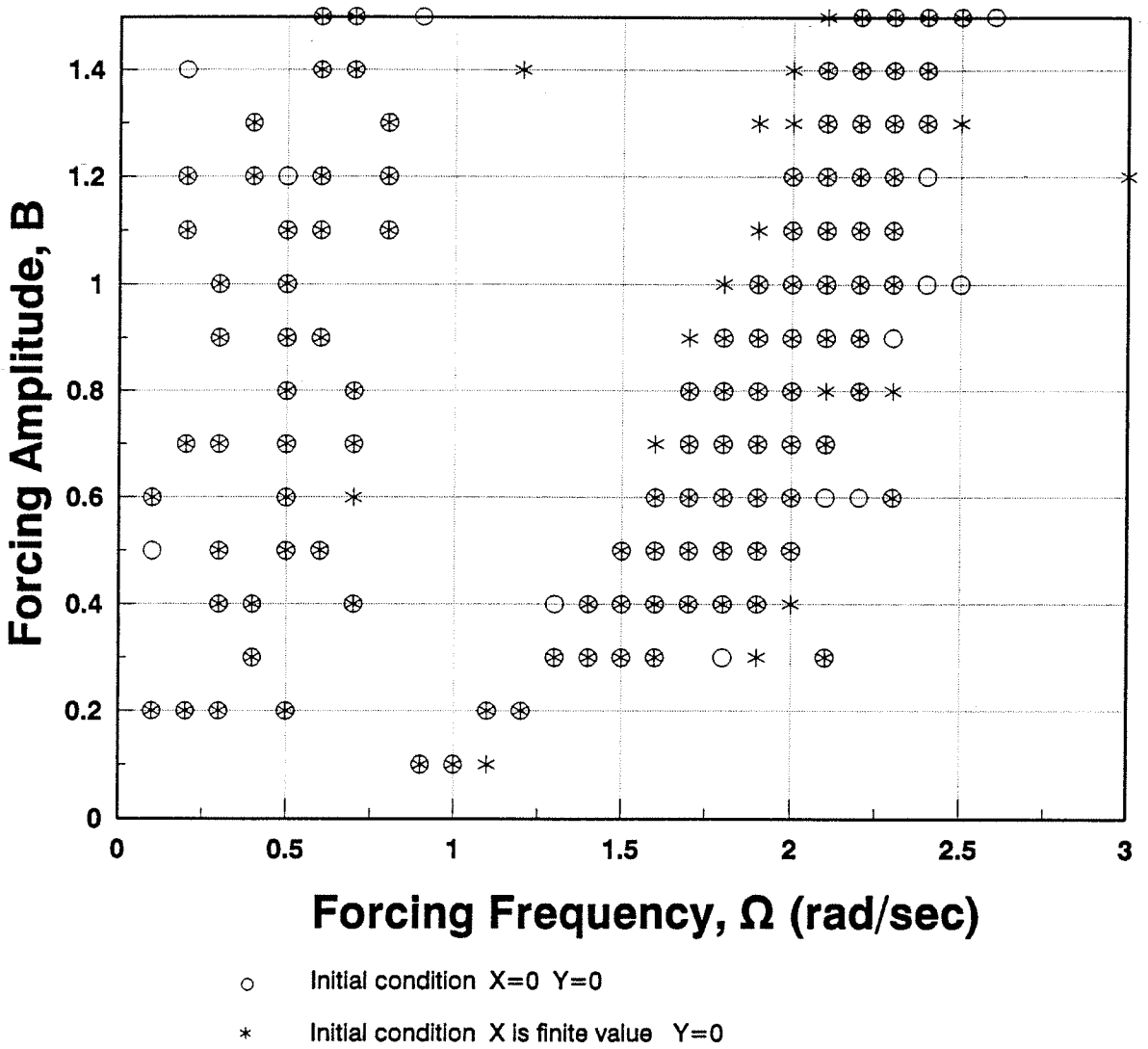

Figure 4.24: Duffing's equation including quadratic nonlinearity (I) in Ω–B plane ($k = -1.0$ $\alpha = 1.0$ $\beta = 1.0$ $c = 0.1$)

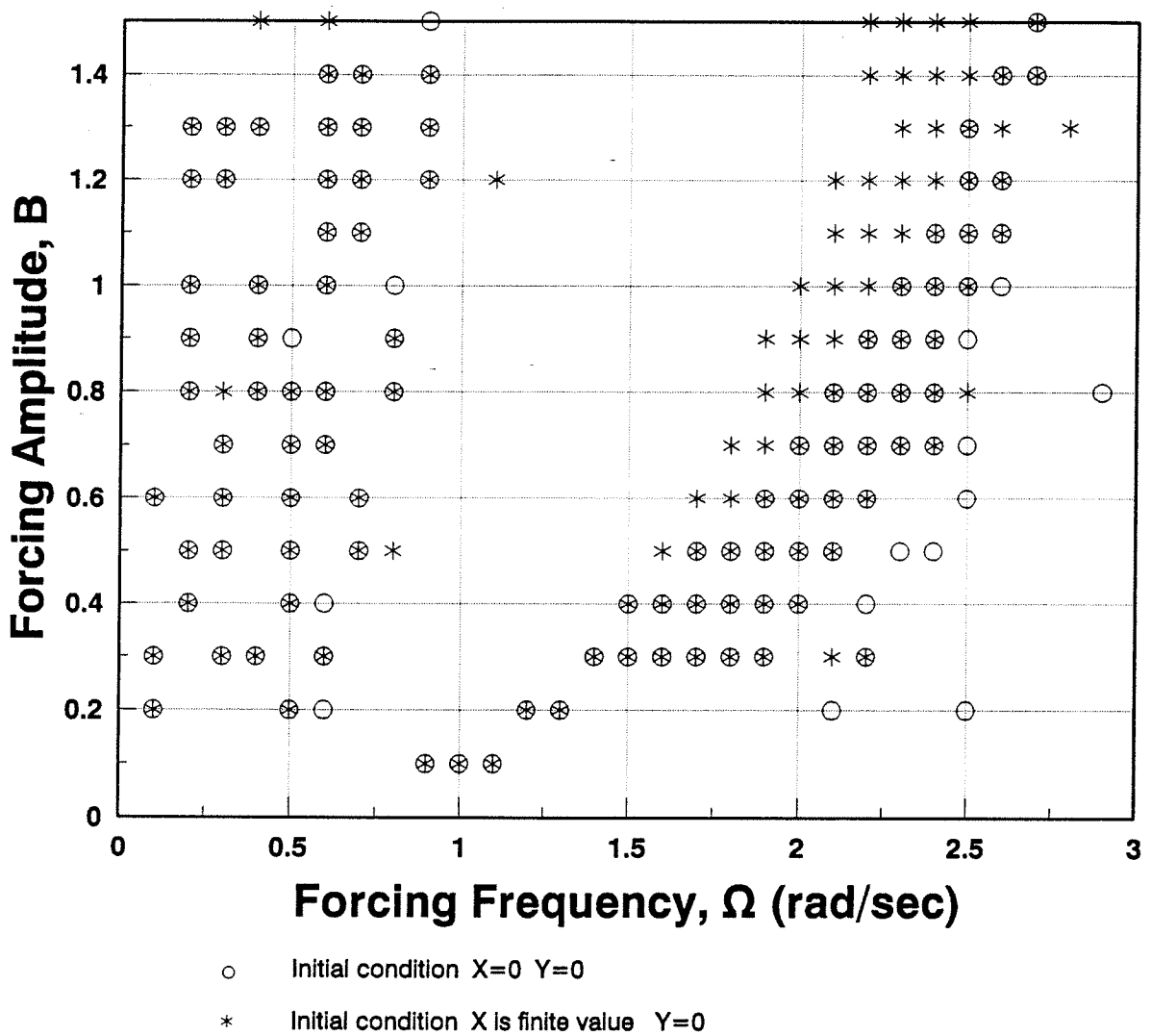

Figure 4.25: Duffing's equation including quadratic nonlinearity (I) in Ω–B plane ($k = -1.0$ $\alpha = 1.0$ $\beta = 2.0$ $c = 0.1$)

Table 4.25: Duffing's equation including quadratic nonlinearity (I)

Parameter		*Value*
Linear coeff.	k	-1.0
Quadratic coeff.	α	1.0
Cubic coeff.	β	2.0
Damping coeff.	c	0.1
Force frequency	Ω	0.0 - 3.0
Force amplitude	B	0.0 - 1.5

Table 4.26: Duffing's equation including quadratic and cubic terms (II)

Parameter		*Value*
Linear coeff.	k	0.0
Quadratic coeff.	α	0.5
Cubic coeff.	β	1.0
Damping coeff.	c	0.1
Force frequency	Ω	0.0 - 3.0
Force amplitude	B	0.0 - 30.0

Table (4.26) - Table (4.31). Chaotic regions are given in Figure (4.26) - Figure (4.31).

From the plots, it is shown that there exist many more chaotic points in this case to compare with Case (I) for the positive linear term. However for negative linear term, there are fewer chaotic points than for Case (I).

4.2.3 PLOTS IN PHASE PLANE AND POINCARÉ MAP

As we mentioned before, we can't rely only on Lyapunov exponent analysis to study chaos. Here, phase plane plots and Poincaré map are used to check some questionable points.

Fig.(4.16) shows a positive λ at $B = 1.1$, $\Omega = 0.7$. The resulting phase plane plot for this point is shown in Fig. 4.32. This plot corresponds to periodic motion. Hence that

Table 4.27: Duffing's equation including quadratic and cubic terms (II)

Parameter		*Value*
Linear coeff.	k	0.0
Quadratic coeff.	α	1.0
Cubic coeff.	β	1.0
Damping coeff.	c	0.1
Force frequency	Ω	0.0 – 3.0
Force amplitude	B	0.0 – 30.0

Table 4.28: Duffing's equation including quadratic nonlinearity (II)

Parameter		*Value*
Linear coeff.	k	0.5
Quadratic coeff.	α	0.5
Cubic coeff.	β	1.0
Damping coeff.	c	0.1
Force frequency	Ω	0.0 – 3.0
Force amplitude	B	0.0 – 30.0

Table 4.29: Duffing's equation including quadratic nonlinearity (II)

Parameter		*Value*
Linear coeff.	k	1.0
Quadratic coeff.	α	0.5
Cubic coeff.	β	1.0
Damping coeff.	c	0.1
Force frequency	Ω	0.0 – 3.0
Force amplitude	B	0.0 – 30.0

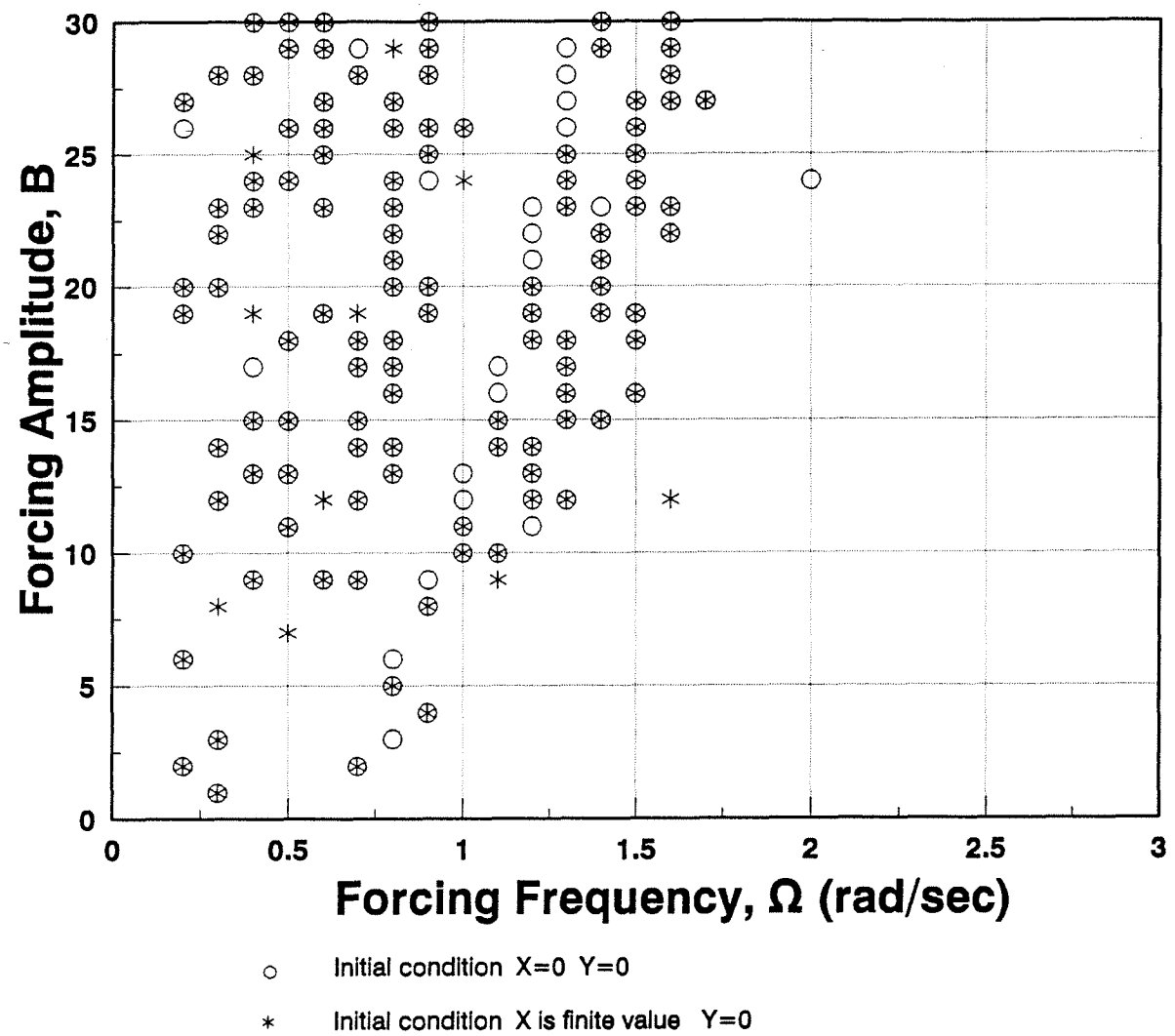

Figure 4.26: Duffing's equation including quadratic and cubic terms (II) in Ω–B plane ($k = 0.0$ $\alpha = 0.5$ $\beta = 1.0$ $c = 0.1$)

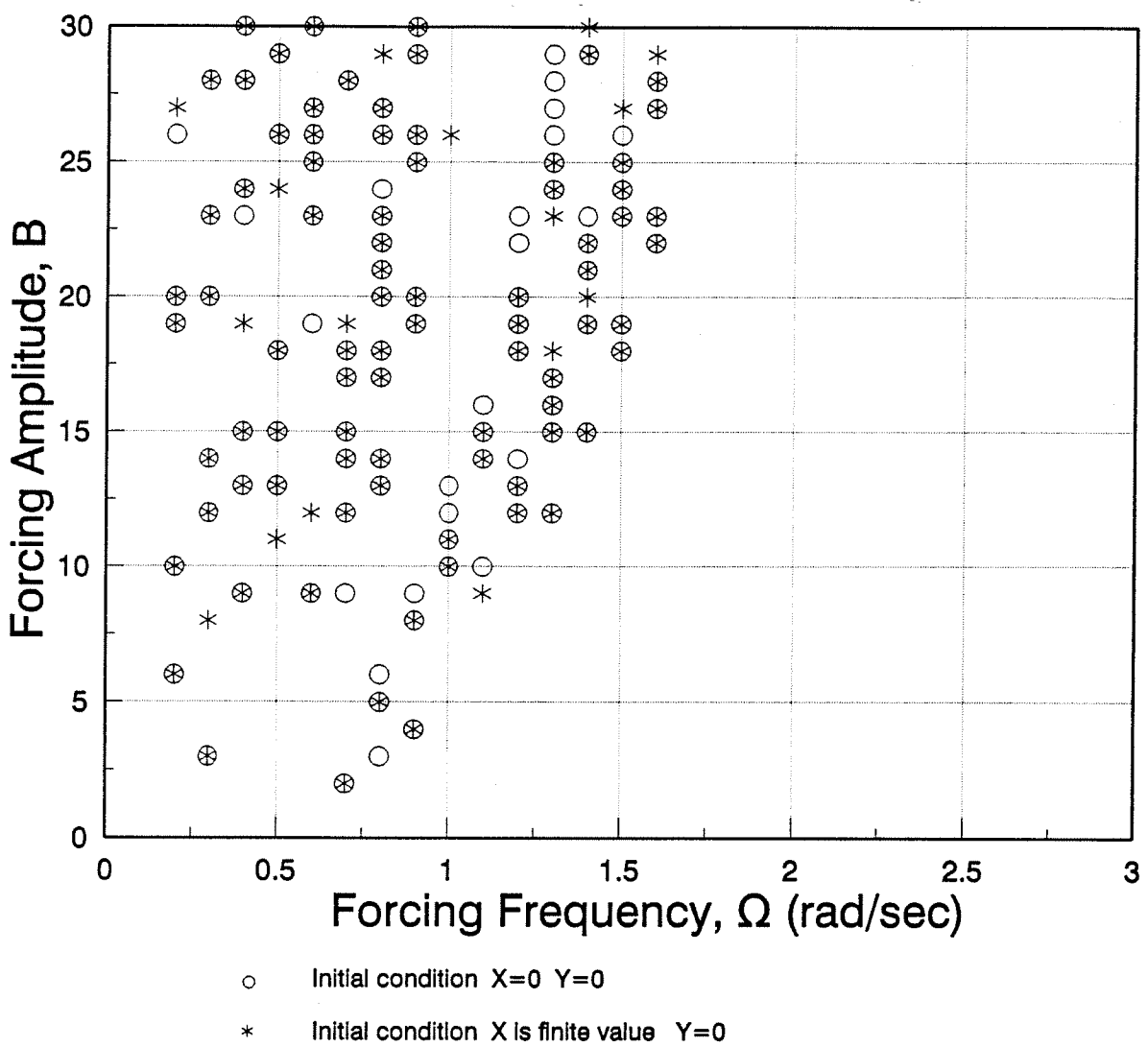

Figure 4.27: Duffing's equation including quadratic and cubic terms (II) in Ω–B plane ($k = 0.0$ $\alpha = 1.0$ $\beta = 1.0$ $c = 0.1$)

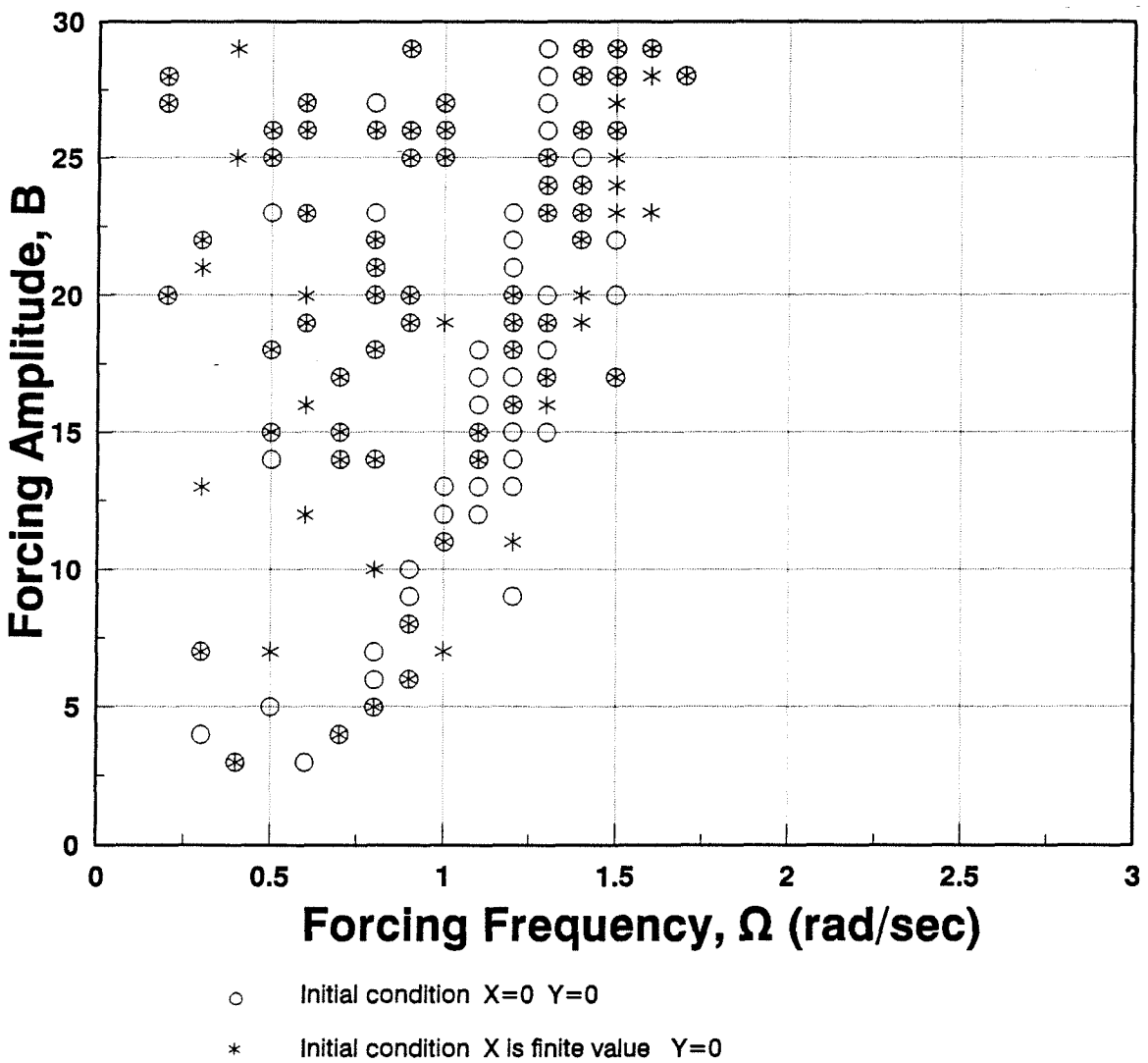

Figure 4.28: Duffing's equation including quadratic nonlinearity (II) in Ω–B plane ($k = 0.5$ $\alpha = 0.5$ $\beta = 1.0$ $c = 0.1$)

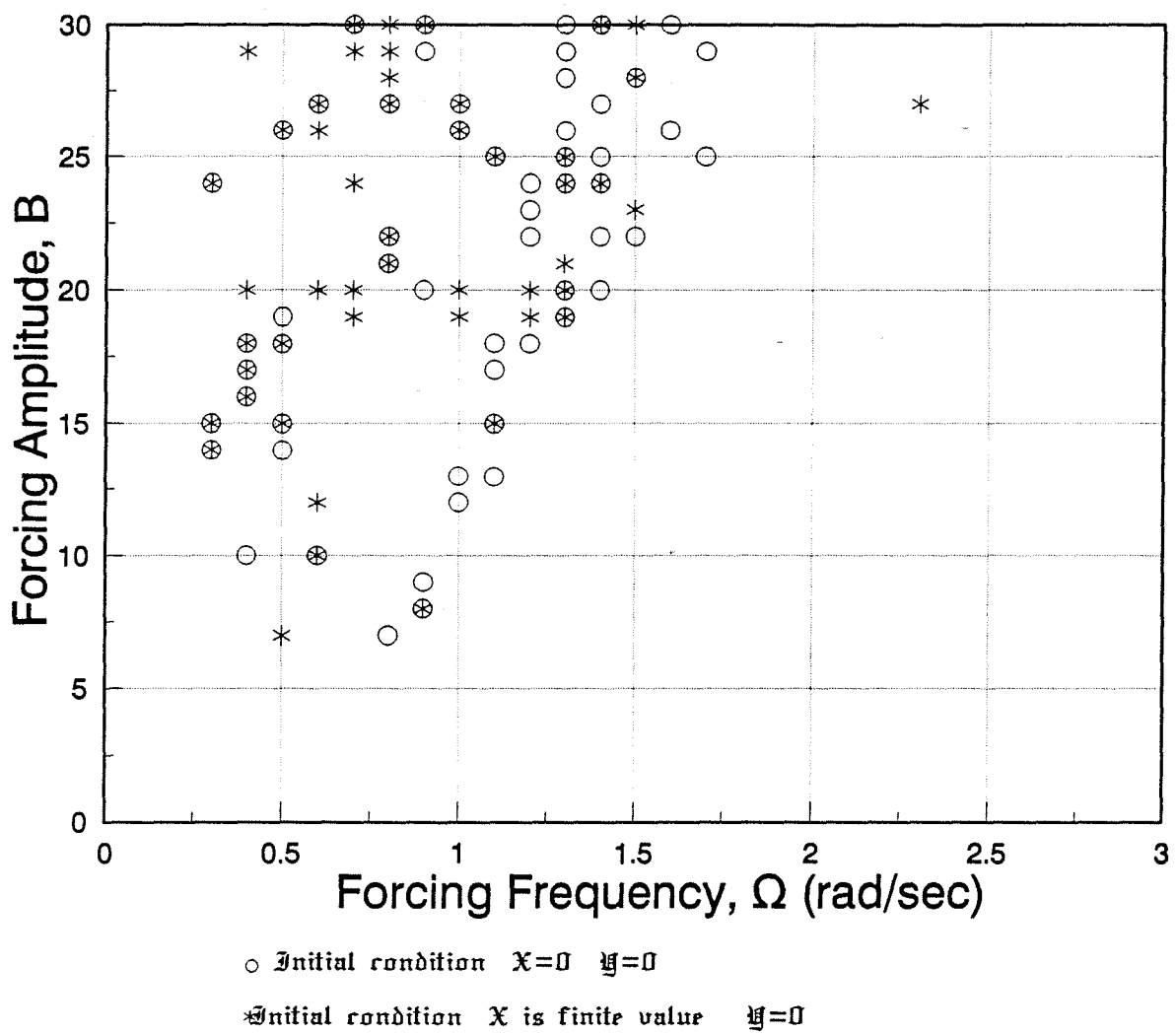

Figure 4.29: Duffing's equation including quadratic nonlinearity (II) in Ω–B plane ($k = 1.0$ $\alpha = 0.5$ $\beta = 1.0$ $c = 0.1$)

Table 4.30: Duffing's equation including quadratic nonlinearity (II)

Parameter		*Value*
Linear coeff.	k	0.5
Quadratic coeff.	α	1.0
Cubic coeff.	β	1.0
Damping coeff.	c	0.1
Force frequency	Ω	0.0 – 3.0
Force amplitude	B	0.0 – 30.0

Table 4.31: Duffing's equation including quadratic nonlinearity (II)

Parameter		*Value*
Linear coeff.	k	-1.0
Quadratic coeff.	α	1.0
Cubic coeff.	β	1.0
Damping coeff.	c	0.1
Force frequency	Ω	0.0 – 3.0
Force amplitude	B	0.0 – 1.5

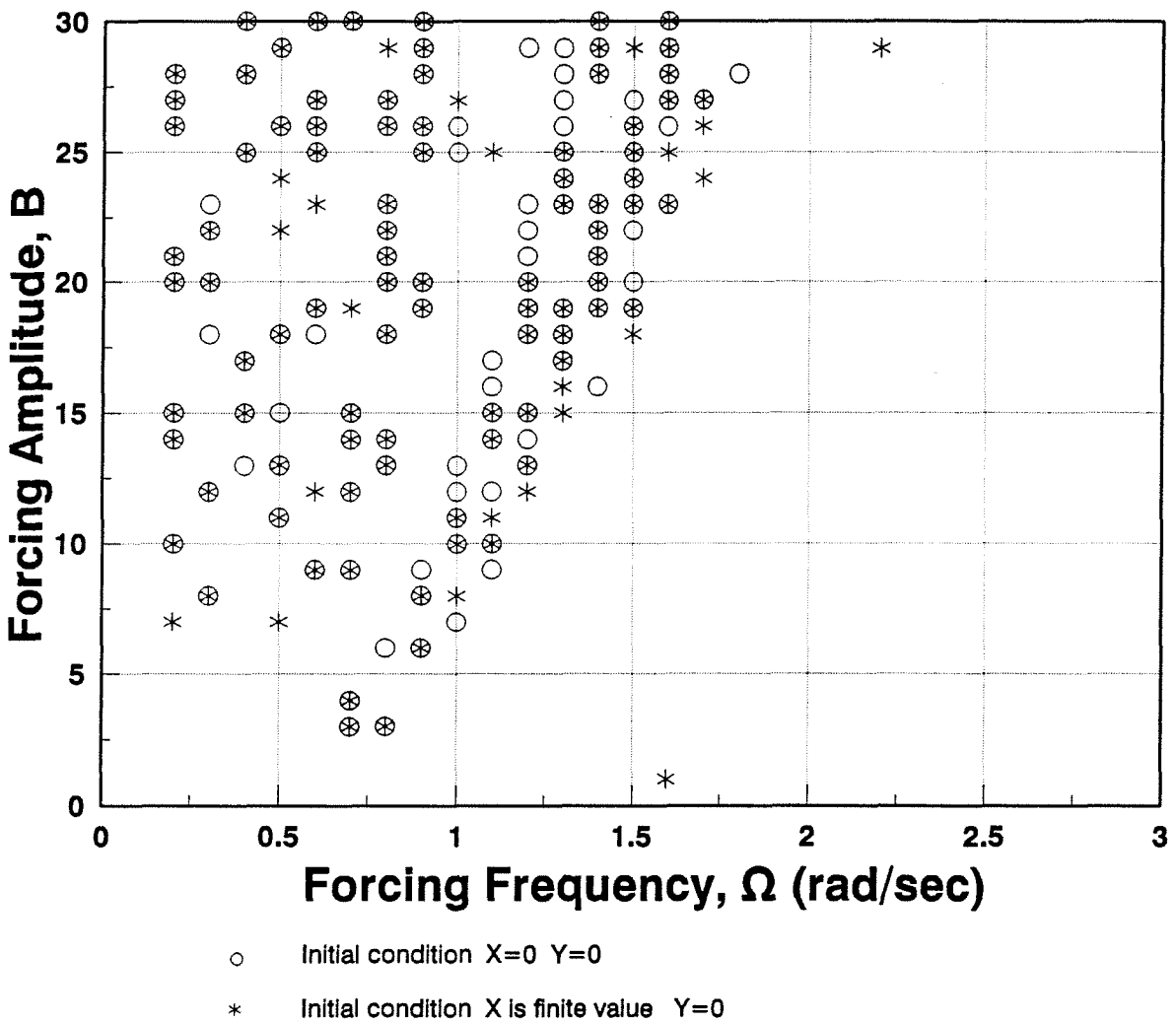

Figure 4.30: Duffing's equation including quadratic nonlinearity (II) in Ω–B plane ($k = 0.5$ $\alpha = 1.0$ $\beta = 1.0$ $c = 0.1$)

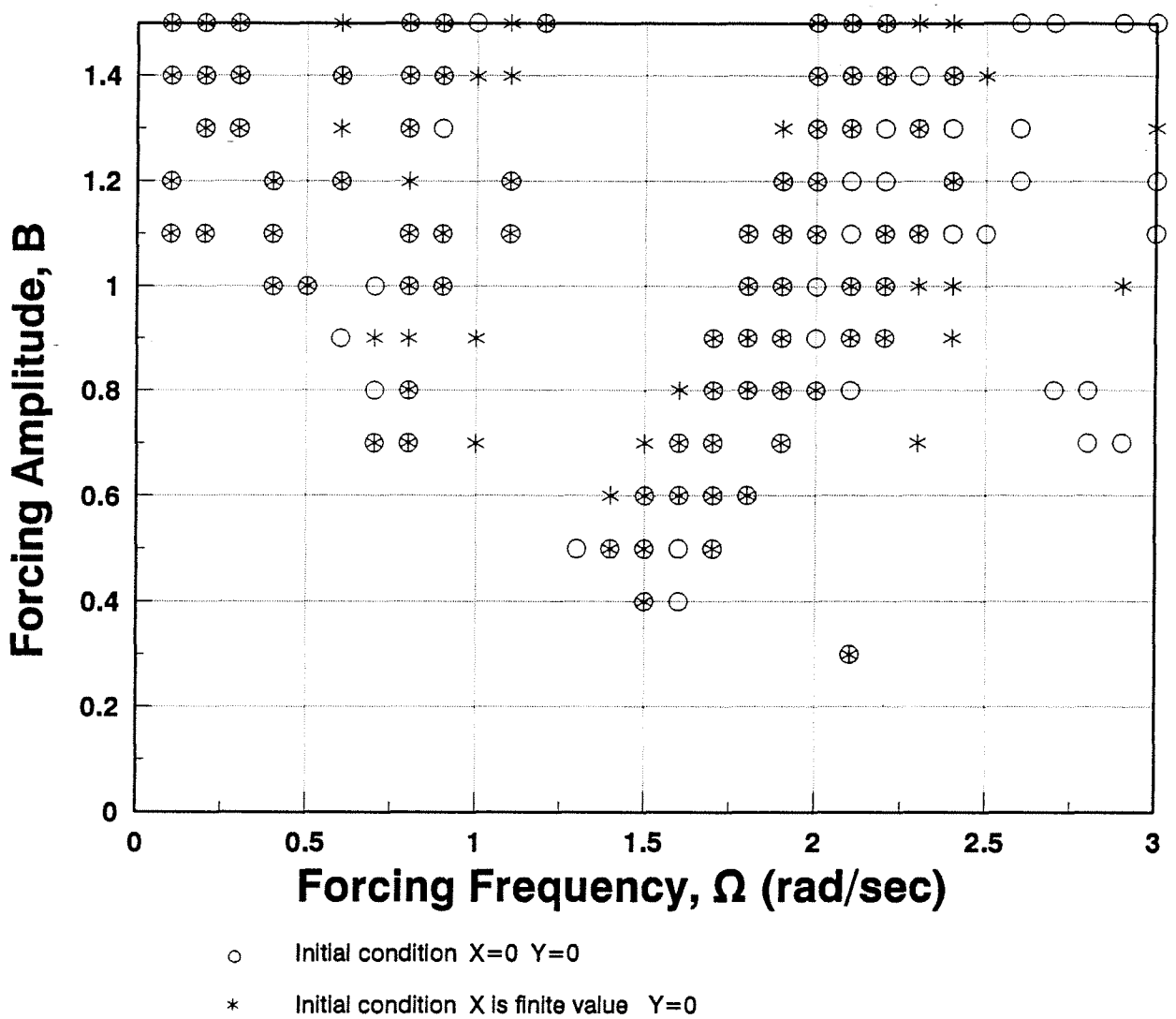

Figure 4.31: Duffing's equation including quadratic nonlinearity (II) in Ω–B plane ($k = -1.0$ $\alpha = 1.0$ $\beta = 1.0$ $c = 0.1$)

point must be eliminated from Fig. 4.16.

Also we consider Fig.(4.13). At $B = 8.0$, $\Omega = 1.5$, the tolerance was not met when the positive λ was recorded. The phase plane plot and Poincaré map for this point are shown in Fig.(4.33) and Fig.(4.34). Hence again this point is not chaotic, but periodic.

Some other points are investigated here. It should be mentioned that chaotic and periodic motions may co-exist at one point for different initial conditions, and phase plane plots are different at one point for different initial conditions (see Fig.(4.35) and Fig.(4.36)).

If the tolerance is met, and $\lambda > 0$, it is always chaos(see Fig.(4.37) and Fig.(4.38)).

It is seen that the checks using phase plane plot and Poincaré map are very important.

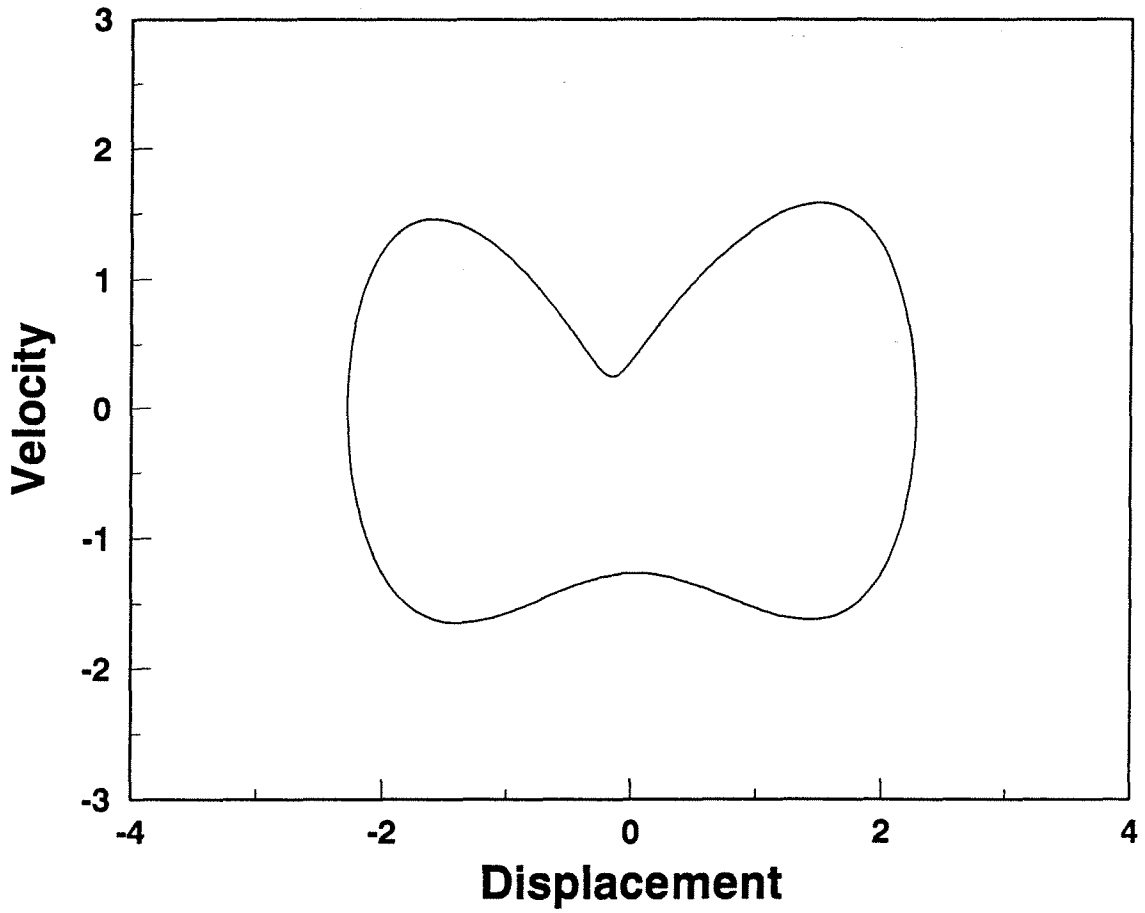

Figure 4.32: Phase plane plot ($k = -0.5$ $\alpha = 0.0$ $\beta = 0.5$ $c = 0.1$ $B = 1.1$ $\Omega = 0.7$)

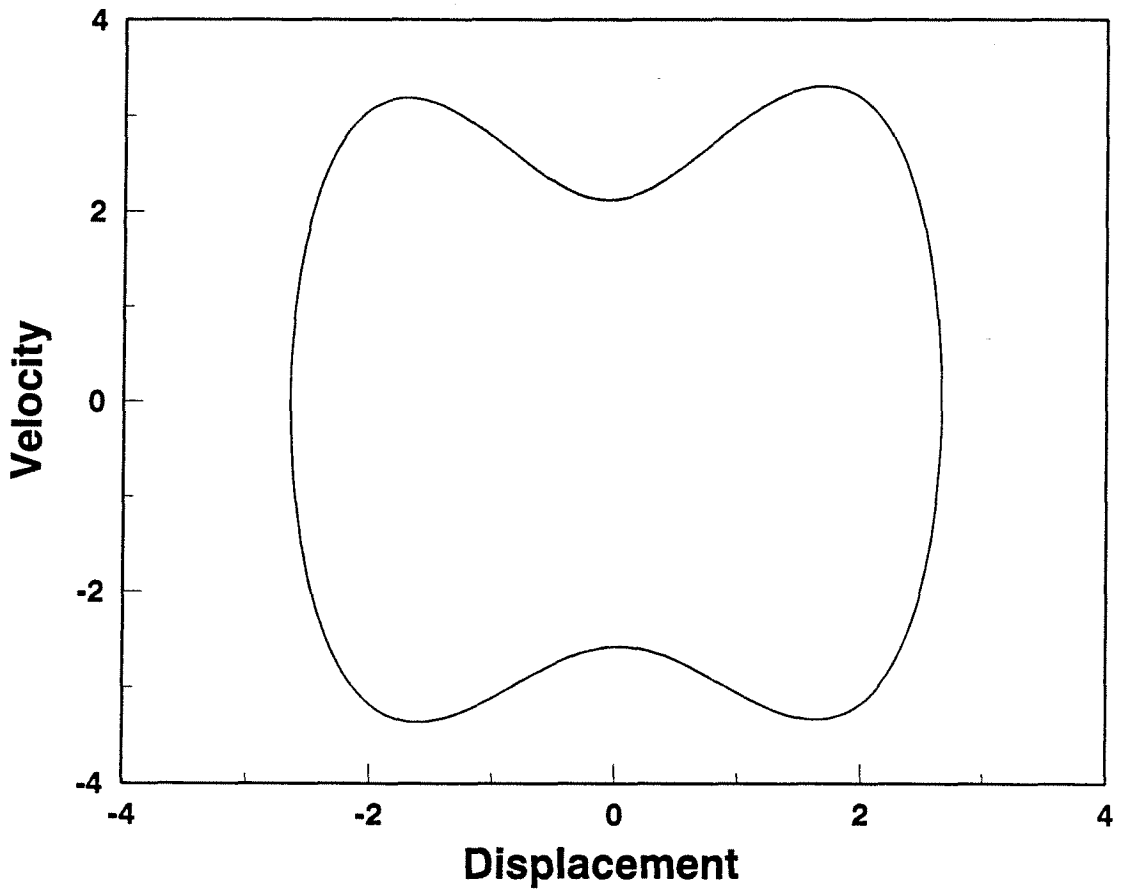

Figure 4.33: Phase plane plot ($k = 1.0$ $\alpha = 0.0$ $\beta = 1.0$ $c = 0.1$ $B = 8.0$ $\Omega = 1.5$)

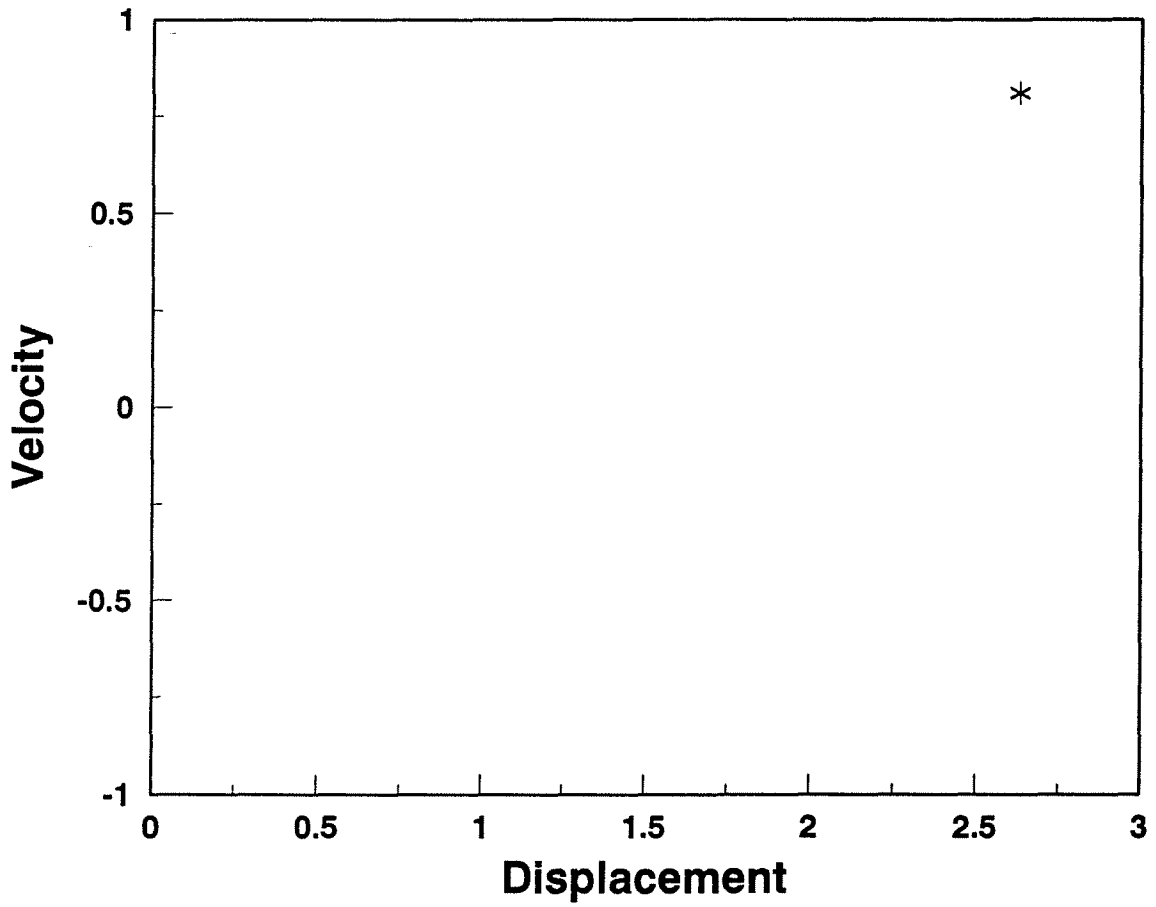

Figure 4.34: Poincaré map ($k = 1.0$ $\alpha = 0.0$ $\beta = 1.0$ $c = 0.1$ $B = 8.0$ $\Omega = 1.5$)

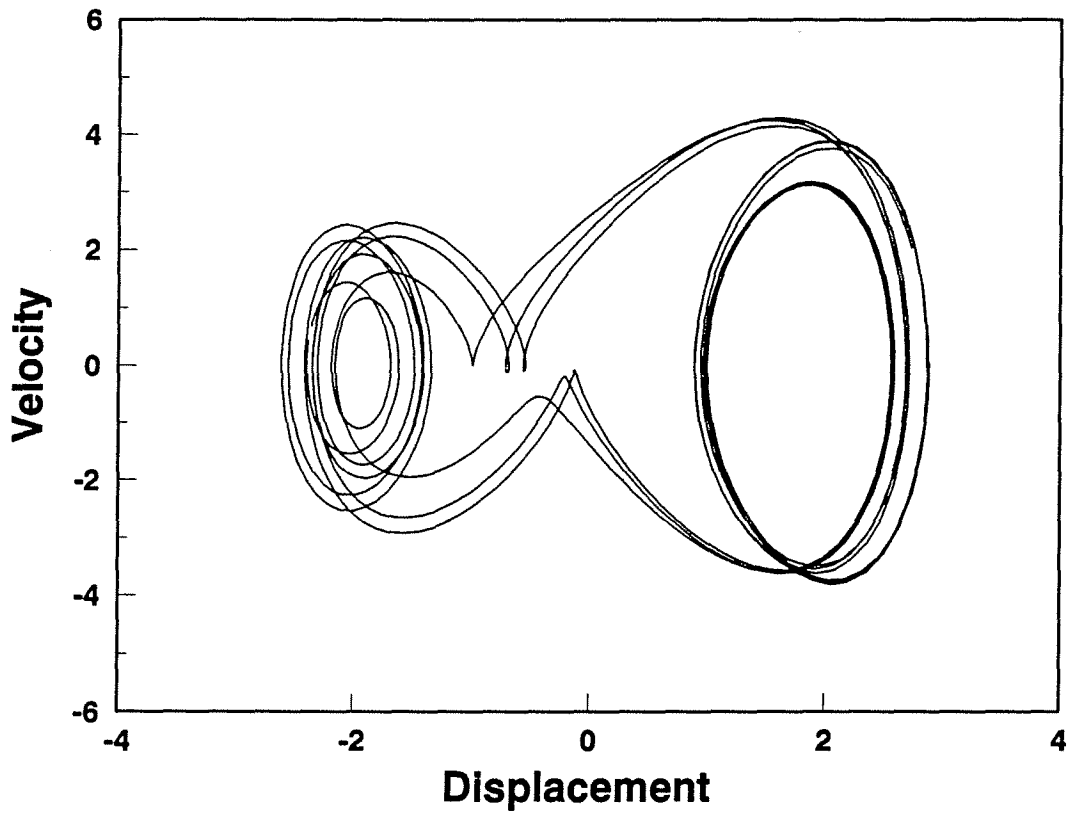

Figure 4.35: Phase plane plot ($k = 0.5$ $\alpha = 1.0$ $\beta = 1.0$ $c = 0.1$ $B = 14.0$ $\Omega = 0.7$ $x_o = 0.0$ $y_o = 0.0$)

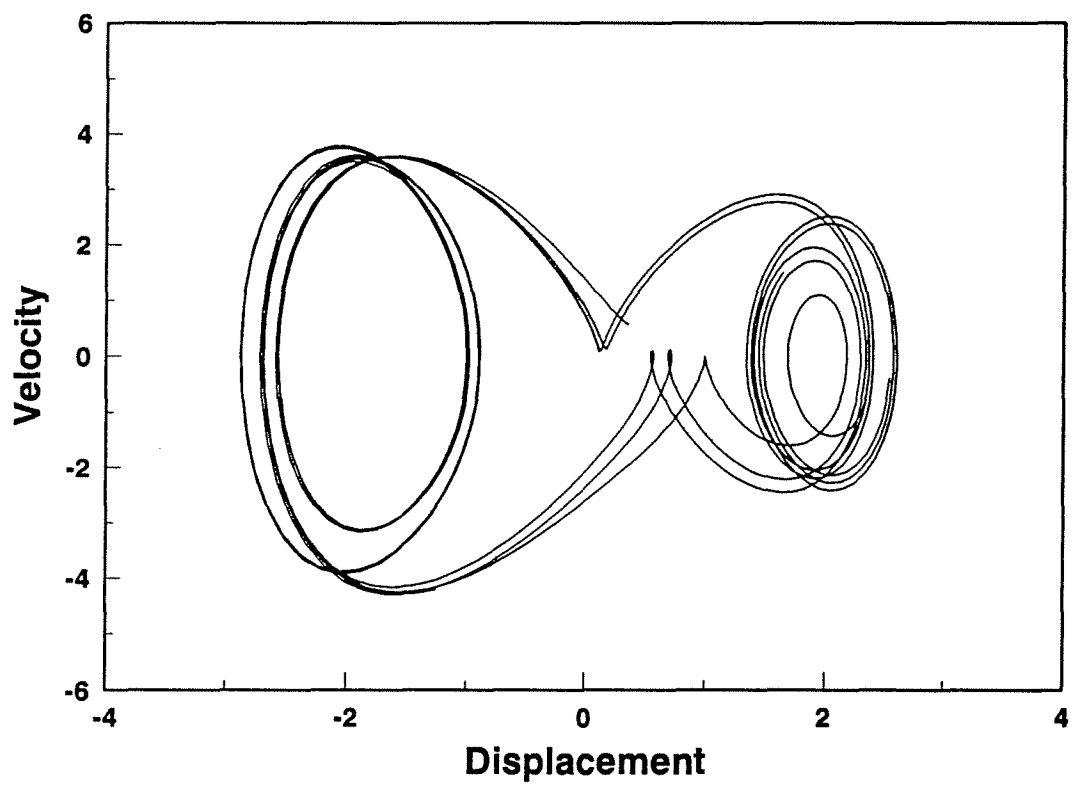

Figure 4.36: Phase plane plot ($k = 0.5$ $\alpha = 1.0$ $\beta = 1.0$ $c = 0.1$ $B = 14.0$ $\Omega = 0.7$ $x_o = -0.243$ $y_o = -3.626$)

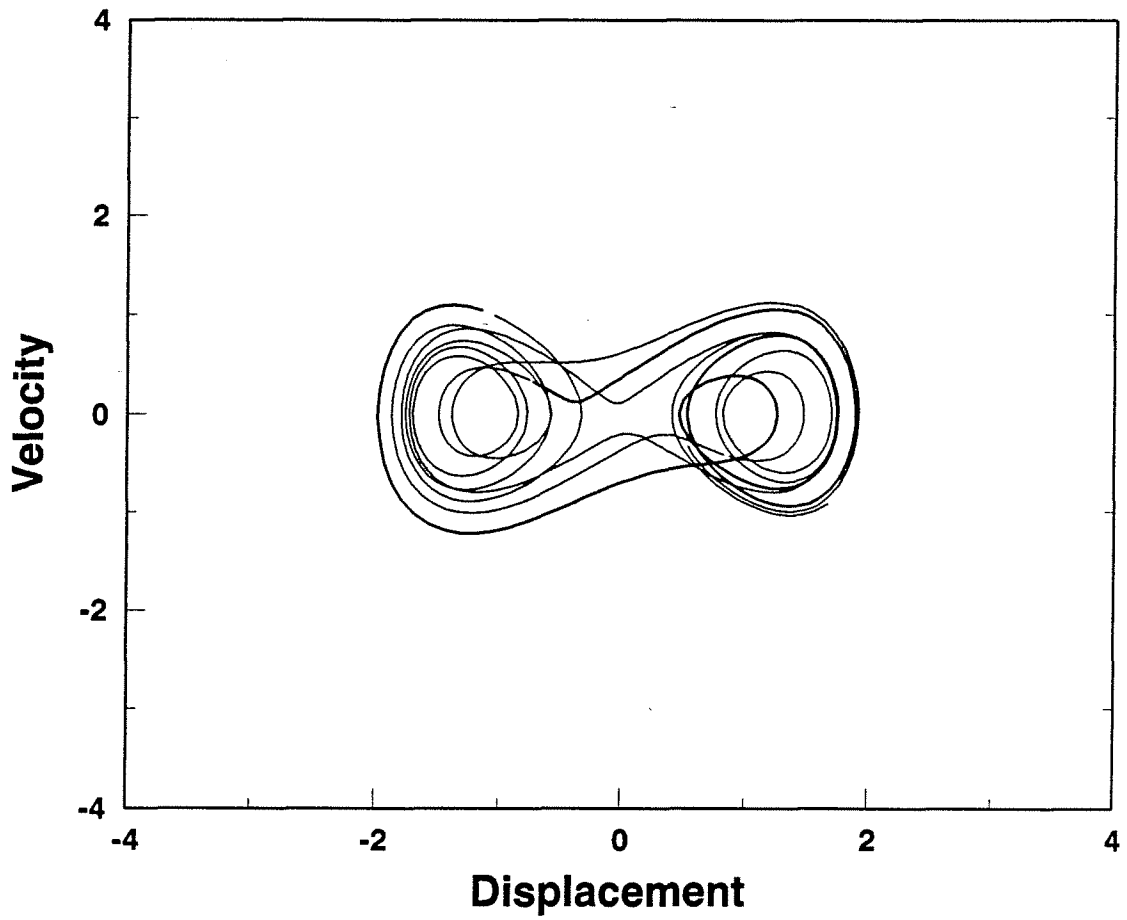

Figure 4.37: Phase plane plot ($k = -0.5$ $\alpha = 0.0$ $\beta = 0.5$ $c = 0.1$ $B = 0.5$ $\Omega = 0.2$)

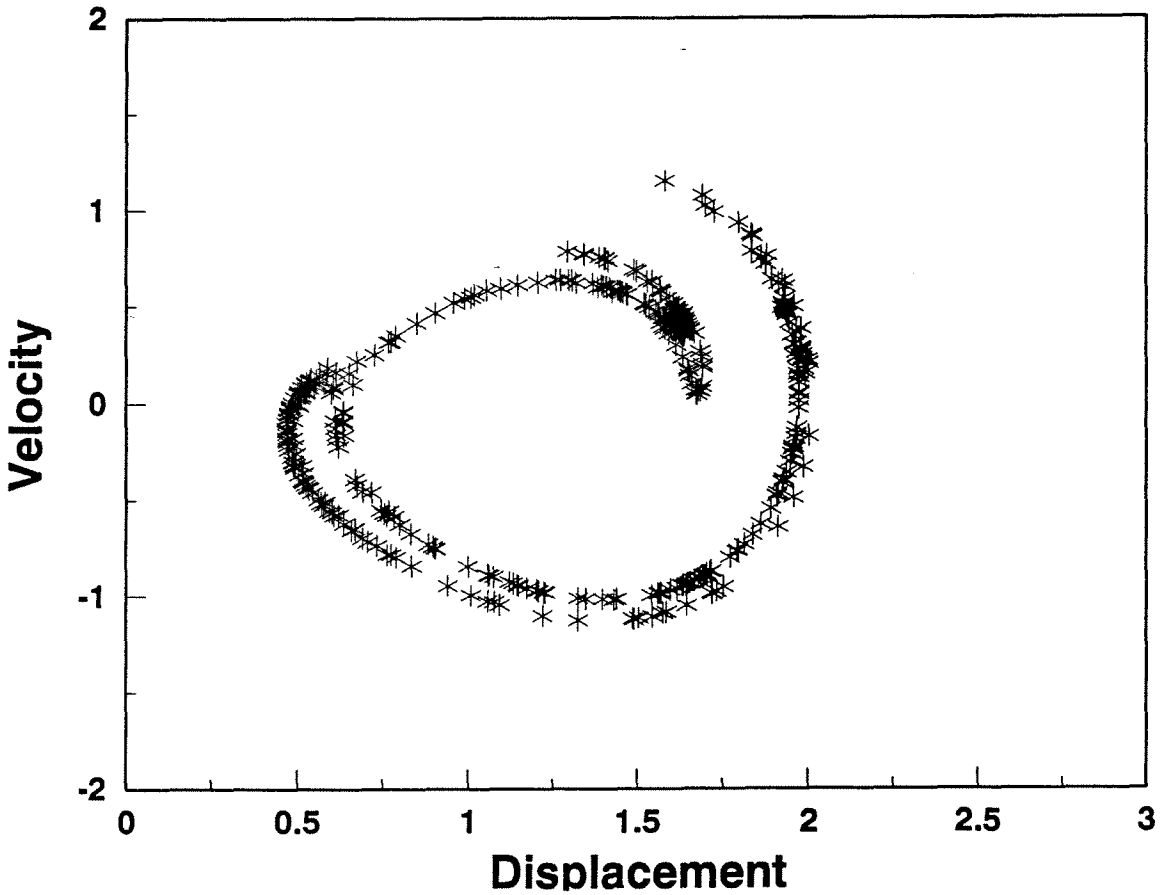

Figure 4.38: Poincaré map ($k = -0.5$ $\alpha = 0.0$ $\beta = 0.5$ $c = 0.1$ $B = 0.5$ $\Omega = 0.2$ $\lambda > 0$)

Chapter 5

CONCLUSIONS

5.1 CONCLUDING REMARKS

A numerical procedure, which estimates the non-negative Lyapunov exponent was used to construct chaotic regions for Duffing's equation including quadratic terms. An extensive parametric investigation was carried out for this equation. Chaotic motion was found to exist for all the cases that included the cubic term and not too large linear and quadratic terms. It was found that there is no chaotic motion for Duffing's system including only linear and quadratic terms. From the investigation of Duffing's systems, we can conclude that only cubic term cause chaos but linear and quadratic terms eliminate chaos. For the case of negative linear term, chaotic motion occurs at quite small forcing amplitude but can exist for all ranges of forcing frequency Ω from $0 - 3.0$. While for the positive linear term, chaos occurs only at quite large forcing amplitude and $\Omega < 2.0$.

Overall, the present method seems to work very well, but there exists some questionable points of chaotic motion, which may mainly be caused by the accuracy of numerical procedures. Therefore, some other methods are needed to check the questionable points.

In order to check the plots of chaotic regions, phase plane and Poincaré map plots were introduced to deal with the questionable points. Depending on all these methods, reliable chaotic regions can be constructed.

The full Newton - Raphson numerical integration procedure for solving the nonlinear Duffing's equations was successful in the present study, and the CPU time of the present

method is relatively low.

Analytical and heuristic criteria were also discussed for some specific cases.

The overall agreement between the numerical results presented here and those available in the literature was satisfactory.

5.2 SUGGESTIONS FOR FURTHER STUDY

Some specific recommendations for further studies based on this work are:

(1) In order to meet tolerance, as we calculate λ, a midsized computer is needed.

(2) Expand the present method to other engineering systems not governed by Duffing's equations. This will be very useful for engineering design.

(3) In order to understand how chaotic motion happens, more mathematical analysis of Duffing's equation including quadratic nonlinearlity is needed.

Bibliography

[1] A.H.Nayfeh and D.T. Mook, "Nonlinear Oscillation", 1979, New York: Wiley-Interscience.

[2] Alan Wolf, Jack B. Swift, Harry L. Swinney and Jone A. Vastano, "Determining Lyapunov Exponents from a Time Series", Physica 16D, 1985, pp 285-317.

[3] Y. Ueda, "Steady Motions Exhibited by Duffing's Equation: A Picture Book of Regular and Chaotic Motions" New Approaches to Nonlinear Problems in Dynamics, 1980, P.J.Holmes(ed.) SIAM, Philadelphia,PA, U.S.A., pp 311-322.

[4] Y.Ueda, "Randomly Transitional Phenonmena in the System Governed by Duffing's Equation", J. Stat. Phys., Vol.20, 1979, 181-196.

[5] P.J. Holmes, "A Nonlinear Oscillator with a Strange Attrector", Trans. R. Soc. London A, 1979, Vol.292, pp 419-448.

[6] F.C. Moon, "Experiments on Chaotic Motions of a Forced Nonlinear Osscillator: Strange Attractors", ASME J.Appl.Mech.,1980, Vol.47, pp 638-644.

[7] P.J. Holmes and F.C. Moon, "Strange Attractors and Chaos in Non- linear Mechanics", ASME J. Appl. Mech.,1983, Vol.50, pp 1021-1032.

[8] E.H. Dowell and C.Pezeshki, "On the Understanding of Chaos in Duffing's Equation Including a Comparison with Experiment", ASME J. Appl. Mech., 1986, Vol.53, pp 5-9.

[9] F.C. Moon, "Chaotic Vibrations",1987,New York: Wiley-Interscience.

[10] G.X. Li, "Chaotic Vibrations of a Nonlinear System with Five Equilibrium States", M.S. Thesis, 1984, Cornell University, N.Y.

[11] T. Fang and E.H. Dowell, "Numerical Simulations of Periodic and Chaotic Responses in a Stable Duffing System", Int.J. Non-linear Mech., 1987, Vol.22, No.5, pp 401-425.

[12] F.C. Moon, "Experimental Models for Strange Attractor Vibrations in Elastic System", New Approaches to Nonlinear Problems in Dynamics, 1980, P.J. Holmes(ed.), SIAM, Philadelphia, PA. U.S.A., pp 487-495.

[13] B.H. Tongue, "Chaotic Behavior of a Simple Single-degree-of- freedom System", Fluid-Structure Interaction and Aerodynamic Damping (E.H. Dowell etc. ed.), 1985, ASME, NY. U.S.A.

[14] L.D. Zavodney and A.H. Nayfeh, "The Response of a Single-degree- of-freedom System with Quadratic and Cubic Non-linearities to a Fundamental Parametric Resonance", J. Sound and Vibr., 1988, Vol.120(1), pp 63-93.

[15] H.L.Neal and A.H. Nayfeh,"Response of a Single-degree-of-freedom System to a Non-Stationary Principal Parametric Excitation", Int. J. Non-linear Mech.,1990, Vol.25, No.2/3, pp 275-284.

[16] N.E. Sanchez and A.H. Nayfeh, "Prediction of Bifurcations in a Parametrically Excited Duffing Oscillator", Int. J. Non-linear Mech., 1990, Vol.25, pp 163-176.

[17] A.H. Nayfeh and L.D. Zavodney, "The Response of Two-degree-of- freedom Systems with Quadratic Non-linearities to a Combination Parametric Resonance", J. Sound and Vibr., 1986, Vol.107(2), pp 329-350.

[18] A.H. Nayfeh and B. Balachandran, "Experimental Investigation of Resonantly Forced Oscillations of a Two-degree-of-freedom Structure", Int. J. Non-linear Mech., 1990, Vol.25, No.2/3, pp 199-209.

[19] M.S. Soliman, J.M.T. Thompson, "Integrity Measures Quantifying the Erosion of Smooth and Fractal Basins of Attraction", J. Sound and Vibr., 1989, Vol.135, pp 453-475.

[20] J.M.T. Thompson, "Chaotic Phenomena Triggering the Escape from a Potential Well", Proc. Roy. Soc. London, 1989, A 421, pp195-225.

[21] A.Y.T. Leung and T.C. Fung, "Construction of Chaotic Regions", J. Sound and Vibr., 1989, Vol.131(3), pp 445-455.

[22] B.Poddar, F.C. Moon and S. Mukherjee, "Chaotic Motion of an Elastic-Plastic Beam", J. Appl. Mech., 1988, Vol.55, pp 185-189.

[23] S.W. Shaw and P.J. Holmes, "A Periodically Forced Piecewise Linear Oscillator", J. Sound and Vibr., 1983, Vol.90(1), pp 129-155.

[24] F.C. Moonand S.W. Shaw, "Chaotic vibrations of a Beam with Non- linear Boundary Conditions", Int. J. Non-linear Mech., 1983, Vol.18, No.6, pp 465-477.

[25] E.H. Dowell, "Flutter of a Buckled Plate as an Example of Chaotic Motion of a Deterministic Autonomous System", J. Sound and Vibr., 1982, Vol.85(3), pp 333-344.

[26] R. Vaziri, "Finite Deflection Dynamic Analysis of Rigid - Plastic Beam", 1985, M.Sc. Thesis, U.B.C., Canada.

[27] A.J. Lichtenberg and M.A. Lieberman, "Regular and Stochastic Motion", 1983, Springer-Verlag, New York.

[28] J. Guckenheimer and P.J. Holmes, "Nonlinear Oscillations, Dynamical Systems and Bifurcations of Vector Fields", 1983, Springer-Verlag, New York.

[29] J.M.T. Thompson and H.B. Stewart, "Nolinear Dynamics and Chaos", 1986, John Wiley and Sons Ltd.